

Final Report

CCQM-K87

“Mono-elemental Calibration Solutions”

Authors:

Olaf Rienitz¹, Detlef Schiel¹, Volker Görlitz¹, Reinhard Jährling¹, Jochen Vogl², Judith Velina Lara-Manzano³, Agnieszka Zoń⁴, Wai-hong Fung⁵, Mirella Buzoianu⁶, Rodrigo Caciano de Sena⁷, Lindomar Augusto dos Reis⁷, Liliana Valiente⁸, Yong-Hyeon Yim⁹, Sarah Hill¹⁰, Rachel Champion¹¹, Paola Fisticaro¹¹, Wu Bing¹², Gregory C. Turk¹³, Michael R. Winchester¹³, David Saxby¹⁴, Jeffrey Merrick¹⁴, Akiharu Hioki¹⁵, Tsutomu Miura¹⁵, Toshihiro Suzuki¹⁵, Maré Linsky¹⁶, Alex Barzev¹⁶, Michal Máriássy¹⁷, Oktay Cankur¹⁸, Betül Ari¹⁸, Murat Tunç¹⁸, L. A. Konopelko¹⁹, Yu. A. Kustikov¹⁹, Marina Bezruchko¹⁹

1	PTB	6	INM	11	LNE	16	NMISA
2	BAM	7	INMETRO	12	NIM	17	SMU
3	CENAM	8	INTI	13	NIST	18	TUBITAK UME
4	GUM	9	KRISS	14	NMIA	19	VNIM
5	HKGL	10	LGC	15	NMIJ		

22 May 2012

Coordinated by: Detlef Schiel and Olaf Rienitz, PTB

Contents

1. Introduction and background	3
2. The samples	5
2.1 General considerations/demonstrated CMCs	5
2.2 Sample preparation	6
2.3 Molar mass of lead	8
2.4 Blanks/trace matrix constituents	9
2.5 Homogeneity/stability	10
3. Gravimetric KCRVs	12
4. Participants	15
5. Instructions to the participants	16
6. Reference materials, methods and instrumentation	16
7. Results	20
7.1 Chromium samples	20
7.2 Cobalt samples	23
7.3 Lead samples	26
7.4 Key comparison reference values	29
7.5 Additional KCRV estimators based on the participants' data	38
7.6 Degrees of equivalence d_i	44
7.7 Precision and accuracy considerations	62
7.8 Dependency of methods and results	70
8. Discussion	72
9. References	76
Appendixes	
A Technical Protocol – CCQM-K87 and CCQM-P124 “Mono-elemental Calibration Solutions”	77
B Table of masses provided with samples (example)	85
C Results from CCQM-P124 compared to CCQM-K87	86
D Accuracy of the participants' standards	95
E Unprocessed results as reported	97
F Conversion applied to results reported for type B solutions	103
G Molar mass of lead, additional data	103
H Remarks on rounding	104

1. Introduction and background

In April 2010 the Working Group on Inorganic Analysis (IAWG) of the *Consultative Committee for Amount of Substance – Metrology in Chemistry* (CCQM) decided to perform this comparison measurement as a joint comparison with the Working Group on Electrochemical Analysis (EAWG). It is intended to improve and to verify the measurement capabilities of the National Metrology Institutes (NMI) for the measurement of mono-elemental calibration solutions with an element mass fraction of $w(E) \approx 1$ g/kg.

In parallel to this key comparison the pilot study CCQM-P124 was organized to give less experienced institutes as well as industrial laboratories also the opportunity to participate.

CCQM-K87 was initiated on request of the KCWG chair in 2009 as a repeat comparison of CCQM-K8, which was conducted by EMPA and LNE in 1999/2000.

Table 1: Timetable of CCQM-K87.

April	2009	First discussion about key comparison based on calibration solutions on request of KCWG chair during IAWG meeting
November	2009	Discussion of possible elements and intended focus
April	2010	Proposal agreed by IAWG
July	2010	Invitation circulated
31 August	2010	Deadline for registration
December	2010	Shipment of the samples
15 March	2011	Deadline for reporting results
1 April	2011	Extended deadline due to delayed sample receipt in several cases
April	2011	Presentation of preliminary results
November	2011	KCRVs accepted by IAWG [1]

Traceability systems in elemental analysis [2] get their fundamental link to the SI via the purity determination of suitable metals or salts. The demonstration of this capability was addressed with CCQM-P62 (purity of Ni) [3] and CCQM-P107 (purity of Zn) [4]. And it is or will be the subject of ongoing or planned comparisons: CCQM-P135 (purity of NaCl) and CCQM-K72 (purity of Zn). The second link in the traceability chain – namely the primary solutions – was covered with CCQM-P46 (preparation of primary solutions of Cu, Mg and Rh). Linking all the measurements in the field to this system is crucial and usually achieved through calibration solutions, which was therefore decided to focus on in the framework of this key comparison (CCQM-K87) and the connected pilot study CCQM-P124.

Three elements (chromium, cobalt and lead) were chosen to represent different kinds of needs and challenges. Chromium becomes increasingly important in environmental analysis. Cobalt as a mono-isotopic element cannot be determined using isotope dilution techniques. Lead usually requires the determination of the isotopic abundances in every sample because of its natural range of variation.

Since the mass fractions of the three elements were adjusted gravimetrically and their original matrix contents were negligible compared to the adjusted content of 1 g/kg, gravimetric refer-

ence values to serve as the *key comparison reference values* (KCRV) are available. These were accepted by the IAWG during the Sydney meeting on 1 November 2011.

Nineteen NMIs from eighteen countries participated and reported their results. The relative deviation of the median of the participants' results from the gravimetric reference value was equal to or smaller than 0.1 % (with an average of 0.05 %) in case of all three elements.

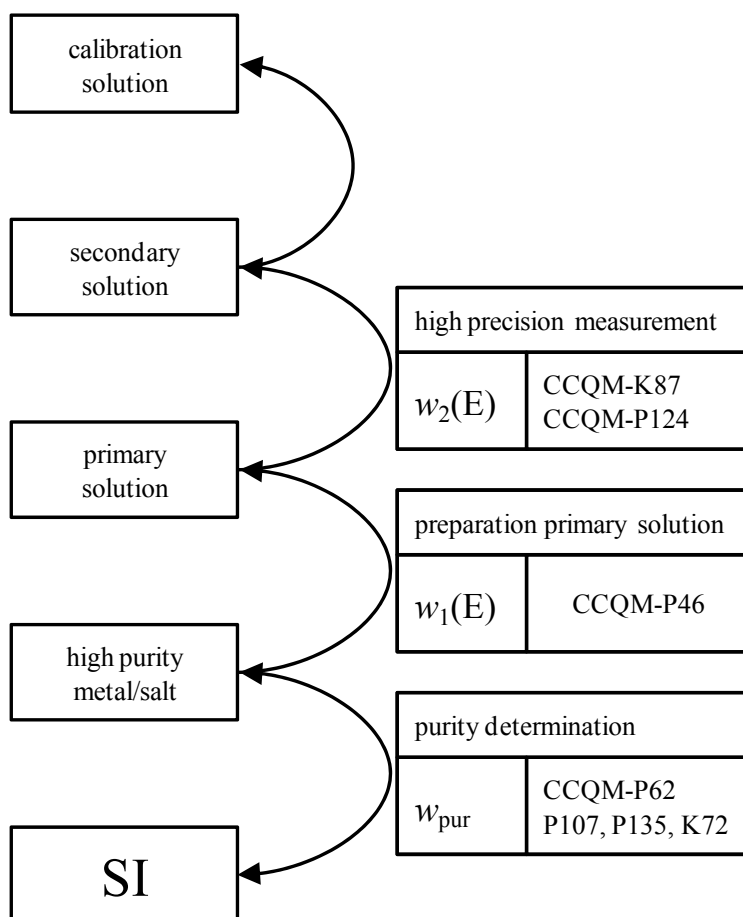


Figure 1: Finalised, ongoing and future CCQM key comparisons and pilot studies aim at demonstrating the participants' ability to set up a traceability system in elemental analysis. CCQM-K87 represents an important part of it.

2. The samples

2.1 General considerations/demonstrated CMCs

Nine mono-elemental solutions were prepared gravimetrically at PTB starting from the German national standards provided by BAM (cobalt and lead) and from a primary material provided by CENAM (chromium), respectively. Table 2 compiles the certified purities w_{pur} of these primary materials along with their associated uncertainties $U(w_{\text{pur}})$.

Table 2: Primary materials used to prepare the key comparison samples.

Element	provided by	w_{pur} g/g	$U(w_{\text{pur}})$ g/g	k 1
Cr	CENAM	0.999 10	0.000 39	2
Co	BAM	0.999 74	0.000 12	2
Pb	BAM	0.999 92	0.000 06	2

Following the outcome of several discussions during IAWG/EAWG meetings three different solutions (A, B, and C) of each element were prepared. Solution type A was meant to serve both as a sample and as the calibration standard against which the participants were asked to measure solution type B assuming an arbitrarily assigned element mass fraction of $w = 1 \text{ g/kg} \pm 0 \text{ g/kg}$. In case the applied method requires no calibration standard (e.g. titrimetry) the participants were asked to skip solution type A. Since trace amounts of matrix constituents may affect the results, in particular those obtained with titrimetry, solution type C was prepared using slightly less pure water and acid with the intention to resemble commercial calibration solutions. Table 3 summarizes these solutions and shows the notation used:

Table 3: Notation of samples prepared.

type of solution	chromium	cobalt	lead
A – calibration solution	Cr-A	Co-A	Pb-A
B – sample solution	Cr-B	Co-B	Pb-B
C – “commercial” sample solution	Cr-C	Co-C	Pb-C

Considering the different challenges and tasks related to the different types of solutions, specific *calibration and measurements capabilities* (CMC) may be claimed by the participants. Table 4 summarizes the demonstrated capabilities in relationship to the type of solution.

Table 4: Solution type and related CMC claims.

type of solution	specific capability
A	determination of element mass fraction using own standard solution and preparation of standard solution
B	1) determination of element mass fraction against another solution provided externally 2) see type A in case solution B was measured without using A as the standard (e.g. titrimetry)
C	see A or B 2) in case of slightly elevated trace matrix constituents (refer to table 8 for details)

2.2 Sample preparation

The sample preparation directly finds the model equation used to calculate the gravimetric element mass fractions their associated uncertainties as well as their ability to serve as KCRVs:

After cleaning the solid starting materials (table 2) following prescribed procedures taken from the certificates, aliquots of approximately 5–6 g were dissolved using stoichiometric amounts of HCl ($w = 0.2$ g/g) in case of Cr and excess amounts of HNO₃ ($w = 0.2$ g/g) in case of Co and Pb. The Cr solutions were adjusted with HNO₃ ($w = 0.2$ g/g) and water to form stock solutions (550 g each) with an element mass fraction of $w(E) \approx 10\,000$ µg/g and an acid mass fraction of $w(\text{HNO}_3) = 0.025$ g/g. In case of Co and Pb only water was added to form the stock solutions (550 g each) with an element mass fraction of $w(E) \approx 10\,000$ µg/g and an acid mass fraction of $w(\text{HNO}_3) = 0.025$ g/g. The final samples were gravimetrically prepared directly from the stock solutions by diluting each 550 g stock solution using HNO₃ ($w = 0.025$ g/g) yielding approximately 5.5 kg of each of the nine solutions. In case of the solution types A and B ultrapure HCl, subboiled HNO₃ and ultrapure water (type 1) was used for the preparation. In order to come as close as possible to a “commercial” solution, trace impurities were introduced into solution type C by using p.a. HNO₃ and p.a. HCl as well as only pure water (type 2) for the preparation instead of the chemicals mentioned above. Since even these p.a. chemicals are extremely pure, the differences between solution type B and C are fairly subtle, reflecting the fact that almost all commercial calibration solutions do not contain impurities above the trace level. All nine solutions were adjusted to feature an element mass fraction of 0.98 g/kg $\leq w(E) \leq 1.02$ g/kg. The solutions were filled in thoroughly cleaned, dried, labelled and weighed 100 mL-PFA bottles. Each bottle contained at least 100 g of the respective solution. Prior to sealing the bottles in film bags, each bottle was weighed again to keep track of losses during shipment and be able to distinguish between unavoidable losses due to evaporation (and correct for them, see appendix A) and losses due to leaking bottles. The bottles were wrapped in tightly sealed film bags (12 µm polyester, 12 µm aluminium, 95 µm LDPE, type A 30 T, C. Waller, Eichstetten, Germany). Altogether 384 bottles were prepared. Table 5 shows the numbers of bottles prepared in more detail.

The table 6 compiles the densities determined at 21 °C immediately after bottling of the samples along with all the other important properties.

Table 5: Number of sample bottles prepared (CCQM-K87 and CCQM-P124).

element, type of solution		number of bottles prepared	total number per element
Cr	A	44	126
	B	42	
	C	40	
Co	A	44	126
	B	42	
	C	40	
Pb	A	46	132
	B	44	
	C	42	

Table 6: Mass densities and major matrix constituents of the samples.

element, type of solution		matrix		element content	density $\rho / (\text{kg/m}^3)$
Cr	A	$w(\text{HCl}) < 0.002 \text{ g/g}$	$w(\text{HNO}_3) \approx 0.025 \text{ g/g}$	$0.98 \text{ g/kg} \leq w(\text{E}) \leq 1.02 \text{ g/kg}$	1014.1
	B				
	C				
Co	A				
	B				
	C				
Pb	A				1012.8
	B				
	C				

2.3 Molar mass of lead

The molar mass of the lead in the samples Pb-A, Pb-B and Pb-C does not match the IUPAC representative molar mass of lead. Therefore, all participants were asked to determine the molar mass in the sample to be able to correct for this issue or (if this was impossible) report their results in terms of an amount content n/m in mol/kg rather than in terms of a mass fraction w in g/kg. The molar mass ($M(\text{Pb}) = (207.17782 \pm 0.00011) \text{ g/mol}$, $k = 2$) of the starting material used to convert these amount content values into mass fractions was determined at PTB on several occasions over the last eight years using both thermal ionisation mass spectrometry (TIMS) and multi-collector ICP mass spectrometry (MC-ICP-MS). It was confirmed in the actual CCQM-K87 samples using TIMS. The PTB value is in good enough agreement with the median of all molar masses reported by the participants ($M_m(\text{Pb}) = (207.17799 \pm 0.00014) \text{ g/mol}$, $k = 2.2$), refer to figure 2 for details.

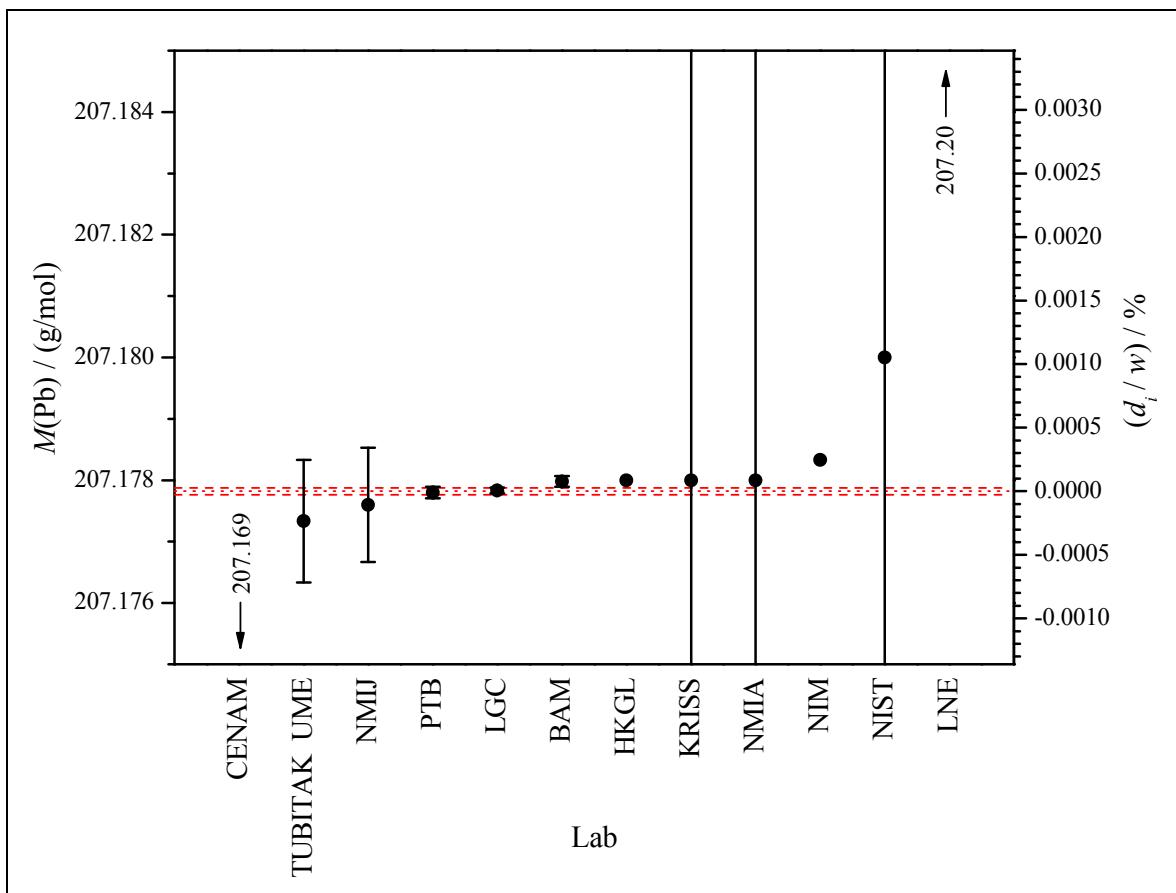


Figure 2: Molar mass of lead (dotted red line) used to convert lead results reported in terms of amount content into mass fractions together with the molar masses as reported by the participants (error bars and dashed red line denote respective standard uncertainties). Please be aware that several institutes determined the molar mass with an effort “fit for purpose”, which does not reflect their actual abilities to perform this kind of measurement.

2.4 Blanks/trace matrix constituents

A blank element content arising from the water, acids, glassware, and tools like pipettes used during sample preparation might limit the possibility to calculate a reliable gravimetric KCRV from the preparation itself. Therefore, these blanks were determined at PTB using an IDMS standard addition technique (Cr, Pb) and gravimetric standard addition [5] in case of Co, respectively. Table 7 summarizes the upper limits found in individual samples. Since these blanks would not affect the gravimetric KCRVs, they were calculated using a blank fraction of $w_0(E) = (0 \pm 100)$ ng/g to account for the conservatively estimated uncertainty associated with the blank determination without changing the actual KCRVs.

Table 7: Blank mass fractions determined using an IDMS standard addition technique (Cr, Pb) and gravimetric standard addition (Co).

Element E	$w(E)$
	ng/g
Cr	< 0.06
Co	< 0.06
Pb	<0.4

The slightly different trace matrix contents in solutions of type A, B and C were determined using a high resolution ICP-mass spectrometer (HR-ICP-MS) applying a semi-quantitative one-point calibration approach. Therefore, the results shown in table 8 are by no means absolute values, they rather illustrate the order of magnitude of the contents to reveal how the matrix of solution type C differs from A, B.

Table 8: Different trace element patterns in solutions type A, B and C. Blank mass fractions determined using a semi-quantitative one-point calibration. Iron was not determined.

Type	A, B	C
Element E	$w(E)$	$w(E)$
	ng/g	ng/g
Li	2	2
B	1	1
Na	1	4
Mg	0.04	0.2
Al	0.3	0.3
Si	6	11
K	2	2
Ca	0.4	2
Cu	0.04	0.3
Sn	0.02	0.2
Ba	0.005	0.1

2.5 Homogeneity/stability

In accordance with ISO Guide 35 [6] all nine samples were checked for homogeneity and stability issues. Altogether 45 bottles (15 per element) out of 384 were uniformly withdrawn from each batch of bottles to perform homogeneity and stability measurements. All measurements were carried out on an ICP OES applying a bracketing method with an internal standard to ensure a maximum relative within-bottle standard deviation of less than 0.017 %. Using one-way ANOVA the between-bottle uncertainty u_{bb} due to homogeneity was calculated from the results of 40 samples per element as the “difference” of the variances among and within the bottles measured (n_0 = effective number of subsamples, k = number of bottles, n_i = number of subsamples per bottle):

$$u_{bb}^2 = s_{bb}^2 = \frac{S_{\text{among}}^2 - S_{\text{within}}^2}{n_0} \quad (1)$$

$$n_0 = \frac{1}{k-1} \left[\sum_{i=1}^k n_i - \frac{\sum_{i=1}^k n_i^2}{\sum_{i=1}^k n_i} \right] \quad (2)$$

Stability was monitored from 15 December 2010 to 8 April 2011. From $n = 24$ samples per element the stability related uncertainty u_{ts} was calculated applying a linear approach to describe possible changes of the element mass fraction w over time t :

$$w = a_0 + a_1 \cdot t \quad (3)$$

No stability issues can be detected in case the slope a_1 (calculated applying an OLS algorithm) is insignificant regarding its standard deviation $s(a_1)$. Symbols: t = student t-factor, p = probability.

$$a_1 = \frac{n \sum_{i=1}^n t_i w_i - \sum_{i=1}^n t_i \sum_{i=1}^n w_i}{n \sum_{i=1}^n t_i^2 - \left(\sum_{i=1}^n t_i \right)^2} \quad (4)$$

$$u^2(a_1) = \frac{n \cdot S^2}{n \sum_{i=1}^n t_i^2 - \left(\sum_{i=1}^n t_i \right)^2} \quad \text{with } S^2 = \frac{1}{n-2} \sum_{i=1}^n [w_i - (a_0 + a_1 t_i)]^2 \quad (5)$$

$$|a_1| < t(p = 0.95, n-2) \cdot s(a_1) \quad (6)$$

With an extended shelf life of $t_{\Delta} = 137$ d the complete time period from sample preparation to the receipt of the last result was covered. This way a very conservative stability related uncertainty u_{ts} was estimated:

$$u_{\text{ts}} = t_{\Delta} \cdot s(a_1) \quad (7)$$

Since no evidence of any homogeneity or stability issue was found no correction had to be applied. In order to account for the uncertainty associated with this finding a “correction” fac-

for $k_{\text{homstab}} = 1$ was defined which allowed to introduce the uncertainty associated with the stability/homogeneity determination into the gravimetric KCRVs without changing their values. The contributions due to homogeneity u_{bb} and stability u_{Its} were combined accordingly to yield the relative uncertainty associated with the “correction” factor $u_{\text{rel}}(k_{\text{homstab}})$. Its value depends on the particular element E (eq. (9)) and on the solution type. Since the solution types differ only slightly the largest uncertainty was chosen for all three solution types of one element.

$$u(k_{\text{homstab}}) = \sqrt{u_{\text{bb}}^2 + u_{\text{Its}}^2} \quad (8)$$

$$u_{\text{rel}}(k_{\text{homstab}}) = \frac{u(k_{\text{homstab}})}{w_{\text{KCRV}}(\text{E})} \quad (9)$$

Table 9 summarizes all uncertainty contributions due to homogeneity and stability. These uncertainties reflect the limits of the ICP OES procedure applied rather than actual homogeneity or stability issues.

Table 9: Uncertainty contributions due to homogeneity u_{bb} and stability u_{Its} along with their combined contribution $u(k_{\text{homstab}})$; the relative combined contribution is related to the gravimetric KCRV (see next section and eq. (9)).

		Cr	Co	Pb
u_{bb}	μg/g	0.2347	0.1969	0.0917
u_{Its}	μg/g	0.2151	0.1958	0.1538
$u(k_{\text{homstab}})$	μg/g	0.3184	0.2777	0.1790
$u_{\text{rel}}(k_{\text{homstab}})$	%	0.032	0.028	0.018

3. Gravimetric KCRVs

The mass fraction $w_{\text{KCRV}}(\text{E})$ of an element E was calculated as the sum of the added mass fraction $w_{\text{add}}(\text{E})$ plus the blank mass fraction $w_0(\text{E})$ according to section 2.4 considering the homogeneity/stability contribution according section 2.5 yielding eq. (10):

$$w_{\text{KCRV}}(\text{E}) = w_{\text{add}}(\text{E}) + w_0(\text{E}) \quad (10)$$

The added element mass concentration $w_{\text{add}}(\text{E})$ was calculated from the preparation of the samples. A 5 L-borosilicate bottle was thoroughly cleaned, checked for the respective element E and dried. After weighing (m_{1r}), an approximate volume of 4 L nitric acid ($w(\text{HNO}_3) = 0.025 \text{ g/g}$) was added. After weighing (m_{2r}), approximately 0.5 kg of the primary reference solution ($w_z = w(\text{E}) \approx 10\,000 \text{ }\mu\text{g/g}$) was added. After weighing (m_{3r}), another 0.8—1.2 L nitric acid ($w(\text{HNO}_3) = 0.025 \text{ g/g}$) was added (m_{4r}) to adjust added element mass fractions of $0.98 \text{ g/kg} \leq w_{\text{add}}(\text{E}) \leq 1.02 \text{ g/kg}$. Since all weighing steps had to be corrected for air buoyancy using correction factors (K_{ij}) taking into account the air density (air temperature, pressure and humidity) as well as the density of the sample (j) at any particular step (i) of the preparation procedure, the equation below was used to calculate the element mass fractions (KCRVs) $w_{\text{KCRV}}(\text{E})$:

$$w_{\text{KCRV}}(\text{E}) = k_{\text{homstab}} \left[\frac{w_z \left[K_{3x} \left(m_{3r} - \frac{K_{1\text{BSG}} \cdot m_{1r}}{K_{3\text{BSG}}} \right) - K_{2\text{NAc}} \left(m_{2r} - \frac{K_{1\text{BSG}} \cdot m_{1r}}{K_{2\text{BSG}}} \right) \right]}{K_{4x} \left(m_{4r} - \frac{K_{1\text{BSG}} \cdot m_{1r}}{K_{4\text{BSG}}} \right)} + w_0(\text{E}) \right] \quad (11)$$

The blank mass fraction $w_0(\text{E})$ was determined by PTB using a gravimetric standard addition technique combined with IDMS (Cr, Pb) and an internal standard (Co). Please refer to section 2.4 (table 7) for details. Equation (11) served as the model equation used to calculate the uncertainty associated with the KCRVs (meaning of the symbols used are compiled in table 10) in accordance with [7]. No significant homogeneity or stability issues were determined within the reproducibility of the ICP OES method applied. The factor k_{homstab} featuring a value of one accounts for this limitation with its associated uncertainty. Please refer to section 2.5 for details.

Table 10: Meaning of symbols used in equation (11).

Symbol	Unit	Quantity
$w_{\text{KCRV}}(\text{E})$	g/kg	KCRV, mass fraction of element E (E = Cr, Co, Pb)
w_z	g/kg	Mass fraction of element E in the primary reference solution z
m_{1r}	kg	Apparent mass of the empty 5 L glass container
m_{2r}	kg	Apparent mass of the empty 5 L glass container plus 4 L nitric acid ($w(\text{HNO}_3) = 0.025 \text{ g/g}$)
m_{3r}	kg	Apparent mass of the empty 5 L glass container plus 4 L nitric acid ($w(\text{HNO}_3) = 0.025 \text{ g/g}$) plus 0.5 kg primary reference solution z ($w_z \approx 10 \text{ g/kg}$)
m_{4r}	kg	Apparent mass of the empty 5 L glass container plus final sample solution
$K_{1\text{BSG}}$	kg/kg	Air buoyancy correction factor of borosilicate glass under the conditions when weighing the empty bottle (m_{1r})
$K_{2\text{BSG}}$	kg/kg	see $K_{1\text{BSG}}$, but when weighing m_{2r}
$K_{3\text{BSG}}$	kg/kg	see $K_{1\text{BSG}}$, but when weighing m_{3r}
$K_{4\text{BSG}}$	kg/kg	see $K_{1\text{BSG}}$, but when weighing m_{4r}
$K_{2\text{NAc}}$	kg/kg	Air buoyancy correction factor of the 4 L nitric acid ($w(\text{HNO}_3) = 0.025 \text{ g/g}$) under the conditions when weighing m_{2r}
K_{3x}	kg/kg	Air buoyancy correction factor of the 4 L nitric acid ($w(\text{HNO}_3) = 0.025 \text{ g/g}$) after adding the primary elemental solution z under the conditions when weighing m_{3r}
K_{4x}	kg/kg	Air buoyancy correction factor of the final sample under the conditions when weighing m_{4r}
k_{homstab}	1	“Correction” factor to introduce the uncertainty contribution due to homogeneity and stability of the samples over the duration of the comparison
$w_0(\text{E})$	g/kg	Blank mass fraction of element E

The KCRVs (mass fractions) $w_{\text{KCRV}}(\text{E})$ as well as their associated uncertainties according to [7] were calculated using equation (11). Table 11 shows a compilation of the KCRVs and their associated uncertainties. The main contributions to the uncertainty are the apparent masses m_{2r} and m_{3r} as well as the uncertainty due to the homogeneity/stability determination.

Table 11: Mass fractions (KCRVs) $w_{\text{KCRV}}(\text{E})$ of the elements E in the three different sample solutions (type A, B, and C). The uncertainties are expanded uncertainties U with a coverage factor of $k = 2$.

E	type of solution	$w_{\text{KCRV}}(\text{E})$ g/kg	$U(w(\text{E}))$ g/kg	$U_{\text{rel}}(w(\text{E}))$ %	k 1
Cr	A – calibration	1.0100			
	B – sample	1.0050	0.0013	0.13	2
	C – “commercial” sample	0.9850			
Co	A – calibration	0.9800			
	B – sample	1.0000	0.0012	0.12	2
	C – “commercial” sample	1.0180			
Pb	A – calibration	0.9800			
	B – sample	0.9940	0.0011	0.11	2
	C – “commercial” sample	0.9830			

4. Participants

Nineteen NMIs from eighteen countries participated in CCQM-K87. For more details refer to table 12.

Table 12: Participants of CCQM-K87 in alphabetical order of their acronyms.

Institute	Country	Contact
BAM – Federal Institute for Materials Research and Testing	Germany	Jochen Vogl
CENAM – Centro Nacional de Metrología	Mexico	Judith Velina Lara-Manzano
GUM – Central Office of Measures	Poland	Agnieszka Zoń
HKGL – Government Laboratory Hong Kong	Hong Kong, China	Wai-hong Fung
INM – National Institute of Metrology	Romania	Mirella Buzoianu
INMETRO – National Institute of Metrology, Standardization and Industrial Quality	Brazil	Rodrigo Caciano de Sena
INTI – Instituto Nacional de Tecnología Industrial	República Argentina	Liliana Valiente
KRISS – Korea Research Institute of Standards and Science	Republic of Korea	Yong-Hyeon Yim
LGC – LGC Ltd.	United Kingdom	Sarah Hill
LNE – Laboratoire National de Métrologie et d'Essais	France	Rachel Champion, Paola Fisicaro
NIM – National Institute of Metrology P. R. China	P. R. China	Wu Bing
NIST – National Institute of Standards and Technology	United States of America	Gregory C. Turk, Michael R. Winchester
NMIA – Australian Government - National Measurement Institute	Australia	David Saxby, Jeffrey Merrick
NMIJ – National Metrology Institute of Japan	Japan	Akiharu Hioki
NMISA – National Metrology Institute of South Africa	South Africa	Maré Linsky
PTB – Physikalisch-Technische Bundesanstalt	Germany	Reinhard Jährling, Volker Görlitz

Institute	Country	Contact
SMU – Slovak Institute of Metrology	Slovakia	Michal Máriássy
TUBITAK UME – TUBITAK National Metrology Institute	Turkey	Oktay Cankur
VNIIM – D. I. Mendeleev Institute for Metrology	Russian Federation	L. A. Konopelko, Yu. A. Kustikov, Marina Bezruchko

5. Instructions to the participants

A technical protocol was sent to all participants of CCQM-K87, prior to the sample distribution providing information about the properties of the samples, the sample handling and the recommended procedure to check for losses and correct for evaporation effects during storage. Together with the reporting deadline specific – method dependent – issues concerning the report – were given. The sample bottles were accompanied by an individual table compiling the masses of the empty bottles and of the respective solutions needed to carry out the loss checking/evaporation correction procedure.

Appendix A shows the technical protocol of CCQM-K87. Appendix B gives an example of one of the above mentioned masses tables.

6. Reference materials, methods and instrumentation

Participants were free to use a method of their choice. All participants measured the samples as received. No digestion was necessary. A majority – though a small one – used ICP OES combined with different calibration strategies.

Table 13: Reference materials (sources of traceability) used as reported by the participants. In case of Pb the second material usually served as the isotopic reference material.

Reference material/source of traceability			
Institute	Cr	Co	Pb
BAM	BAM PRM		BAM-Y004, NIST SRM 981
CENAM	DMR-440f	DMR-458a	DMR-463a, NIST SRM 981
GUM	in-house, traceable to SMU B10	in-house, traceable to SMU B09	in-house, traceable to SMU B26
HKGL	NIST SRM 3112a	NIST SRM 3113	NIST SRM 3128, NIST SRM 981

Reference material/source of traceability			
Institute	Cr	Co	Pb
INM	NIST SRM 3112a	NIST SRM 3113	NIST SRM 3128
INMETRO		in-house	
INTI	NIST SRM 3112a	NIST SRM 3113	NIST SRM 3128
KRISS	in-house	in-house	in-house, NIST SRM 981
LGC	NIST SRM 3112a, Lot No. 990607	in-house	in-house, NIST SRM 981
LNE	NIST SRM 136d	Fer BNM 0001	Fer BNM 0001
NIM	GBW08614	GBW08613	GBW08619
NIST	NIST Primary Material	NIST Primary Material	NIST Primary Material
NMIA	NIST SRM 3112a	NIST SRM 3113	NIST SRM 3128, NIST SRM 981
NMIJ		in-house	in-house, NIST SRM 981
NMISA	NIST SRM 3112a	NIST SRM 3113	NIST SRM 3128
PTB	BAM-A-primary-Cr-1	BAM-A-primary-Co-1	BAM-Y004, NIST SRM 981
SMU	coulometry	EDTA, in-house, LM01-07	EDTA, in-house, LM01-07
TUBITAK UME	NIST SRM 3112a	NIST SRM 3113	NIST SRM 981, NIST SRM 982
VNIIM	GSO 7984-2002	GOST 123-2008	GOST 22861-77

Table 14: Instrumentation/method and calibration strategy used as reported by the participants (IS = internal standard).

Instrumentation/method/calibration strategy			
Institute	Cr	Co	Pb
BAM	MC-TIMS, double IDMS		MC-TIMS, double IDMS
CENAM-1	ICP OES, one-point- calibration + IS	ICP OES, one-point- calibration + IS	ICP OES, one-point- calibration + IS
CENAM-2			titrimetry
GUM	ICP OES, one-point-calibration	ICP OES, one-point-calibration	ICP OES, one-point-calibration
HKGL	ICP OES, one-point- calibration + IS	ICP OES, one-point- calibration + IS	ICP OES, one-point- calibration + IS
INM	Q-ICP-MS, calibration curve	Q-ICP-MS, calibration curve	Q-ICP-MS, calibration curve
INMETRO		ICP OES, calibration curve	
INTI	FAAS, one-point-calibration	ICP OES, one-point-calibration	FAAS, one-point-calibration
KRISS	ICP OES, one-point- calibration + IS	ICP OES, one-point- calibration + IS	ICP OES, one-point- calibration + IS
LGC	MC-ICP-MS, double IDMS	Q-ICP-MS, one-point- calibration + IS	MC-ICP-MS, double IDMS
LNE	Q-ICP-MS, double IDMS	titrimetry	titrimetry
NIM	Q-ICP-MS, bracketing + IS	Q-ICP-MS, bracketing + IS	Q-ICP-MS, bracketing + IS
NIST	ICP OES, one-point- calibration + IS	ICP OES, one-point- calibration + IS	ICP OES, one-point- calibration + IS
NMIA	HR-ICP-MS, double IDMS	HR-ICP-MS, one- point-calibration + IS	HR-ICP-MS, double IDMS
NMIJ		titrimetry	titrimetry
NMISA	ICP OES, bracketing + IS	ICP OES, bracketing + IS	ICP OES, bracketing + IS
PTB	ICP OES, bracketing + IS	ICP OES, bracketing + IS	ICP OES, bracketing + IS

Instrumentation/method/calibration strategy			
Institute	Cr	Co	Pb
SMU	coulometric titrimetry	titrimetry	titrimetry
TUBITAK UME	Q-ICP-MS, four-point- calibration + IS	Q-ICP-MS, four-point- calibration + IS	Q-ICP-MS, double IDMS
VNIIM	ICP OES, one-point-calibration	ICP OES, one-point-calibration	ICP OES, one-point-calibration

7. Results

The participants' results as reported to the coordinating laboratory are shown in tables 18–26, and 31–39 as well as figures 3–11, and 12–20.

7.1 Chromium samples

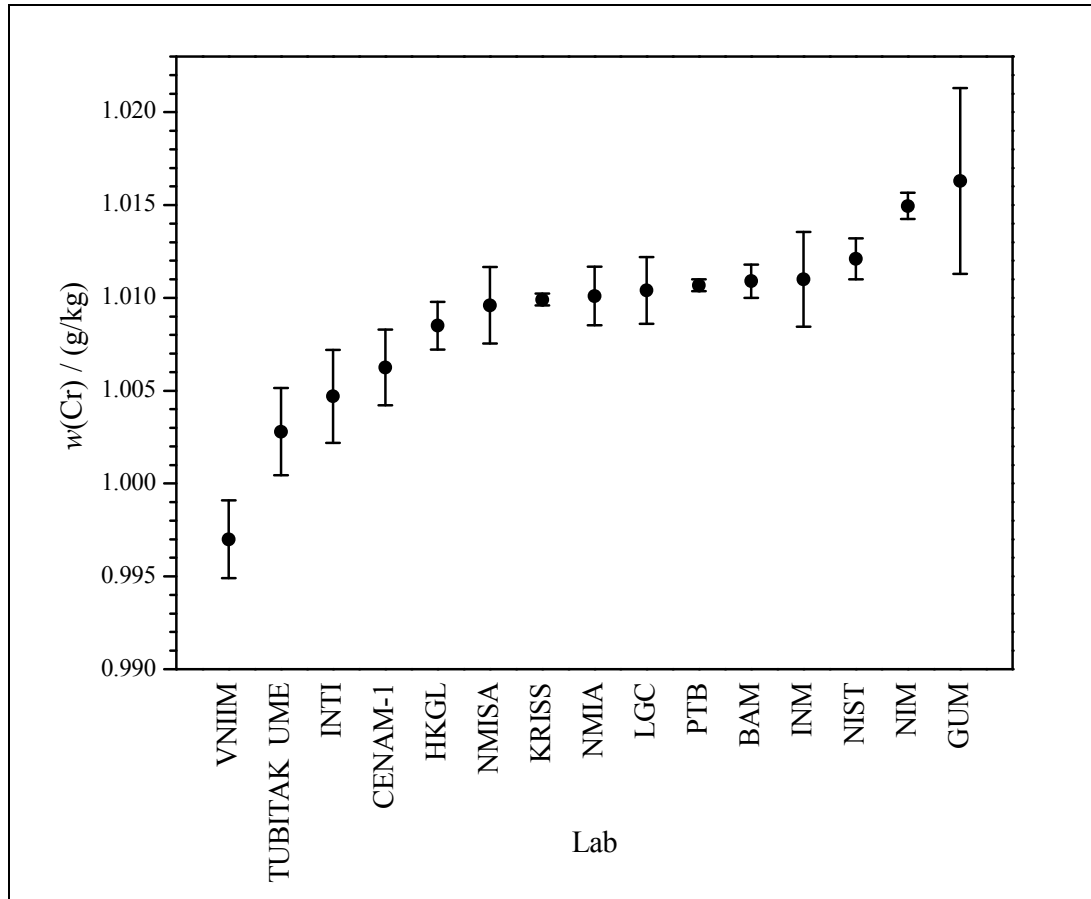


Figure 3: Chromium mass fraction $w(\text{Cr})$ in sample **Cr-A** as reported by the CCQM-K87 participants. Error bars denote the combined uncertainty $u_c(w(\text{Cr}))$ for a coverage factor of $k = 1$ as reported.

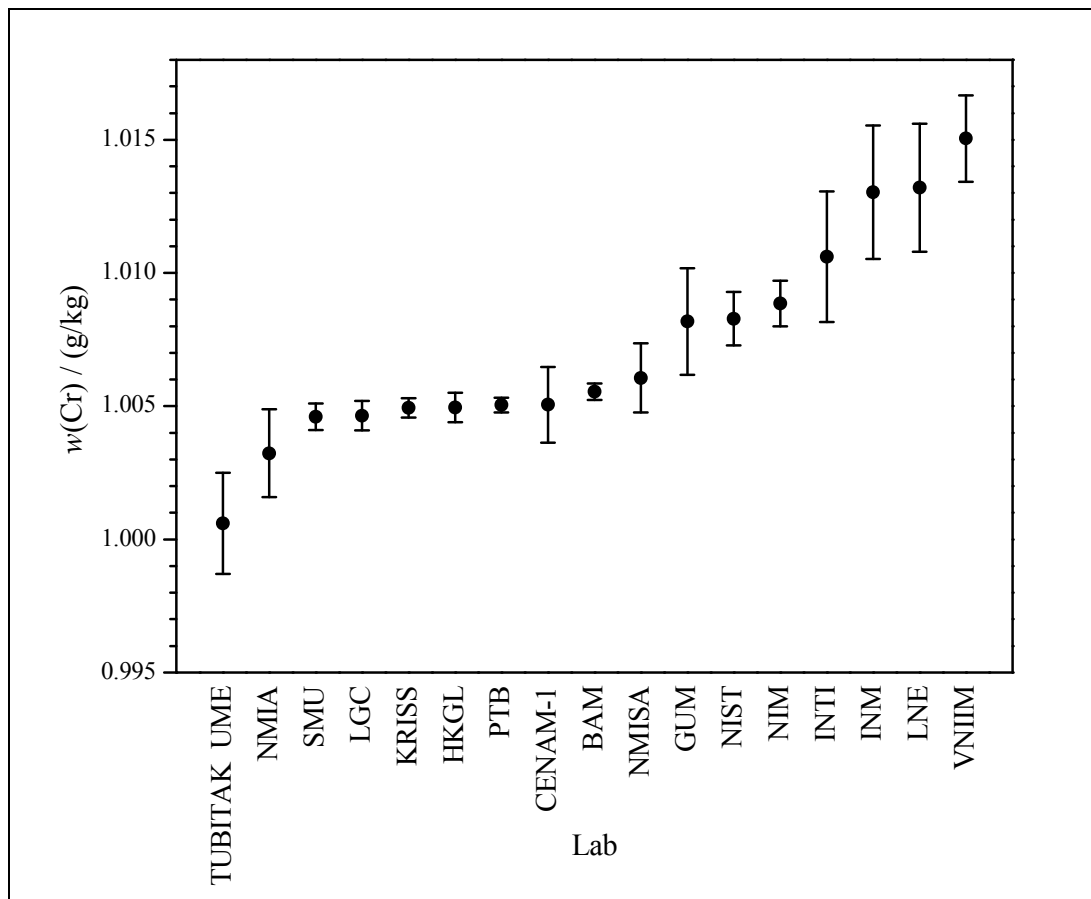


Figure 4: Chromium mass fraction $w(\text{Cr})$ in sample **Cr-B** as reported by the CCQM-K87 participants. Error bars denote the combined uncertainty $u_c(w(\text{Cr}))$ for a coverage factor of $k = 1$ as reported. All results reported as measured against Cr-A under the assumption of $w(\text{Cr}) = 1 \text{ g/kg} \pm 0 \text{ g/kg}$ were converted using the actual value (KCRV) of Cr-A (appendix F).

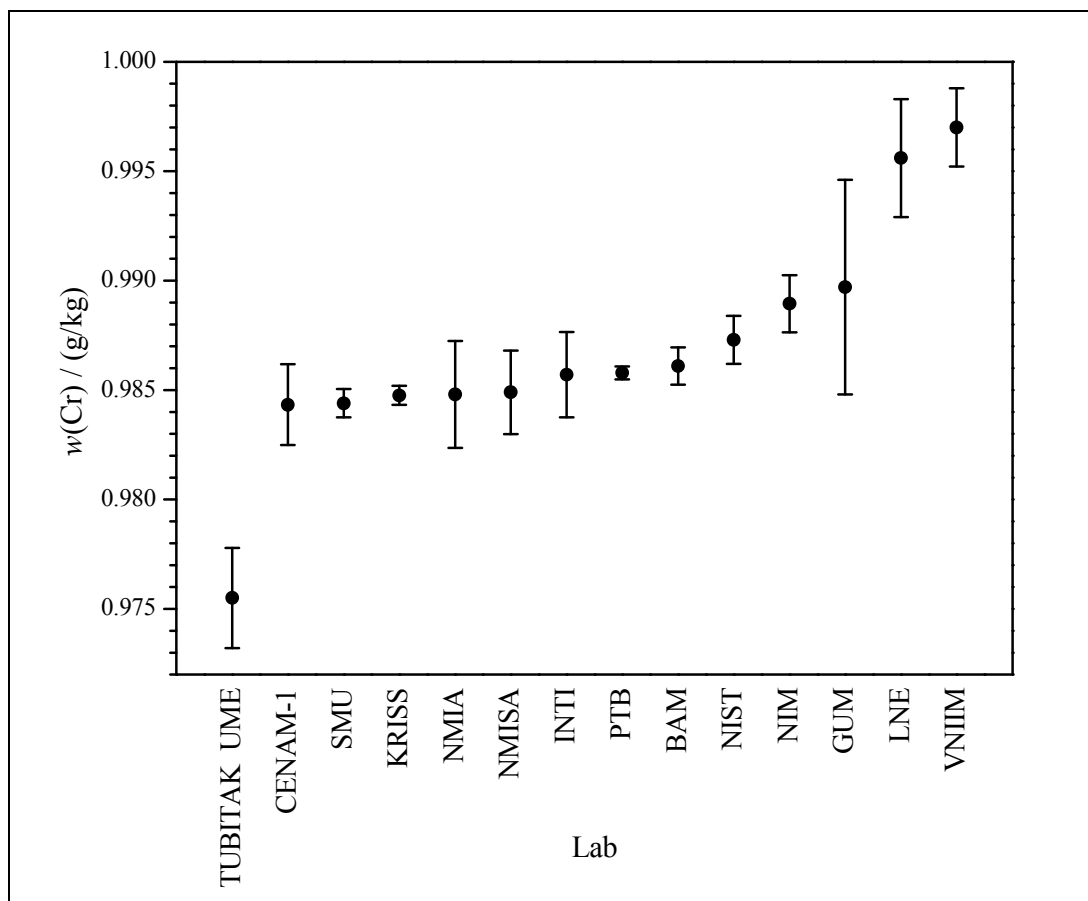


Figure 5: Chromium mass fraction $w(\text{Cr})$ in sample Cr-C as reported by the CCQM-K87 participants. Error bars denote the combined uncertainty $u_c(w(\text{Cr}))$ for a coverage factor of $k = 1$ as reported.

7.2 Cobalt samples

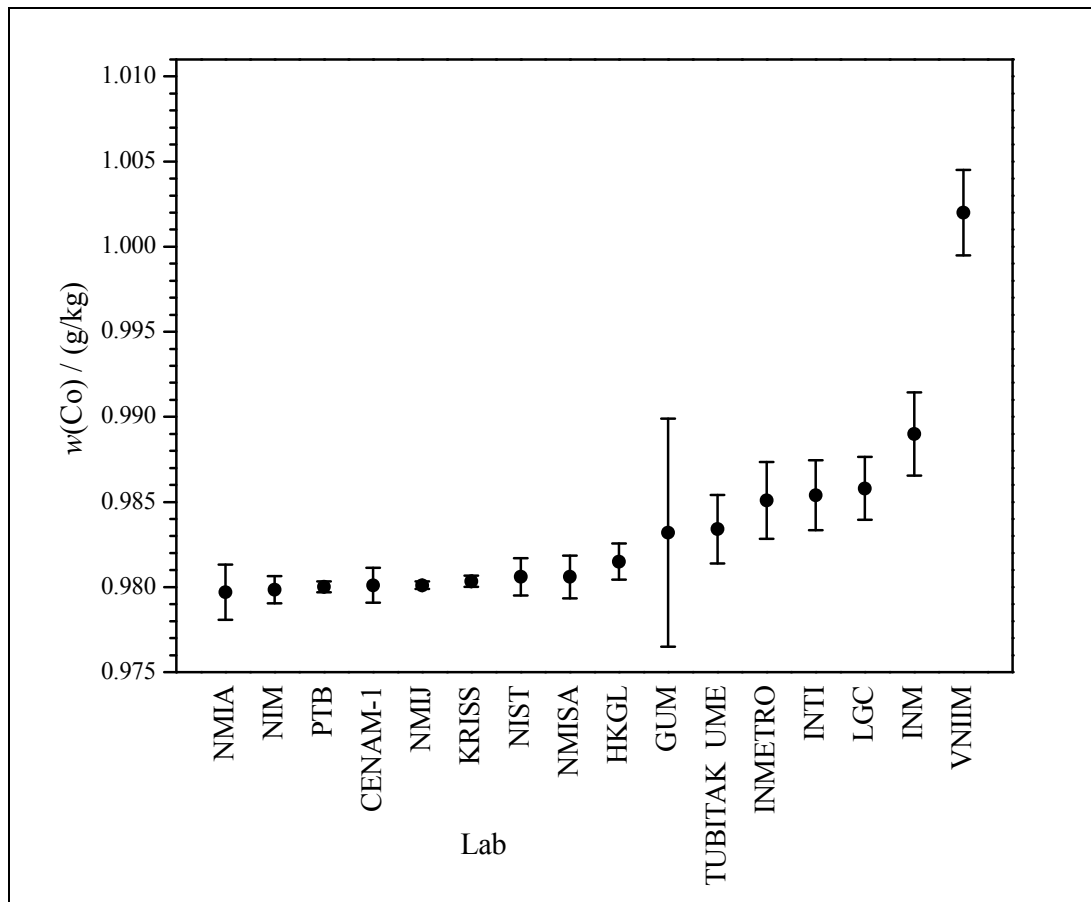


Figure 6: Cobalt mass fraction $w(\text{Co})$ in sample **Co-A** as reported by the CCQM-K87 participants. Error bars denote the combined uncertainty $u_c(w(\text{Co}))$ for a coverage factor of $k = 1$ as reported.

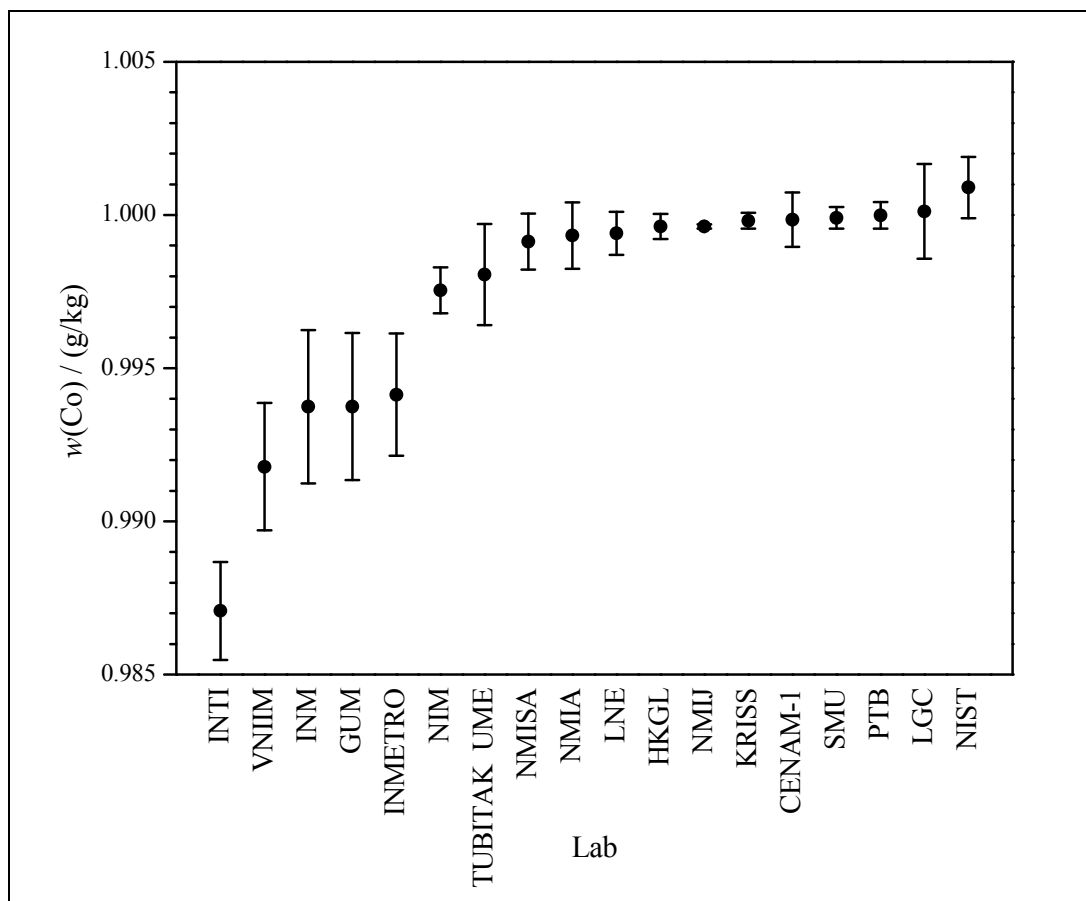


Figure 7: Cobalt mass fraction $w(\text{Co})$ in sample **Co-B** as reported by the CCQM-K87 participants. Error bars denote the combined uncertainty $u_c(w(\text{Co}))$ for a coverage factor of $k = 1$ as reported. All results reported as measured against Co-A under the assumption of $w(\text{Co}) = 1 \text{ g/kg} \pm 0 \text{ g/kg}$ were converted using the actual value (KCRV) of Co-A (appendix F).

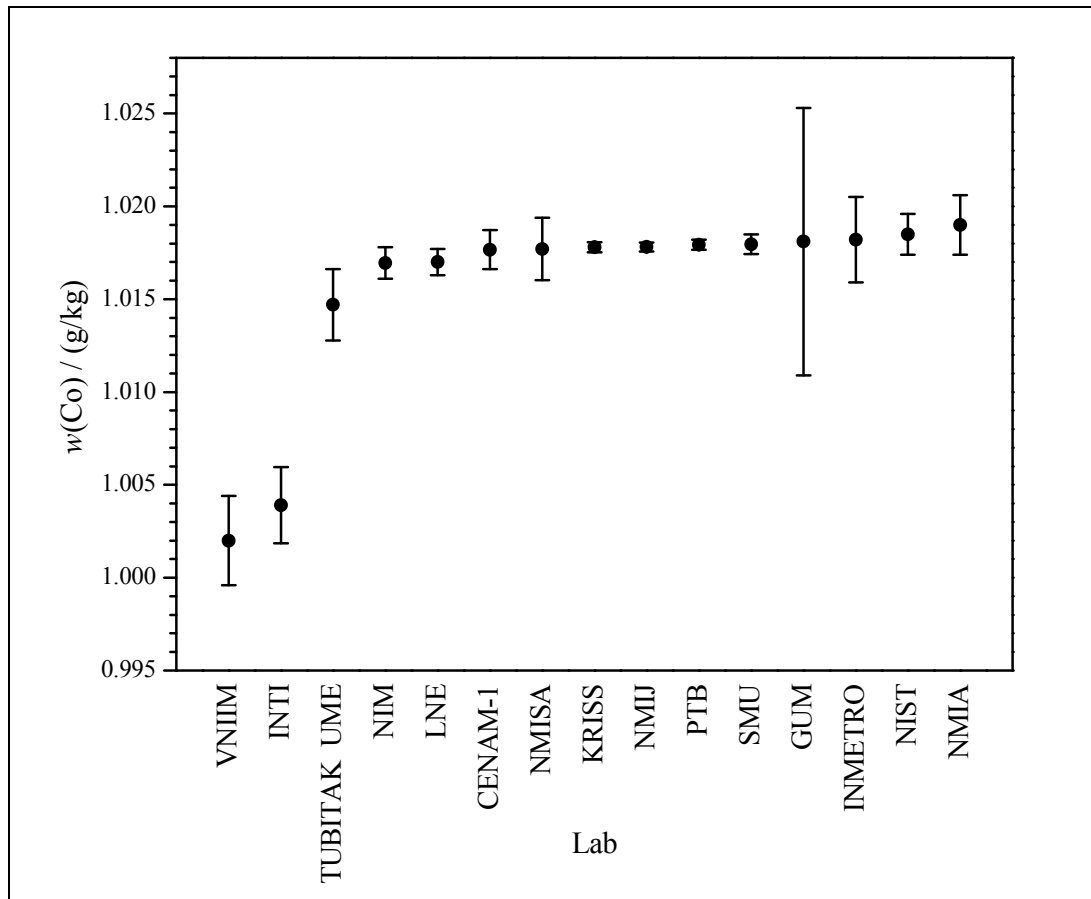


Figure 8: Cobalt mass fraction $w(\text{Co})$ in sample **Co-C** as reported by the CCQM-K87 participants. Error bars denote the combined uncertainty $u_c(w(\text{Co}))$ for a coverage factor of $k = 1$ as reported.

7.3 Lead samples

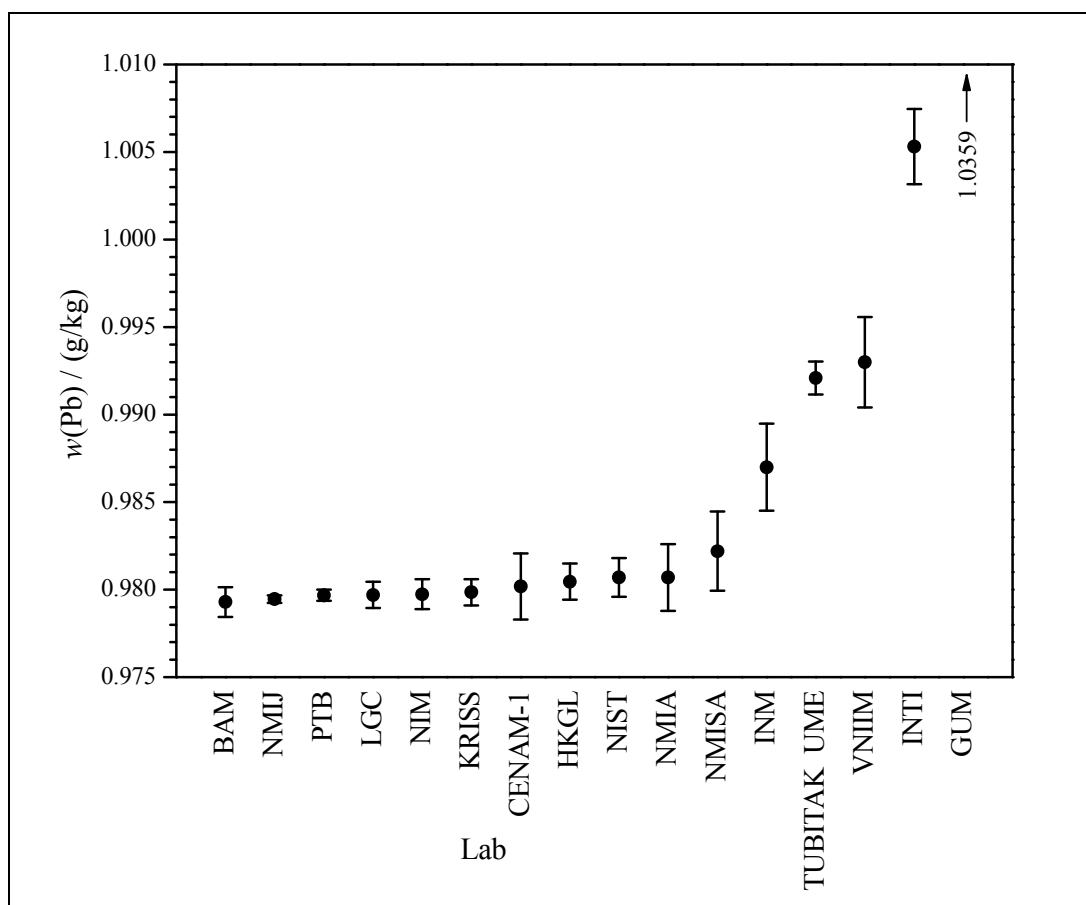


Figure 9: Lead mass fraction $w(\text{Pb})$ in sample **Pb-A** as reported by the CCQM-K87 participants. Error bars denote the combined uncertainty $u_c(w(\text{Pb}))$ for a coverage factor of $k = 1$ as reported. Results reported in terms of amount contents n/m converted in mass fractions w applying a molar mass of $M(\text{Pb}) = (207.17782 \pm 0.00011) \text{ g/mol}$ ($k = 2$), refer to section 2.3 for details.

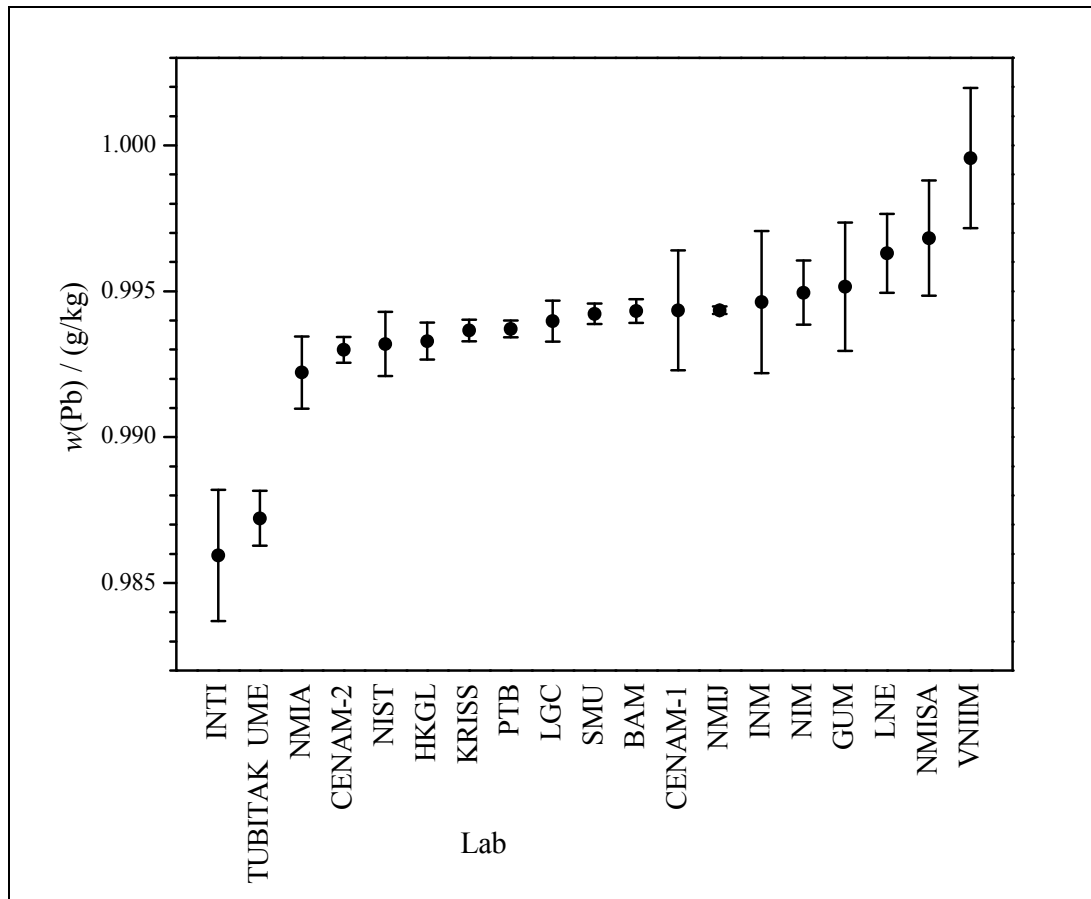


Figure 10: Lead mass fraction $w(\text{Pb})$ in sample **Pb-B** as reported by the CCQM-K87 participants. Error bars denote the combined uncertainty $u_c(w(\text{Pb}))$ for a coverage factor of $k = 1$ as reported. All results reported as measured against Pb-A under the assumption of $w(\text{Pb}) = 1 \text{ g/kg} \pm 0 \text{ g/kg}$ were converted using the actual value (KCRV) of Pb-A (appendix F). Results reported in terms of amount contents n/m converted in mass fractions w applying a molar mass of $M(\text{Pb}) = (207.17782 \pm 0.00011) \text{ g/mol}$ ($k = 2$), refer to section 2.3 for details.

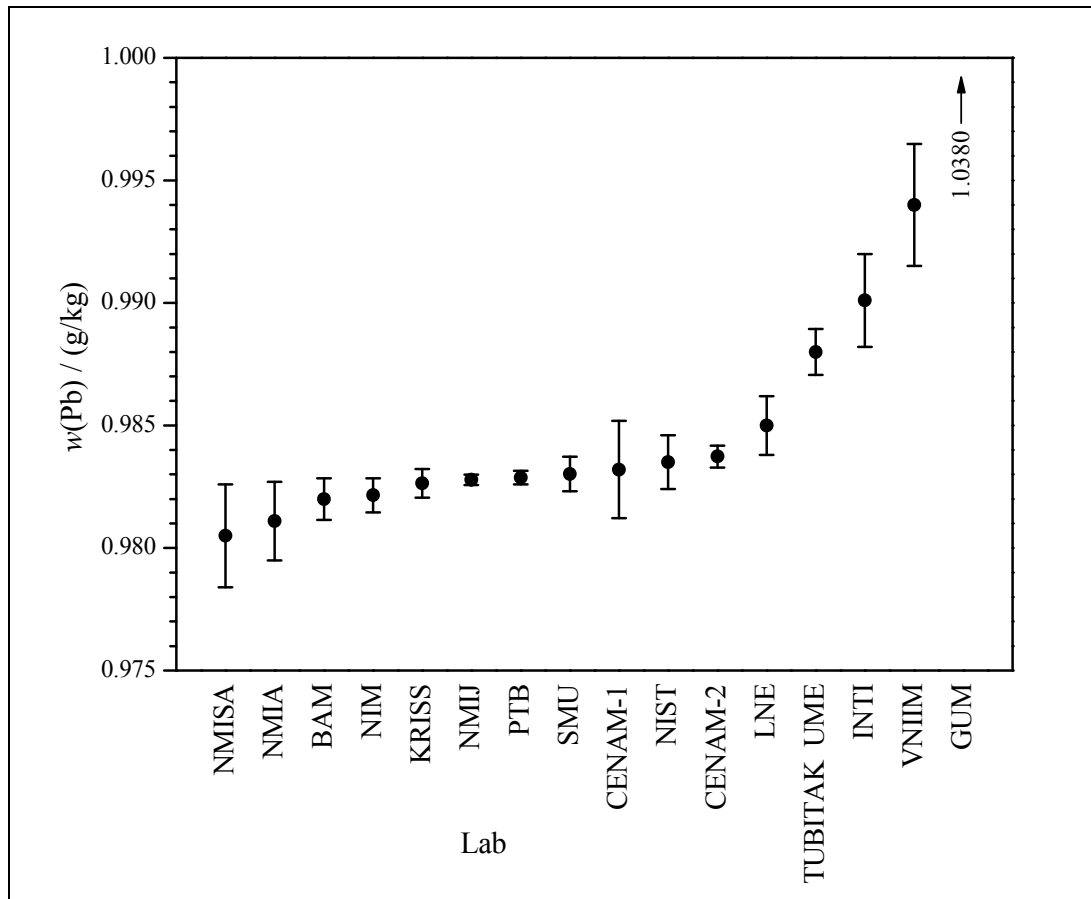


Figure 11: Lead mass fraction $w(\text{Pb})$ in sample **Pb-C** as reported by the CCQM-K87 participants. Error bars denote the combined uncertainty $u_c(w(\text{Pb}))$ for a coverage factor of $k = 1$ as reported. Results reported in terms of amount contents n/m converted in mass fractions w applying a molar mass of $M(\text{Pb}) = (207.17782 \pm 0.00011) \text{ g/mol}$ ($k = 2$), refer to section 2.3 for details.

7.4 Key comparison reference values

Since gravimetric reference values based on the sample preparation were available for all nine samples (section 3, summarized in table 11) it seemed reasonable to recommend these values as the key comparison reference values (KCRV) w_{KCRV} . This decision was agreed upon during the IAWG autumn meeting in Sydney 2011 [1]. Figures 12–20 show the participants results as well as their associated uncertainties along with the particular gravimetric KCRV.

7.4.1 Chromium

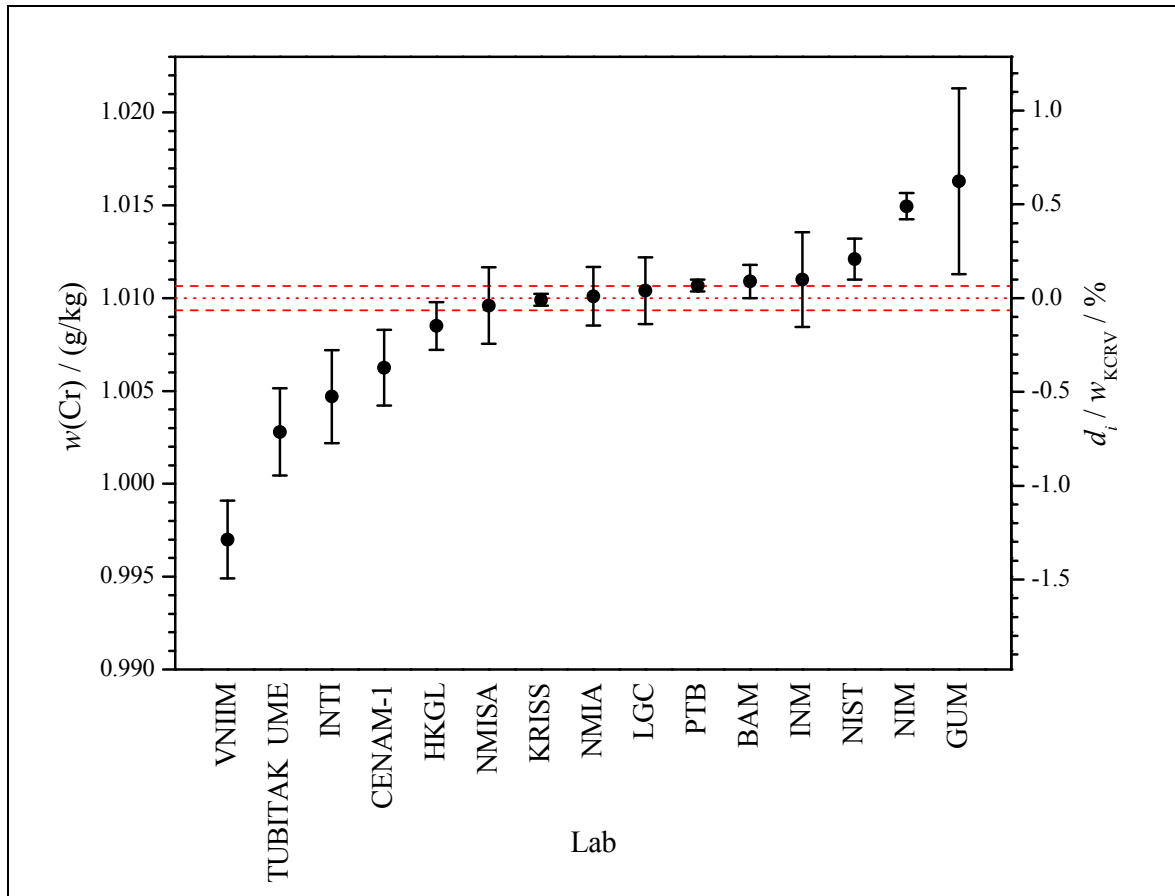


Figure 12: Chromium mass fraction $w(\text{Cr})$ in sample **Cr-A** as reported by the CCQM-K87 participants. Error bars denote the combined uncertainty $u_c(w(\text{Cr}))$ for a coverage factor of $k = 1$ as reported. The dotted red line shows the **gravimetric KCRV**: $w_{\text{KCRV}}(\text{Cr}) = 1.0100 \text{ g/kg}$. The dashed red lines indicate the range of the combined uncertainty $u_c(w_{\text{KCRV}}(\text{Cr}))$ associated with the KCRV. The right y-axis shows the degree of equivalence d_i relative to the KCRV (for more details see section 7.6).

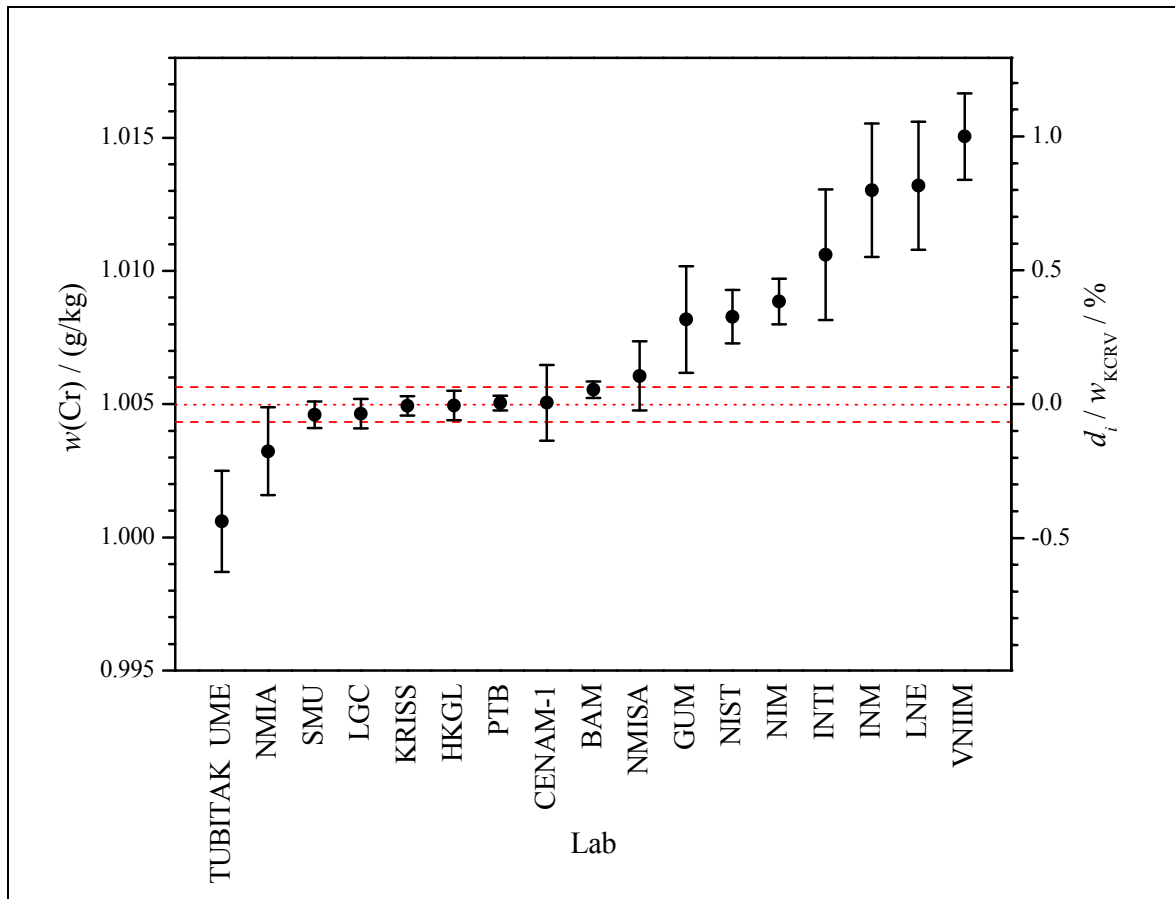


Figure 13: Chromium mass fraction $w(\text{Cr})$ in sample **Cr-B** as reported by the CCQM-K87 participants. All results reported as measured against Cr-A under the assumption of $w(\text{Cr}) = 1 \text{ g/kg} \pm 0 \text{ g/kg}$ were converted using the actual value (KCRV) of Cr-A (appendix F). Error bars denote the combined uncertainty $u_c(w(\text{Cr}))$ for a coverage factor of $k = 1$ as reported. The dotted red line shows the **gravimetric KCRV**: $w_{\text{KCRV}}(\text{Cr}) = 1.0050 \text{ g/kg}$. The dashed red lines indicate the range of the combined uncertainty $u_c(w_{\text{KCRV}}(\text{Cr}))$ associated with the KCRV. The right y-axis shows the degree of equivalence d_i relative to the KCRV (for more details see section 7.6).

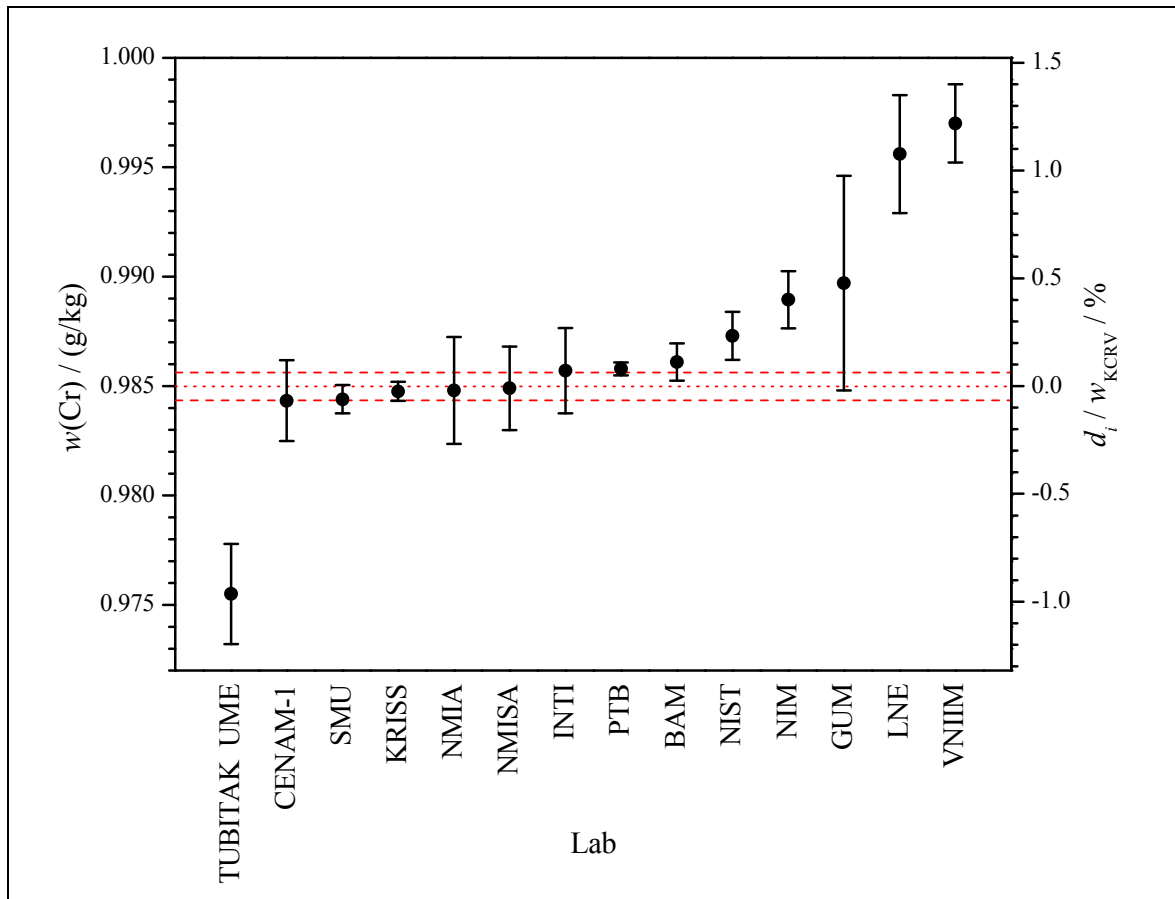


Figure 14: Chromium mass fraction $w(\text{Cr})$ in sample **Cr-C** as reported by the CCQM-K87 participants. Error bars denote the combined uncertainty $u_c(w(\text{Cr}))$ for a coverage factor of $k = 1$ as reported. The dotted red line shows the **gravimetric KCRV**: $w_{\text{KCRV}}(\text{Cr}) = 0.9850 \text{ g/kg}$. The dashed red lines indicate the range of the combined uncertainty $u_c(w_{\text{KCRV}}(\text{Cr}))$ associated with the KCRV. The right y-axis shows the degree of equivalence d_i relative to the KCRV (for more details see section 7.6).

7.4.2 Cobalt

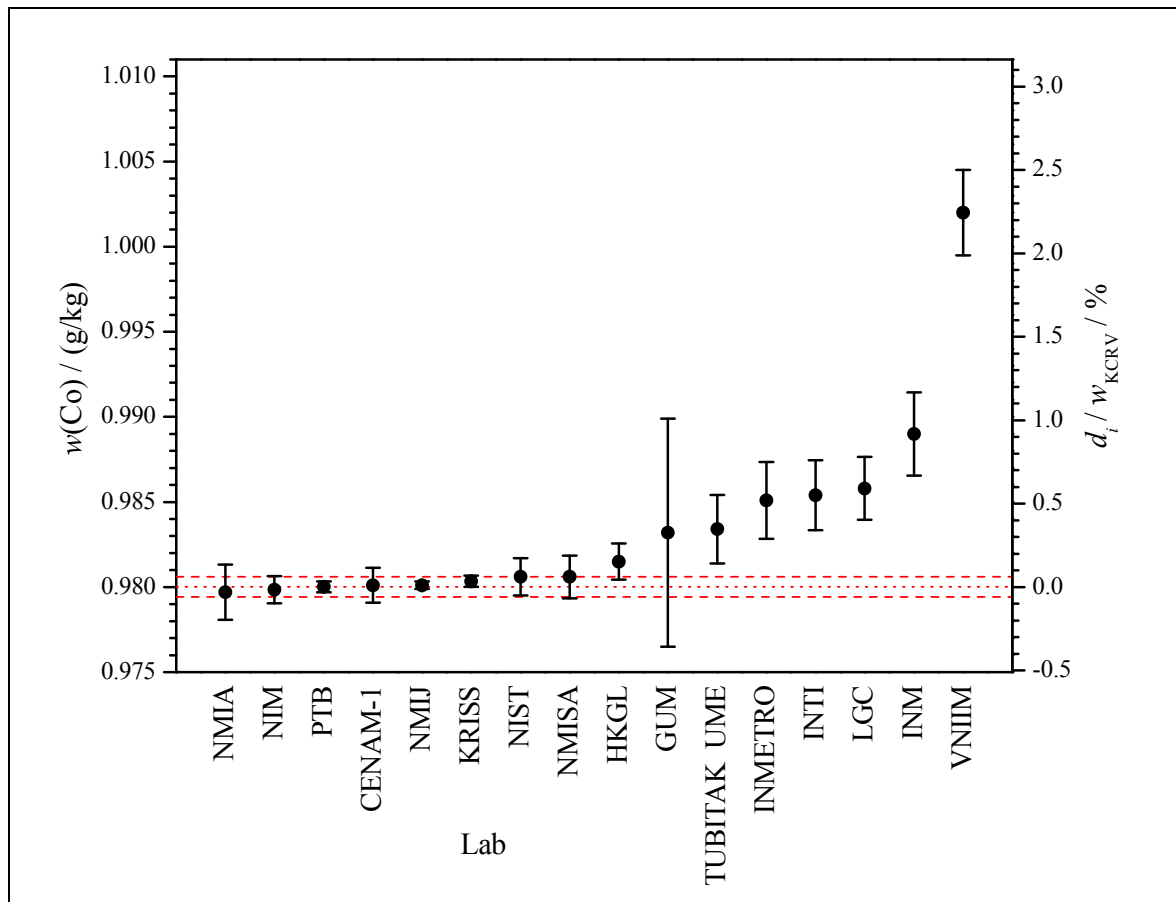


Figure 15: Cobalt mass fraction $w(\text{Co})$ in sample **Co-A** as reported by the CCQM-K87 participants. Error bars denote the combined uncertainty $u_c(w(\text{Co}))$ for a coverage factor of $k = 1$ as reported. The dotted red line shows the **gravimetric KCRV**: $w_{\text{KCRV}}(\text{Co}) = 0.9800 \text{ g/kg}$. The dashed red lines indicate the range of the combined uncertainty $u_c(w_{\text{KCRV}}(\text{Co}))$ associated with the KCRV. The right y-axis shows the degree of equivalence d_i relative to the KCRV (for more details see section 7.6).

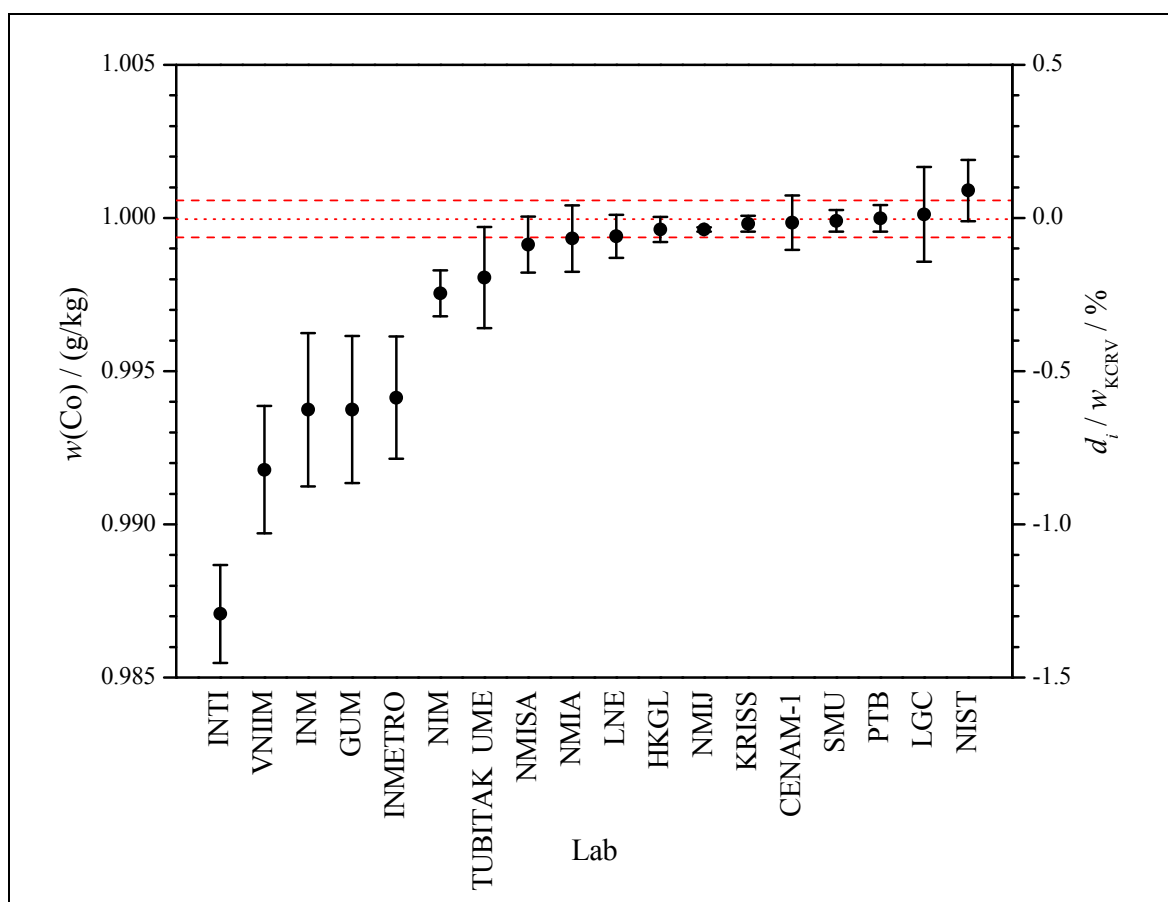


Figure 16: Cobalt mass fraction $w(\text{Co})$ in sample **Co-B** as reported by the CCQM-K87 participants. All results reported as measured against Co-A under the assumption of $w(\text{Co}) = 1 \text{ g/kg} \pm 0 \text{ g/kg}$ were converted using the actual value (KCRV) of Co-A (appendix F). Error bars denote the combined uncertainty $u_c(w(\text{Co}))$ for a coverage factor of $k = 1$ as reported. The dotted red line shows the **gravimetric KCRV**: $w_{\text{KCRV}}(\text{Co}) = 1.0000 \text{ g/kg}$. The dashed red lines indicate the range of the combined uncertainty $u_c(w_{\text{KCRV}}(\text{Co}))$ associated with the KCRV. The right y-axis shows the degree of equivalence d_i relative to the KCRV (for more details see section 7.6).

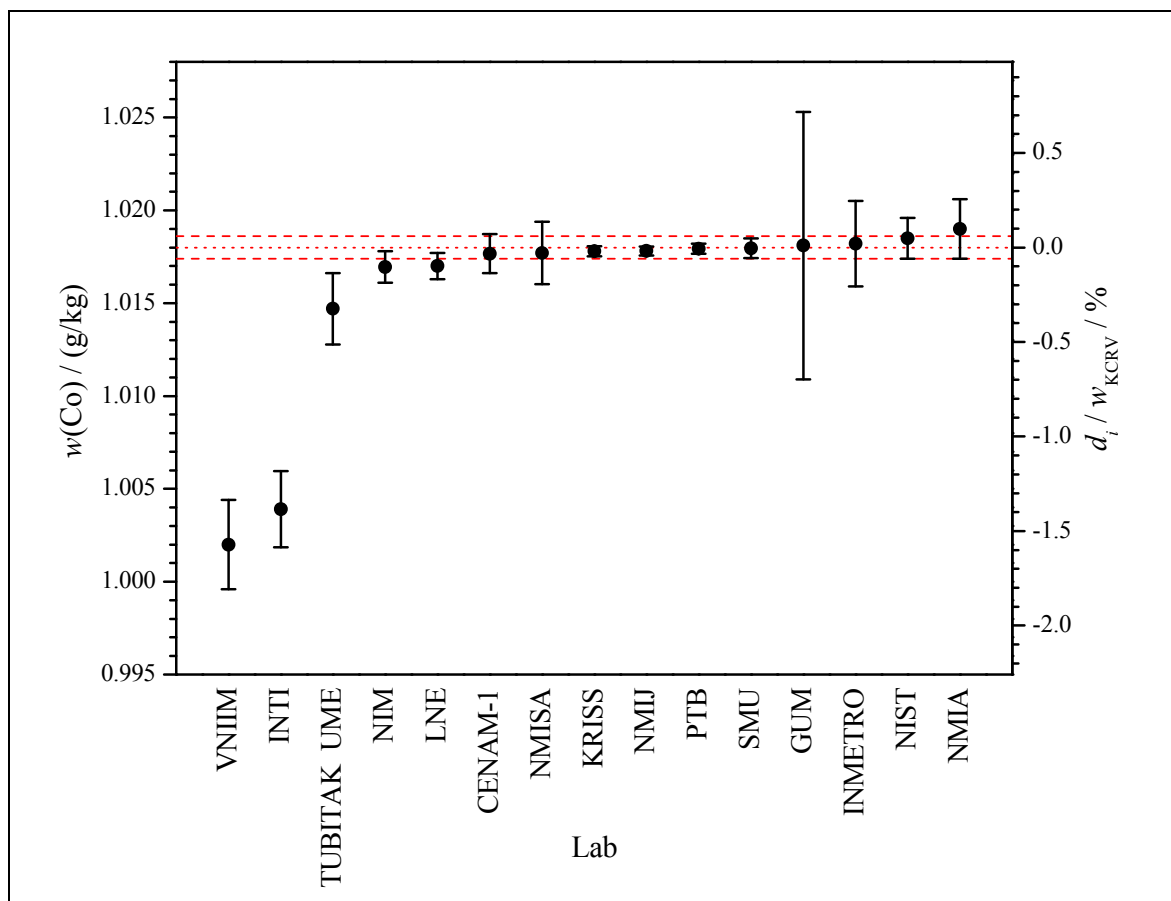


Figure 17: Cobalt mass fraction $w(\text{Co})$ in sample **Co-C** as reported by the CCQM-K87 participants. Error bars denote the combined uncertainty $u_c(w(\text{Co}))$ for a coverage factor of $k = 1$ as reported. The dotted red line shows the **gravimetric KCRV**: $w_{\text{KCRV}}(\text{Co}) = 1.0180 \text{ g/kg}$. The dashed red lines indicate the range of the combined uncertainty $u_c(w_{\text{KCRV}}(\text{Co}))$ associated with the KCRV. The right y-axis shows the degree of equivalence d_i relative to the KCRV (for more details see section 7.6).

7.4.3 Lead

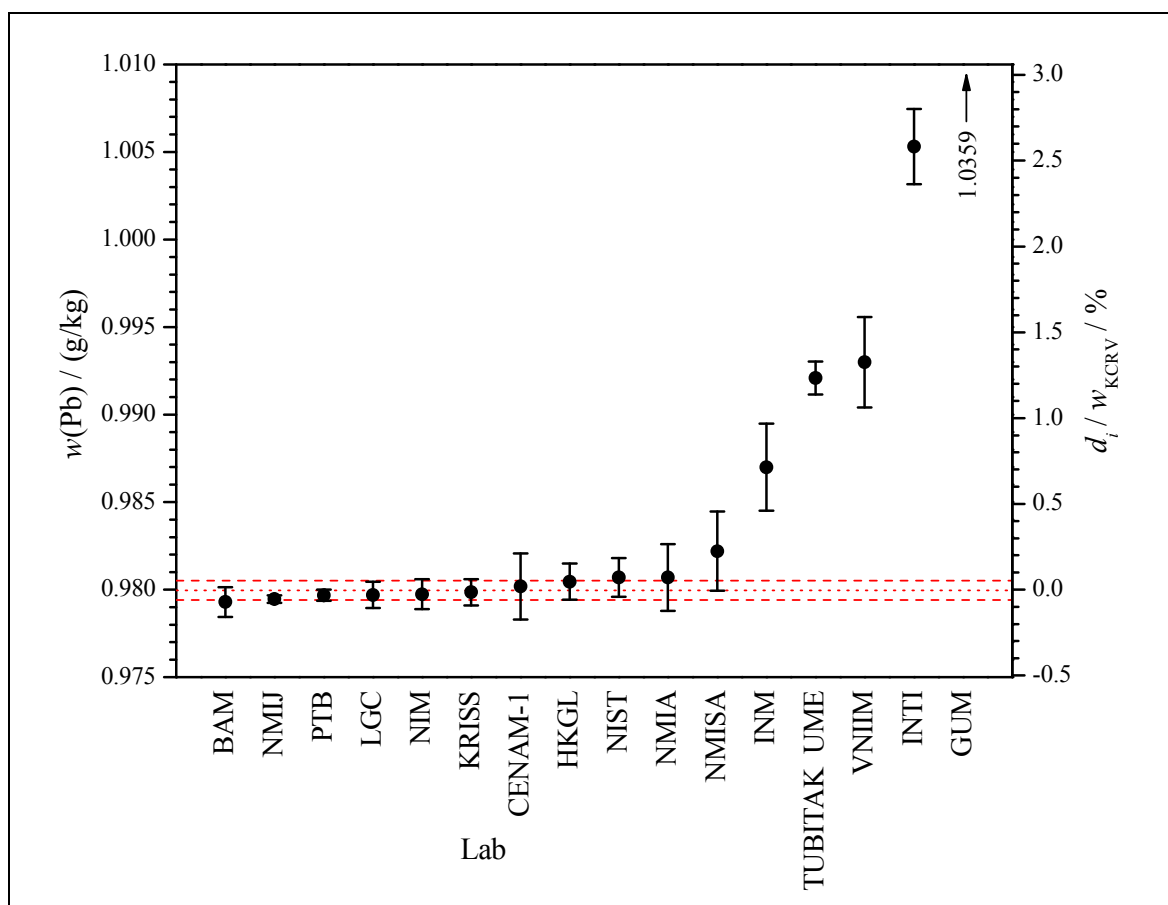


Figure 18: Lead mass fraction $w(\text{Pb})$ in sample **Pb-A** as reported by the CCQM-K87 participants. Results reported in terms of amount contents n/m converted in mass fractions w applying a molar mass of $M(\text{Pb}) = (207.17782 \pm 0.00011) \text{ g/mol}$ ($k = 2$), refer to section 2.3 for details. Error bars denote the combined uncertainty $u_c(w(\text{Pb}))$ for a coverage factor of $k = 1$ as reported. The dotted red line shows the **gravimetric KCRV**: $w_{\text{KCRV}}(\text{Pb}) = 0.9800 \text{ g/kg}$. The dashed red lines indicate the range of the combined uncertainty $u_c(w_{\text{KCRV}}(\text{Pb}))$ associated with the KCRV. The right y-axis shows the degree of equivalence d_i relative to the KCRV (for more details see section 7.6).

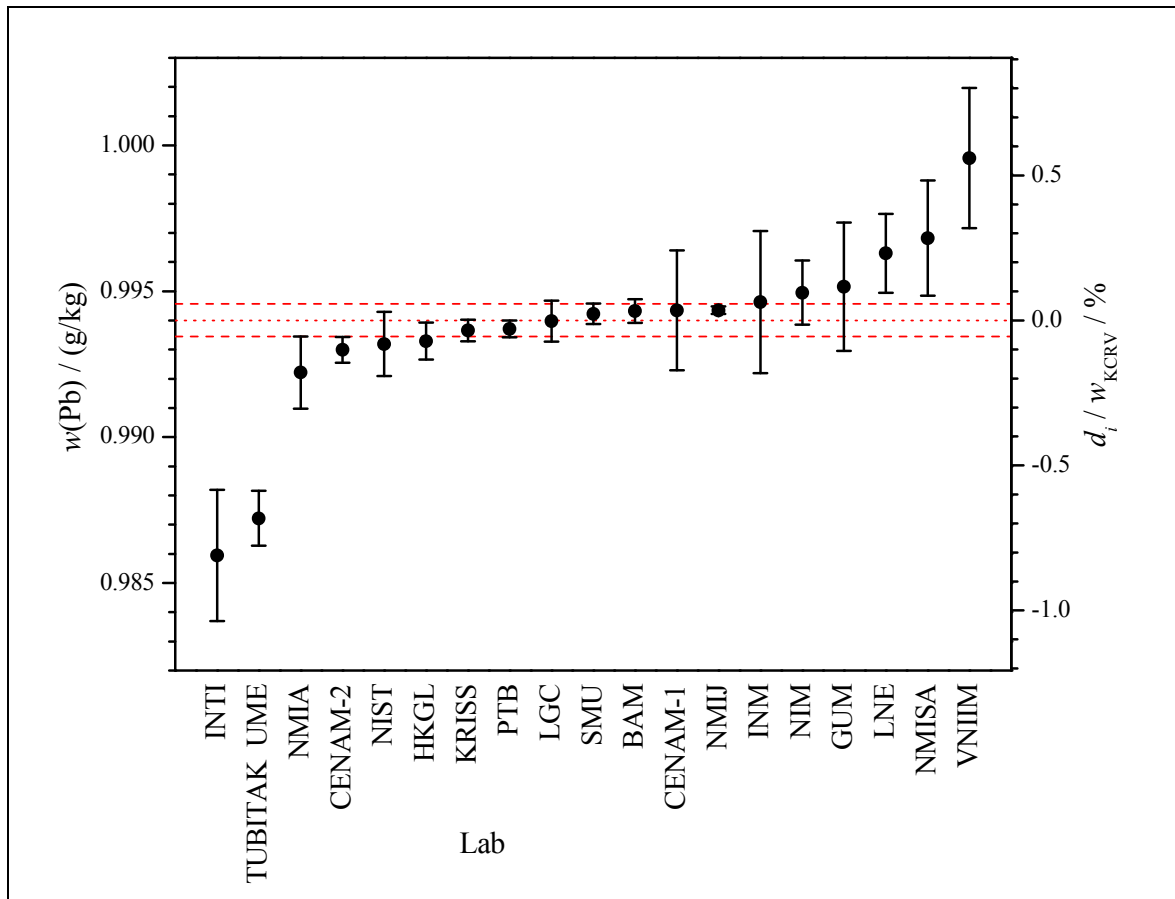


Figure 19: Lead mass fraction $w(\text{Pb})$ in sample **Pb-B** as reported by the CCQM-K87 participants. All results reported as measured against Pb-A under the assumption of $w(\text{Pb}) = 1 \text{ g/kg} \pm 0 \text{ g/kg}$ were converted using the actual value (KCRV) of Pb-A (appendix F). Results reported in terms of amount contents n/m converted in mass fractions w applying a molar mass of $M(\text{Pb}) = (207.17782 \pm 0.00011) \text{ g/mol}$ ($k = 2$), refer to section 2.3 for details. Error bars denote the combined uncertainty $u_c(w(\text{Pb}))$ for a coverage factor of $k = 1$ as reported. The dotted red line shows the **gravimetric KCRV**: $w_{\text{KCRV}}(\text{Pb}) = 0.9940 \text{ g/kg}$. The dashed red lines indicate the range of the combined uncertainty $u_c(w_{\text{KCRV}}(\text{Pb}))$ associated with the KCRV. The right y-axis shows the degree of equivalence d_i relative to the KCRV (for more details see section 7.6).

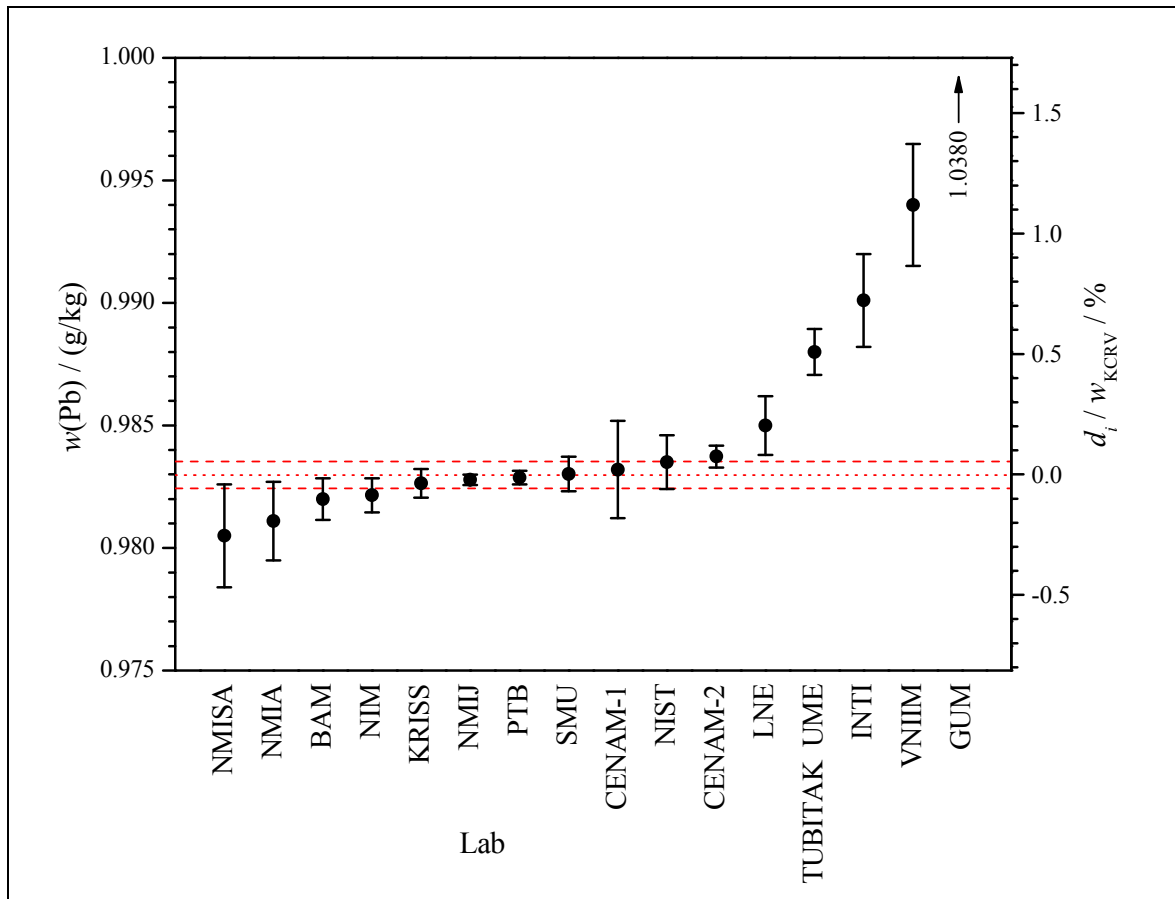


Figure 20: Lead mass fraction $w(\text{Pb})$ in sample **Pb-C** as reported by the CCQM-K87 participants. Results reported in terms of amount contents n/m converted in mass fractions w applying a molar mass of $M(\text{Pb}) = (207.17782 \pm 0.00011) \text{ g/mol}$ ($k = 2$), refer to section 2.3 for details. Error bars denote the combined uncertainty $u_c(w(\text{Pb}))$ for a coverage factor of $k = 1$ as reported. The dotted red line shows the **gravimetric KCRV**: $w_{\text{KCRV}}(\text{Pb}) = 0.9830 \text{ g/kg}$. The dashed red lines indicate the range of the combined uncertainty $u_c(w_{\text{KCRV}}(\text{Pb}))$ associated with the KCRV. The right y-axis shows the degree of equivalence d_i relative to the KCRV (for more details see section 7.6).

7.5 Additional KCRV estimators based on the participants' data

In case no independent reference values are available, usually location estimators basing on the participants' results are considered to be used as the KCRVs. For the sake of completeness three most common of these consensus values will be calculated and discussed here. Following a systematic approach proposed in [8], first the data sets were checked for outliers. The Dixon test was chosen because of its suitability for small data sets [9-13]. The lower and upper limit criteria were calculated from the reported data (table 18–26) considering the respective total numbers of participants N . These limit criteria were compared to the particular allowed limits. All data sets except for those of sample Cr-A and Cr-B showed evidence indicating the presence of outliers (table 15).

Table 15: Results of Dixon test [9-13] applied to all data sets (E = element; N = number of participants; red numbers = indicating the possible presence of outliers).

E	type of solution	N	calculated limit criteria		Dixon	
			lower	upper	allowed limit	outlier(s)
Cr	A	15	0.510	0.362	0.525	no
	B	17	0.322	0.193	0.490	no
	C	14	0.627	0.579	0.546	yes
Co	A	16	0.052	0.737	0.507	yes
	B	18	0.516	0.127	0.475	yes
	C	15	0.784	0.186	0.525	yes
Pb	A	16	0.028	0.763	0.507	yes
	B	19	0.606	0.444	0.462	yes
	C	16	0.156	0.855	0.507	yes

Subsequently the data sets were checked for consistency using the chi-squared test proposed in [8]. The uncertainty weighted means \bar{w}_u were calculated according to eq. (12)

$$\bar{w}_u = \frac{\sum_{i=1}^N \frac{w_i}{u^2(w_i)}}{\sum_{i=1}^N \frac{1}{u^2(w_i)}} \quad (12)$$

yielding chi-squared χ_{obs}^2 according to eq. (13)

$$\chi_{\text{obs}}^2 = \sum_{i=1}^N \left(\frac{w_i - \bar{w}_u}{u(w_i)} \right)^2 \quad (13)$$

In case the 95 percentile of χ^2 with $N-1$ degrees of freedom $\chi_{0.05, N-1}^2$ (from [13]) is smaller than χ_{obs}^2 the respective data set should be considered mutually inconsistent [8]. Please note that the number of participants N in case of samples Pb-B and Pb-C (table 16) is not equal to the numbers found in table 15 because the data of CENAM-2 were excluded from the calculation of χ_{obs}^2 complying with the agreements of the IAWG Sydney meeting [1] allowing more

than one result to be reported in a key comparison but allowing only one of these to be included in a (potential) KCRV estimator. All nine data sets did not pass the chi-squared test (table 16). This finding renders any KCRV estimator based on the participants' results questionable considering the availability of a gravimetric reference value.

Table 16: Results of chi-squared test [8] applied to all data sets (E = element, N = number of participants). Values rounded to yield integer numbers.

E	type of solution	N	χ_{obs}^2	$\chi_{0.05, N-1}^2$	mutually consistent?
Cr	A	15	113	24	no
	B	17	103	26	no
	C	14	92	22	no
Co	A	16	113	25	no
	B	18	107	28	no
	C	15	95	24	no
Pb	A	16	404	25	no
	B	18	90	28	no
	C	15	116	24	no

Nevertheless the uncertainty weighted mean \bar{w}_u (eq. (12)) as well as the arithmetic mean \bar{w} (eq. (14)) and the median \bar{w}_m (eq. (15)) were calculated along with their associated uncertainties $u(\bar{w}_u)$, $u(\bar{w})$ and $u(\bar{w}_m)$ (equations 17–19).

$$\bar{w} = \frac{1}{N} \sum_{i=1}^N w_i \quad (14)$$

$$\bar{w}_m = \frac{1}{2} (w_{N/2} + w_{N/2+1}) \quad N \text{ even} \quad (15)$$

$$\bar{w}_m = w_{(N+1)/2} \quad N \text{ odd} \quad (16)$$

Due to the observed mutual inconsistency of all data sets the uncertainty $u(\bar{w}_u)$ associated with the uncertainty weighted mean was corrected for the observed dispersion according to [8].

$$u(\bar{w}_u) = \sqrt{\frac{\chi_{\text{obs}}^2}{N-1} \left(\sum_{i=1}^N \frac{1}{u^2(w_i)} \right)^{-1}} \quad (17)$$

$$u(\bar{w}) = \sqrt{\frac{1}{N \cdot (N-1)} \sum_{i=1}^N (w_i - \bar{w})^2} \quad (18)$$

$$u(\bar{w}_m) = \sqrt{\frac{\pi}{2N}} \cdot 1.483 \cdot \text{med}(|w_i - \bar{w}_m|) \quad (19)$$

Please note that when carrying out eq. (15) and (16), respectively, the participants' results w_i have to be arranged in the order of increasing values, while when carrying out equation (19) the absolute deviations of the participants' results from the median $|w_i - \bar{w}_m|$ have to be arranged in the order of increasing values.

Table 17 compares the gravimetric KCRV to the uncertainty weighted and the arithmetic mean as well as the median according to equations (12)–(19). In order to discuss the additional consensus estimators their deviations d_i from the gravimetric KCRV and the uncertainties associated with these deviations were calculated similar to the calculation of the degrees of equivalence (section 7.6) and plotted (figures 21–23). Within the limits of uncertainty no significant differences were observed between the gravimetric KCRVs and the consensus estimators as well as among the consensus estimators except for the arithmetic means of Co-A and Co-B. In principal the median and the uncertainty weighted means are in contrast to the arithmetic means in excellent agreement with the gravimetric KCRVs. The relative deviations of all consensus estimators from the respective KCRVs was calculated to illustrate this (eq. (20) and table 17).

$$\Delta_{\text{rel}}w = \frac{|d_i|}{w_{\text{KCRV}}} \quad (20)$$

Table 17: Compilation of the gravimetric KCRVs w_{KCRV} and three additional consensus KCRV estimators. The associated expanded uncertainties were calculated using a coverage factor of $k = 2$ according to $U(w_i) = k \cdot u_c(w_i)$. Numbers were rounded to the number of digits of the uncertainty of the KCRVs. Degrees of equivalence d_i (section 7.6) were calculated and graphs were drawn using all available digits without rounding. For more information refer to the text above and figures 21–23. (UWM = uncertainty weighted mean, M = median, AM = arithmetic mean, E = element, t = type of solution, i = type of estimator).

E	t	i	$w_i(\text{E})$	d_i	$U(d_i)$	$d_i/U(d_i)$	$\Delta_{\text{rel}}w$
			g/kg	g/kg	g/kg	1	%
Cr	A	KCRV	1.0100	0.0000			0.00
		M	1.0101	0.0001	0.0020	0.0501	0.01
		AM	1.0090	-0.0010	0.0028	0.3521	0.10
		UWM	1.0105	0.0005	0.0017	0.2662	0.05
Cr	B	KCRV	1.0050	0.0000			0.00
		M	1.0055	0.0006	0.0025	0.2292	0.06
		AM	1.0072	0.0022	0.0023	0.9516	0.22
		UWM	1.0054	0.0004	0.0015	0.2732	0.04
Cr	C	KCRV	0.9850	0.0000			0.00
		M	0.9857	0.0008	0.0019	0.4067	0.08
		AM	0.9868	0.0018	0.0030	0.5880	0.18
		UWM	0.9857	0.0007	0.0017	0.4045	0.07
Co	A	KCRV	0.9800	0.0000			0.00
		M	0.9811	0.0010	0.0017	0.6123	0.10
		AM	0.9835	0.0035	0.0031	1.1511	0.36
		UWM	0.9804	0.0004	0.0014	0.2484	0.04

E	t	i	$w_i(\mathbf{E})$ g/kg	d_i g/kg	$U(d_i)$ g/kg	$d_i/U(d_i)$ 1	$\Delta_{\text{rel}}w$ %
Co	B	KCRV	1.0000	0.0000			0.00
		M	0.9994	-0.0006	0.0013	0.4489	0.06
		AM	0.9974	-0.0025	0.0021	1.1837	0.25
		UWM	0.9996	-0.0004	0.0012	0.2979	0.04
Co	C	KCRV	1.0180	0.0000			0.00
		M	1.0178	-0.0002	0.0013	0.1546	0.02
		AM	1.0157	-0.0023	0.0030	0.7771	0.23
		UWM	1.0177	-0.0003	0.0014	0.2204	0.03
Pb	A	KCRV	0.9800	0.0000			0.00
		M	0.9806	0.0006	0.0014	0.4263	0.06
		AM	0.9872	0.0072	0.0075	0.9649	0.74
		UWM	0.9802	0.0002	0.0019	0.1186	0.02
Pb	B	KCRV	0.9940	0.0000			0.00
		M	0.9943	0.0003	0.0013	0.2070	0.03
		AM	0.9938	-0.0002	0.0018	0.1269	0.02
		UWM	0.9941	0.0001	0.0012	0.0778	0.01
Pb	C	KCRV	0.9830	0.0000			0.00
		M	0.9830	0.0000	0.0015	0.0237	0.00
		AM	0.9879	0.0049	0.0075	0.6607	0.50
		UWM	0.9830	0.0000	0.0014	0.0174	0.00

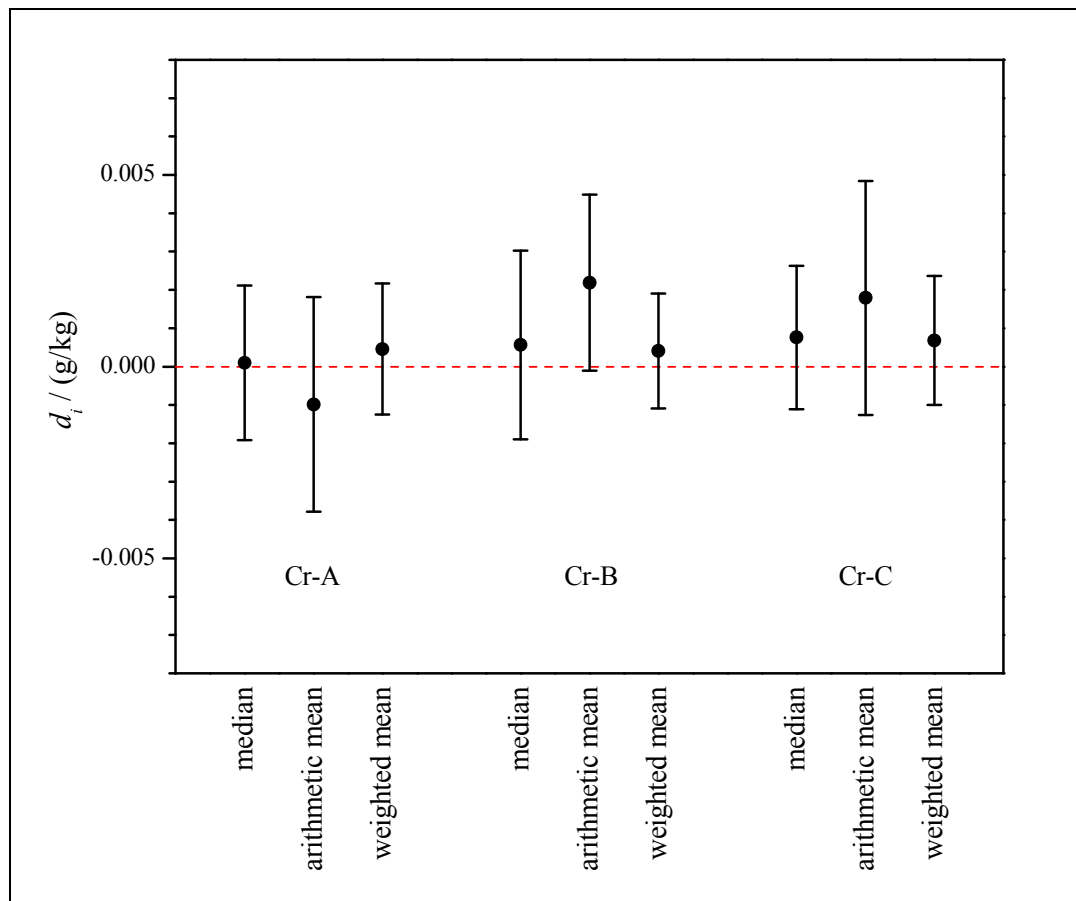


Figure 21: Chromium samples. Deviation d_i of the medians, arithmetic means, and uncertainty weighted means from the gravimetric KCRVs along with the expanded uncertainties associated with these deviations; d_i calculated similar to degrees of equivalence (section 7.6). The dashed red line indicates the relative location of the gravimetric KCRVs. Within the limits of uncertainty no significant differences between the estimators were observed. Medians and uncertainty weighted means are in excellent agreement with the KCRVs.

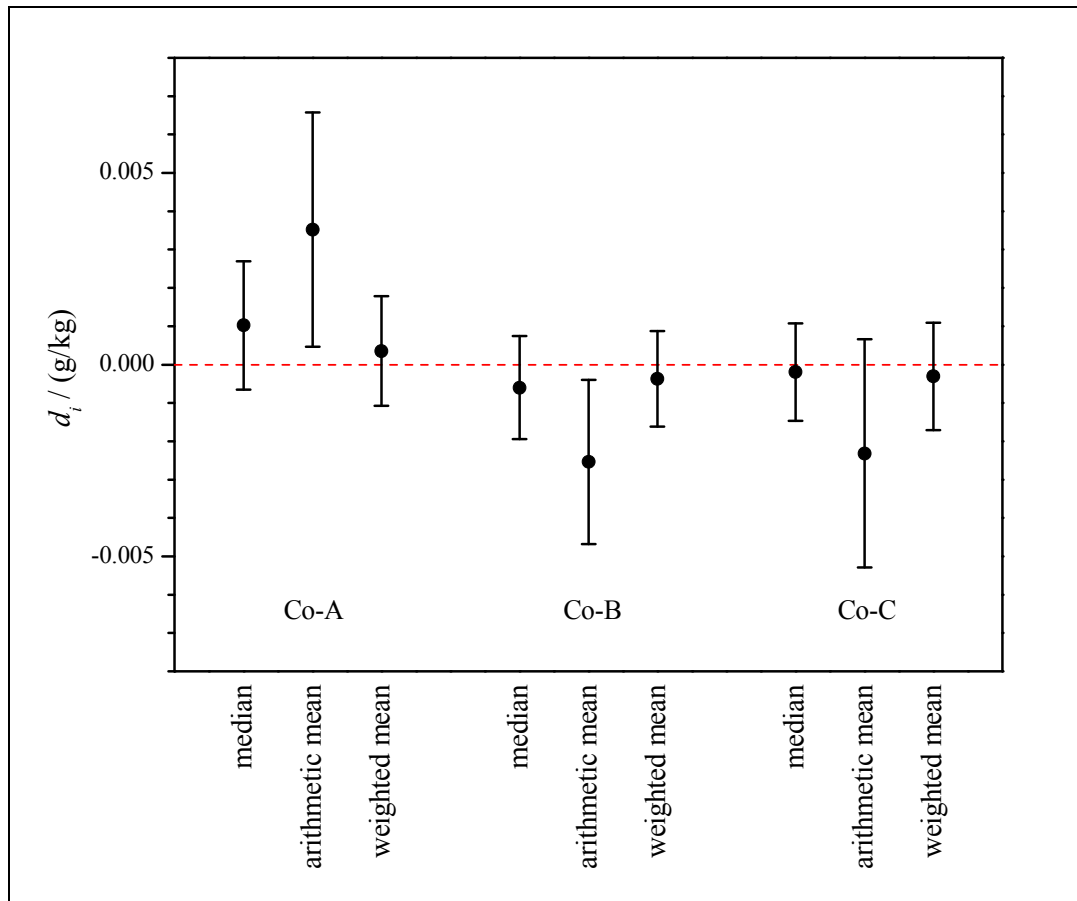


Figure 22: Cobalt samples. Deviation d_i of the medians, arithmetic means, and uncertainty weighted means from the gravimetric KCRVs along with the expanded uncertainties associated with these deviations; d_i calculated similar to degrees of equivalence (section 7.6). The dashed red line indicates the relative location of the gravimetric KCRVs. Within the limits of uncertainty no significant differences between the estimators were observed. Medians and uncertainty weighted means are in excellent agreement with the KCRVs.

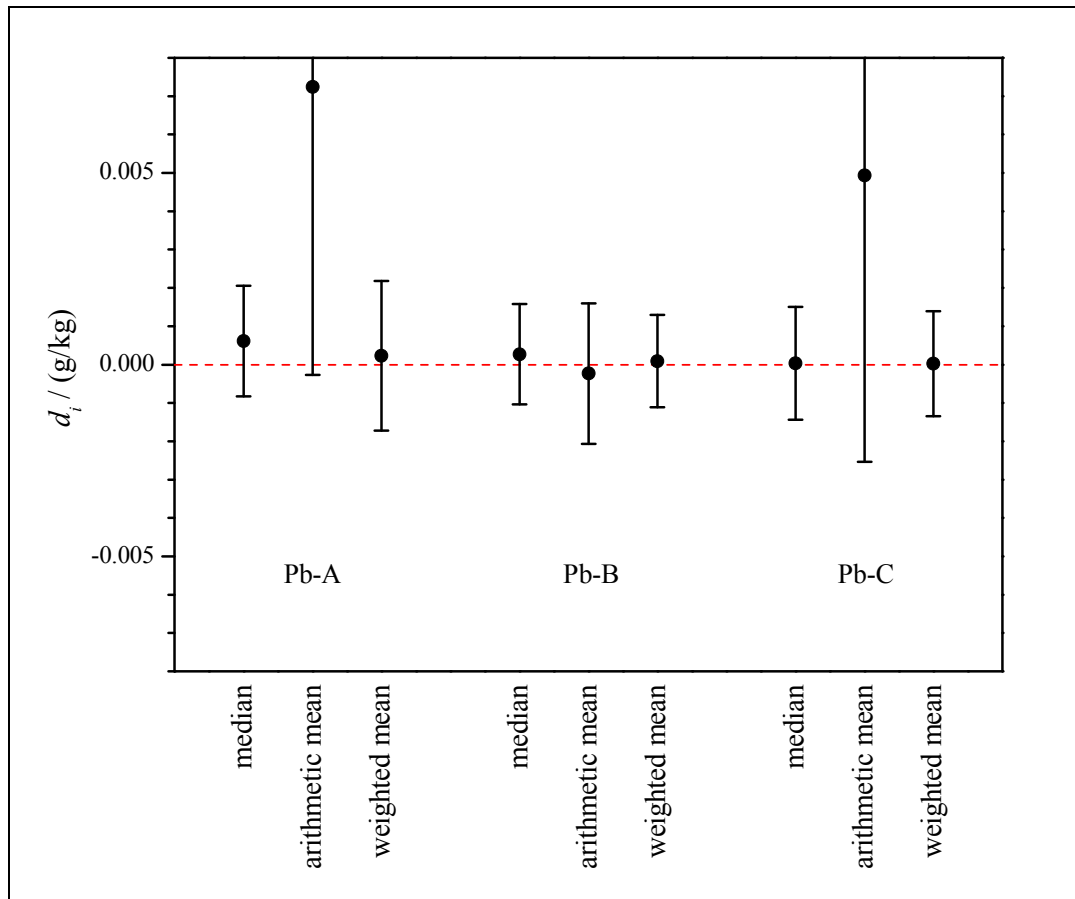


Figure 23: Lead samples. Deviation d_i of the medians, arithmetic means, and uncertainty weighted means from the gravimetric KCRVs along with the expanded uncertainties associated with these deviations; d_i calculated similar to degrees of equivalence (section 7.6). The dashed red line indicates the relative location of the gravimetric KCRVs. Within the limits of uncertainty no significant differences between the estimators were observed. Medians and uncertainty weighted means are in excellent agreement with the KCRVs.

7.6 Degrees of equivalence d_i

The degree of equivalence d_i (DoE) of an individual NMI result w_i and the *key comparison reference value* w_{KCRV} as well as the uncertainty $u(d_i)$ associated with d_i was calculated following [8,14] according to equations (21) and (22). The results were summarized in tables 18–26 and plotted in figures 24–32.

$$d_i = w_i - w_{\text{KCRV}} \quad (21)$$

$$u(d_i) = \sqrt{u^2(w_i) + u^2(w_{\text{KCRV}})} \quad (22)$$

Even though the technical protocol (appendix A) recommended to determine the element contents with a maximum relative expanded uncertainty of $U_{\text{rel,max}}(w) \leq 0.5\%$ the uncertainty $u(d_i)$ associated with d_i was calculated with the actual uncertainty reported also in cases the uncertainty reported exceeded the recommended limit.

Table 18: Chromium sample **Cr-A**. Mass fractions $w_i(\text{Cr})$ and their associated combined and relative expanded uncertainties $u_c(w_i)$ and $U_{\text{rel}}(w_i)$, resp., together with the coverage factor k_i as reported by the participants in the order of increasing mass fraction values. In case only expanded or relative combined uncertainties were reported the values compiled were calculated accordingly. Degrees of equivalence d_i and their associated combined and expanded uncertainty $u(d_i)$ and $U(d_i)$, resp., according to equation (21) and (22). A coverage factor of $k = 2$ was used to calculate $U(d_i) = k \cdot u(d_i)$.

Cr-A							
$w_{\text{KCRV}}(\text{Cr}) = (1.0100 \pm 0.0013) \text{ g/kg}$							
NMI	$w_i(\text{Cr})$	$u_c(w_i)$	k_i	$U_{\text{rel}}(w_i)$	d_i	$u(d_i)$	$U(d_i)$
	g/kg	g/kg	1	%	g/kg	g/kg	g/kg
VNIIM	0.997	0.00209	2	0.42	-0.01300	0.0022	0.0044
TUBITAK UME	1.0028	0.00236	2	0.47	-0.00720	0.0024	0.0049
INTI	1.0047	0.00250	2	0.50	-0.00530	0.0026	0.0052
CENAM-1	1.0063	0.00203	2	0.40	-0.00374	0.0021	0.0043
HKGL	1.0085	0.00129	2.11	0.27	-0.00150	0.0014	0.0029
NMISA	1.0096	0.00206	1.99	0.41	-0.00040	0.0022	0.0043
KRISS	1.00991	0.00031	2.57	0.08	-0.00009	0.0007	0.0014
NMIA	1.0101	0.00157	2.10	0.33	0.00010	0.0017	0.0034
LGC	1.0104	0.00180	2	0.36	0.00040	0.0019	0.0038
PTB	1.01068	0.00033	2	0.06	0.00068	0.0007	0.0015
BAM	1.0109	0.00090	2	0.18	0.00090	0.0011	0.0022
INM	1.0110	0.00255	2	0.50	0.00100	0.0026	0.0053
NIST	1.0121	0.00110	2.045	0.22	0.00210	0.0013	0.0026
NIM	1.0150	0.00070	2	0.14	0.00495	0.0010	0.0019
GUM	1.0163	0.00500	2	0.98	0.00630	0.0050	0.0101

Table 19: Chromium sample **Cr-B**. Mass fractions $w_i(\text{Cr})$ and their associated combined and relative expanded uncertainties $u_c(w_i)$ and $U_{\text{rel}}(w_i)$, resp., together with the coverage factor k_i as reported by the participants in the order of increasing mass fraction values. All results reported as measured against Cr-A under the assumption of $w(\text{Cr}) = 1 \text{ g/kg} \pm 0 \text{ g/kg}$ were converted using the actual value (KCRV) of Cr-A (appendix F). In case only expanded or relative combined uncertainties were reported the values compiled were calculated accordingly. Degrees of equivalence d_i and their associated combined and expanded uncertainty $u(d_i)$ and $U(d_i)$, resp., according to equation (21) and (22). A coverage factor of $k = 2$ was used to calculate $U(d_i) = k \cdot u(d_i)$.

Cr-B							
$w_{\text{KCRV}}(\text{Cr}) = (1.0050 \pm 0.0013) \text{ g/kg}$							
NMI	$w_i(\text{Cr})$ g/kg	$u_c(w_i)$ g/kg	k_i 1	$U_{\text{rel}}(w_i)$ %	d_i g/kg	$u(d_i)$ g/kg	$U(d_i)$ g/kg
TUBITAK UME	1.0006	0.00190	2	0.38	-0.00438	0.0020	0.0040
NMIA	1.0032	0.00165	2.36	0.39	-0.00175	0.0018	0.0036
SMU	1.0046	0.00050	2	0.10	-0.00038	0.0008	0.0016
LGC	1.0046	0.00055	2	0.11	-0.00034	0.0009	0.0017
KRISS	1.0049	0.00036	2.45	0.09	-0.00004	0.0007	0.0015
HKGL	1.0049	0.00055	2.36	0.13	-0.00003	0.0009	0.0017
PTB	1.0050	0.00028	2	0.05	0.00006	0.0007	0.0014
CENAM-1	1.0051	0.00142	2	0.28	0.00007	0.0016	0.0031
BAM	1.0055	0.00031	2	0.06	0.00056	0.0007	0.0014
NMISA	1.0061	0.00130	2.00	0.26	0.00108	0.0015	0.0029
GUM	1.0082	0.00200	2	0.40	0.00320	0.0021	0.0042
NIST	1.0083	0.00100	2.052	0.21	0.00330	0.0012	0.0024
NIM	1.0089	0.00085	2	0.17	0.00387	0.0011	0.0021
INTI	1.0106	0.00245	2	0.48	0.00562	0.0025	0.0051
INM	1.0130	0.00250	2	0.49	0.00805	0.0026	0.0052
LNE	1.0132	0.00240	2	0.47	0.00822	0.0025	0.0050
VNIIM	1.0150	0.00162	2	0.32	0.01007	0.0017	0.0035

Table 20: Chromium sample **Cr-C**. Mass fractions $w_i(\text{Cr})$ and their associated combined and relative expanded uncertainties $u_c(w_i)$ and $U_{\text{rel}}(w_i)$, resp., together with the coverage factor k_i as reported by the participants in the order of increasing mass fraction values. In case only expanded or relative combined uncertainties were reported the values compiled were calculated accordingly. Degrees of equivalence d_i and their associated combined and expanded uncertainty $u(d_i)$ and $U(d_i)$, resp., according to equation (21) and (22). A coverage factor of $k = 2$ was used to calculate $U(d_i) = k \cdot u(d_i)$.

Cr-C							
$w_{\text{KCRV}}(\text{Cr}) = (0.9850 \pm 0.0013) \text{ g/kg}$							
NMI	$w_i(\text{Cr})$	$u_c(w_i)$	k_i	$U_{\text{rel}}(w_i)$	d_i	$u(d_i)$	$U(d_i)$
	g/kg	g/kg	1	%	g/kg	g/kg	g/kg
TUBITAK UME	0.9755	0.00229	2	0.47	-0.00948	0.0024	0.0048
CENAM-1	0.9843	0.00184	2	0.37	-0.00064	0.0019	0.0039
SMU	0.9844	0.00065	2	0.13	-0.00058	0.0009	0.0018
KRISS	0.98476	0.00044	2.78	0.12	-0.00022	0.0008	0.0016
NMIA	0.9848	0.00244	2.01	0.50	-0.00018	0.0025	0.0050
NMISA	0.9849	0.00191	1.99	0.39	-0.00008	0.0020	0.0040
INTI	0.9857	0.00195	2	0.40	0.00072	0.0021	0.0041
PTB	0.98578	0.00030	2	0.06	0.00080	0.0007	0.0014
BAM	0.9861	0.00085	2	0.17	0.00112	0.0011	0.0021
NIST	0.9873	0.00110	2.042	0.22	0.00232	0.0013	0.0025
NIM	0.9889	0.00130	2	0.26	0.00397	0.0014	0.0029
GUM	0.9897	0.00490	2	0.99	0.00472	0.0049	0.0099
LNE	0.9956	0.00270	2	0.54	0.01062	0.0028	0.0055
VNIIM	0.997	0.00179	2	0.36	0.01202	0.0019	0.0038

Table 21: Cobalt sample **Co-A**. Mass fractions $w_i(\text{Co})$ and their associated combined and relative expanded uncertainties $u_c(w_i)$ and $U_{\text{rel}}(w_i)$, resp., together with the coverage factor k_i as reported by the participants in the order of increasing mass fraction values. In case only expanded or relative combined uncertainties were reported the values compiled were calculated accordingly. Degrees of equivalence d_i and their associated combined and expanded uncertainty $u(d_i)$ and $U(d_i)$, resp., according to equation (21) and (22). A coverage factor of $k = 2$ was used to calculate $U(d_i) = k \cdot u(d_i)$.

Co-A							
$w_{\text{KCRV}}(\text{Co}) = (0.9800 \pm 0.0012) \text{ g/kg}$							
NMI	$w_i(\text{Co})$	$u_c(w_i)$	k_i	$U_{\text{rel}}(w_i)$	d_i	$u(d_i)$	$U(d_i)$
	g/kg	g/kg	1	%	g/kg	g/kg	g/kg
NMIA	0.9797	0.00163	2.03	0.34	-0.00033	0.0017	0.0035
NIM	0.9798	0.00080	2	0.16	-0.00018	0.0010	0.0020
PTB	0.98002	0.00032	2	0.06	-0.00001	0.0007	0.0013
CENAM-1	0.9801	0.00103	2	0.21	0.00008	0.0012	0.0024
NMIJ	0.98011	0.00023	2	0.05	0.00008	0.0006	0.0013
KRISS	0.98034	0.00032	2.78	0.09	0.00031	0.0007	0.0013
NIST	0.9806	0.00110	2.042	0.22	0.00057	0.0012	0.0025
NMISA	0.9806	0.00126	1.99	0.25	0.00057	0.0014	0.0028
HKGL	0.9815	0.00107	2.2	0.24	0.00147	0.0012	0.0024
GUM	0.9832	0.00670	2	1.36	0.00317	0.0067	0.0135
TUBITAK UME	0.9834	0.00202	2	0.41	0.00337	0.0021	0.0042
INMETRO	0.9851	0.00225	2	0.46	0.00507	0.0023	0.0047
INTI	0.9854	0.00205	2	0.42	0.00537	0.0021	0.0043
LGC	0.9858	0.00185	2	0.38	0.00577	0.0019	0.0039
INM	0.9890	0.00245	2	0.50	0.00897	0.0025	0.0050
VNIIM	1.002	0.00251	2	0.50	0.02197	0.0026	0.0051

Table 22: Cobalt sample Co-B. Mass fractions $w_i(\text{Co})$ and their associated combined and relative expanded uncertainties $u_c(w_i)$ and $U_{\text{rel}}(w_i)$, resp., together with the coverage factor k_i as reported by the participants in the order of increasing mass fraction values. All results reported as measured against Co-A under the assumption of $w(\text{Co}) = 1 \text{ g/kg} \pm 0 \text{ g/kg}$ were converted using the actual value (KCRV) of Co-A (appendix F). In case only expanded or relative combined uncertainties were reported the values compiled were calculated accordingly. Degrees of equivalence d_i and their associated combined and expanded uncertainty $u(d_i)$ and $U(d_i)$, resp., according to equation (21) and (22). A coverage factor of $k = 2$ was used to calculate $U(d_i) = k \cdot u(d_i)$.

Co-B							
$w_{\text{KCRV}}(\text{Co}) = (1.0000 \pm 0.0012) \text{ g/kg}$							
NMI	$w_i(\text{Co})$	$u_c(w_i)$	k_i	$U_{\text{rel}}(w_i)$	d_i	$u(d_i)$	$U(d_i)$
	g/kg	g/kg	1	%	g/kg	g/kg	g/kg
INTI	0.98708	0.00160	2	0.32	-0.01289	0.0017	0.0034
VNIIM	0.99179	0.00208	2	0.42	-0.00818	0.0022	0.0043
INM	0.99375	0.00250	2	0.50	-0.00622	0.0026	0.0051
GUM	0.99375	0.00240	2	0.48	-0.00622	0.0025	0.0049
INMETRO	0.99414	0.00200	2	0.40	-0.00583	0.0021	0.0042
NIM	0.99754	0.00075	2	0.15	-0.00243	0.0010	0.0019
TUBITAK UME	0.99806	0.00165	2	0.33	-0.00191	0.0018	0.0035
NMISA	0.99914	0.00091	1.97	0.18	-0.00083	0.0011	0.0022
NMIA	0.99933	0.00108	2.03	0.22	-0.00064	0.0012	0.0025
LNE	0.9994	0.00070	2	0.14	-0.00057	0.0009	0.0018
HKGL	0.99963	0.00041	2.45	0.10	-0.00034	0.0007	0.0015
NMIJ	0.99963	0.00007	2	0.01	-0.00034	0.0006	0.0012
KRISS	0.99981	0.00025	2.45	0.06	-0.00016	0.0007	0.0013
CENAM-1	0.99985	0.00089	2	0.18	-0.00012	0.0011	0.0021
SMU	0.99991	0.00035	2	0.07	-0.00006	0.0007	0.0014
PTB	0.99999	0.00043	2	0.09	0.00002	0.0007	0.0015
LGC	1.00012	0.00155	2	0.31	0.00015	0.0017	0.0033
NIST	1.0009	0.00100	2.052	0.22	0.00093	0.0012	0.0023

Table 23: Cobalt sample **Co-C**. Mass fractions $w_i(\text{Co})$ and their associated combined and relative expanded uncertainties $u_c(w_i)$ and $U_{\text{rel}}(w_i)$, resp., together with the coverage factor k_i as reported by the participants in the order of increasing mass fraction values. In case only expanded or relative combined uncertainties were reported the values compiled were calculated accordingly. Degrees of equivalence d_i and their associated combined and expanded uncertainty $u(d_i)$ and $U(d_i)$, resp., according to equation (21) and (22). A coverage factor of $k = 2$ was used to calculate $U(d_i) = k \cdot u(d_i)$.

Co-C							
$w_{\text{KCRV}}(\text{Co}) = (1.0180 \pm 0.0012) \text{ g/kg}$							
NMI	$w_i(\text{Co})$	$u_c(w_i)$	k_i	$U_{\text{rel}}(w_i)$	d_i	$u(d_i)$	$U(d_i)$
	g/kg	g/kg	1	%	g/kg	g/kg	g/kg
VNIIM	1.002	0.00240	2	0.48	-0.01600	0.0025	0.0050
INTI	1.0039	0.00205	2	0.41	-0.01410	0.0021	0.0043
TUBITAK UME	1.0147	0.00193	2	0.38	-0.00330	0.0020	0.0040
NIM	1.0170	0.00085	2	0.17	-0.00105	0.0010	0.0021
LNE	1.0170	0.00070	2	0.14	-0.00100	0.0009	0.0019
CENAM-1	1.0177	0.00106	2	0.21	-0.00033	0.0012	0.0024
NMISA	1.0177	0.00168	2.02	0.33	-0.00030	0.0018	0.0036
KRISS	1.01780	0.00027	2.57	0.07	-0.00020	0.0007	0.0013
NMIJ	1.01781	0.00023	2	0.05	-0.00019	0.0007	0.0013
PTB	1.01793	0.00028	2	0.05	-0.00007	0.0007	0.0013
SMU	1.01796	0.00053	2	0.10	-0.00004	0.0008	0.0016
GUM	1.0181	0.00720	2	1.41	0.00010	0.0072	0.0145
INMETRO	1.0182	0.00230	2	0.45	0.00020	0.0024	0.0048
NIST	1.0185	0.00110	2.052	0.22	0.00050	0.0013	0.0025
NMIA	1.0190	0.00160	2.06	0.32	0.00100	0.0017	0.0034

Table 24: Lead sample **Pb-A**. Mass fractions $w_i(\text{Pb})$ and their associated combined and relative expanded uncertainties $u_c(w_i)$ and $U_{\text{rel}}(w_i)$, resp., together with the coverage factor k_i as reported by the participants in the order of increasing mass fraction values. Results reported in terms of amount contents n/m converted in mass fractions w applying a molar mass of $M(\text{Pb}) = (207.17782 \pm 0.00011)$ g/mol ($k = 2$), refer to section 2.3 for details. In case only expanded or relative combined uncertainties were reported the values compiled were calculated accordingly. Degrees of equivalence d_i and their associated combined and expanded uncertainty $u(d_i)$ and $U(d_i)$, resp., according to equation (21) and (22). A coverage factor of $k = 2$ was used to calculate $U(d_i) = k \cdot u(d_i)$.

Pb-A							
$w_{\text{KCRV}}(\text{Pb}) = (0.9800 \pm 0.0011)$ g/kg							
NMI	$w_i(\text{Pb})$ g/kg	$u_c(w_i)$ g/kg	k_i 1	$U_{\text{rel}}(w_i)$ %	d_i g/kg	$u(d_i)$ g/kg	$U(d_i)$ g/kg
BAM	0.9793	0.00085	2	0.17	-0.00066	0.0010	0.0020
NMIJ	0.97946	0.00022	2	0.04	-0.00050	0.0006	0.0012
PTB	0.97968	0.00033	2	0.07	-0.00028	0.0006	0.0013
LGC	0.9797	0.00075	2	0.15	-0.00026	0.0009	0.0019
NIM	0.9797	0.00085	2	0.17	-0.00023	0.0010	0.0020
KRISS	0.9798	0.00074	2.18	0.16	-0.00012	0.0009	0.0018
CENAM-1	0.9802	0.00189	2	0.38	0.00022	0.0020	0.0039
HKGL	0.98046	0.00104	2.08	0.22	0.00050	0.0012	0.0023
NIST	0.9807	0.00110	2.040	0.22	0.00074	0.0012	0.0025
NMIA	0.9807	0.00190	2.00	0.39	0.00074	0.0020	0.0040
NMISA	0.9822	0.00226	1.99	0.46	0.00224	0.0023	0.0047
INM	0.9870	0.00249	2	0.50	0.00703	0.0025	0.0051
TUBITAK UME	0.9921	0.00094	2	0.19	0.01214	0.0011	0.0022
VNIIM	0.993	0.00258	2	0.52	0.01304	0.0026	0.0053
INTI	1.0053	0.00215	2	0.43	0.02534	0.0022	0.0044
GUM	1.0359	0.00725	2	1.40	0.05592	0.0073	0.0145

*Table 25: Lead sample **Pb-B**. Mass fractions $w_i(\text{Pb})$ and their associated combined and relative expanded uncertainties $u_c(w_i)$ and $U_{\text{rel}}(w_i)$, resp., together with the coverage factor k_i as reported by the participants in the order of increasing mass fraction values. All results reported as measured against Pb-A under the assumption of $w(\text{Pb}) = 1 \text{ g/kg} \pm 0 \text{ g/kg}$ were converted using the actual value (KCRV) of Pb-A (appendix F). Results reported in terms of amount contents n/m converted in mass fractions w applying a molar mass of $M(\text{Pb}) = (207.17782 \pm 0.00011) \text{ g/mol}$ ($k = 2$), refer to section 2.3 for details. In case only expanded or relative combined uncertainties were reported the values compiled were calculated accordingly. Degrees of equivalence d_i and their associated combined and expanded uncertainty $u(d_i)$ and $U(d_i)$, resp., according to equation (21) and (22). A coverage factor of $k = 2$ was used to calculate $U(d_i) = k \cdot u(d_i)$.*

Pb-B							
$w_{\text{KCRV}}(\text{Pb}) = (0.9940 \pm 0.0011) \text{ g/kg}$							
NMI	$w_i(\text{Pb})$	$u_c(w_i)$	k_i	$U_{\text{rel}}(w_i)$	d_i	$u(d_i)$	$U(d_i)$
	g/kg	g/kg	1	%	g/kg	g/kg	g/kg
INTI	0.9859	0.00225	2	0.46	-0.00806	0.0023	0.0046
TUBITAK UME	0.9872	0.00094	2	0.19	-0.00679	0.0011	0.0022
NMIA	0.9922	0.00124	2.02	0.25	-0.00179	0.0014	0.0027
CENAM-2	0.9930	0.00044	2	0.09	-0.00101	0.0007	0.0014
NIST	0.9932	0.00110	2.040	0.23	-0.00081	0.0012	0.0025
HKGL	0.9933	0.00063	2.36	0.15	-0.00071	0.0008	0.0017
KRISS	0.9937	0.00036	2.06	0.08	-0.00035	0.0007	0.0013
PTB	0.99371	0.00029	2	0.06	-0.00029	0.0006	0.0013
LGC	0.9940	0.00070	2	0.14	-0.00002	0.0009	0.0018
SMU	0.9942	0.00035	2	0.07	0.00022	0.0007	0.0013
BAM	0.9943	0.00041	2	0.08	0.00032	0.0007	0.0014
CENAM-1	0.9943	0.00205	2	0.41	0.00034	0.0021	0.0043
NMIJ	0.9944	0.00013	2	0.03	0.00035	0.0006	0.0011
INM	0.9946	0.00244	2	0.49	0.00063	0.0025	0.0050
NIM	0.9950	0.00110	2	0.22	0.00095	0.0012	0.0025
GUM	0.9952	0.00220	2	0.44	0.00115	0.0023	0.0045
LNE	0.9963	0.00135	2	0.27	0.00230	0.0015	0.0029
NMISA	0.9968	0.00197	1.98	0.39	0.00282	0.0020	0.0041
VNIIM	0.9996	0.00240	2	0.48	0.00556	0.0025	0.0049

Table 26: Lead sample **Pb-C**. Mass fractions $w_i(\text{Pb})$ and their associated combined and relative expanded uncertainties $u_c(w_i)$ and $U_{\text{rel}}(w_i)$, resp., together with the coverage factor k_i as reported by the participants in the order of increasing mass fraction values. Results reported in terms of amount contents n/m converted in mass fractions w applying a molar mass of $M(\text{Pb}) = (207.17782 \pm 0.00011)$ g/mol ($k = 2$), refer to section 2.3 for details. In case only expanded or relative combined uncertainties were reported the values compiled were calculated accordingly. Degrees of equivalence d_i and their associated combined and expanded uncertainty $u(d_i)$ and $U(d_i)$, resp., according to equation (21) and (22). A coverage factor of $k = 2$ was used to calculate $U(d_i) = k \cdot u(d_i)$.

Pb-C							
$w_{\text{KCRV}}(\text{Pb}) = (0.9830 \pm 0.0011)$ g/kg							
NMI	$w_i(\text{Pb})$ g/kg	$u_c(w_i)$ g/kg	k_i 1	$U_{\text{rel}}(w_i)$ %	d_i g/kg	$u(d_i)$ g/kg	$U(d_i)$ g/kg
NMISA	0.9805	0.00210	2.00	0.43	-0.00248	0.0022	0.0043
NMIA	0.9811	0.00160	2.00	0.33	-0.00188	0.0017	0.0034
BAM	0.9820	0.00085	2	0.17	-0.00098	0.0010	0.0020
NIM	0.9822	0.00070	2	0.14	-0.00083	0.0009	0.0018
KRISS	0.9826	0.00059	2.23	0.13	-0.00034	0.0008	0.0016
NMIJ	0.98278	0.00022	2	0.04	-0.00020	0.0006	0.0012
PTB	0.98287	0.00028	2	0.06	-0.00011	0.0006	0.0012
SMU	0.9830	0.00070	2	0.14	0.00003	0.0009	0.0018
CENAM-1	0.9832	0.00198	2	0.40	0.00022	0.0021	0.0041
NIST	0.9835	0.00110	2.042	0.22	0.00052	0.0012	0.0025
CENAM-2	0.98373	0.00045	2	0.09	0.00075	0.0007	0.0014
LNE	0.9850	0.00120	2	0.24	0.00202	0.0013	0.0026
TUBITAK UME	0.9880	0.00094	2	0.19	0.00502	0.0011	0.0022
INTI	0.9901	0.00190	2	0.38	0.00712	0.0020	0.0040
VNIIM	0.994	0.00249	2	0.50	0.01102	0.0025	0.0051
GUM	1.0380	0.00829	2	1.60	0.05498	0.0083	0.0166

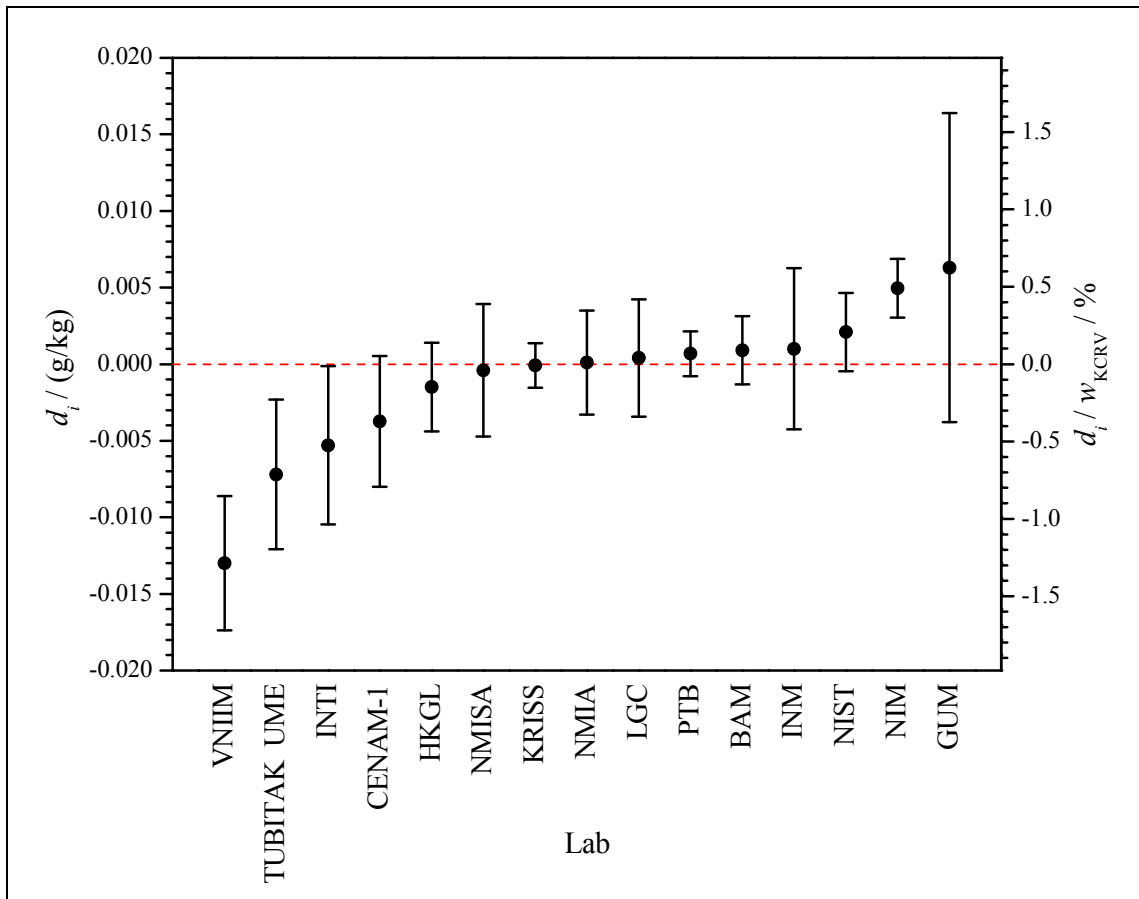


Figure 24: Chromium sample Cr-A. Graphical representation of the equivalence statements related to the gravimetric KCRV – DoE-plot of the data reported by the CCQM-K87 participants according to table 18. The black dots show the degree of equivalence d_i (DoE), while the error bars denote the expanded uncertainty associated with the degree of equivalence $U(d_i)$ according to eq. (22), calculated applying a coverage factor of $k = 2$, using $U(d_i) = k \cdot u(d_i)$. Results enclosing zero with their uncertainty interval are considered to be consistent with the KCRV.

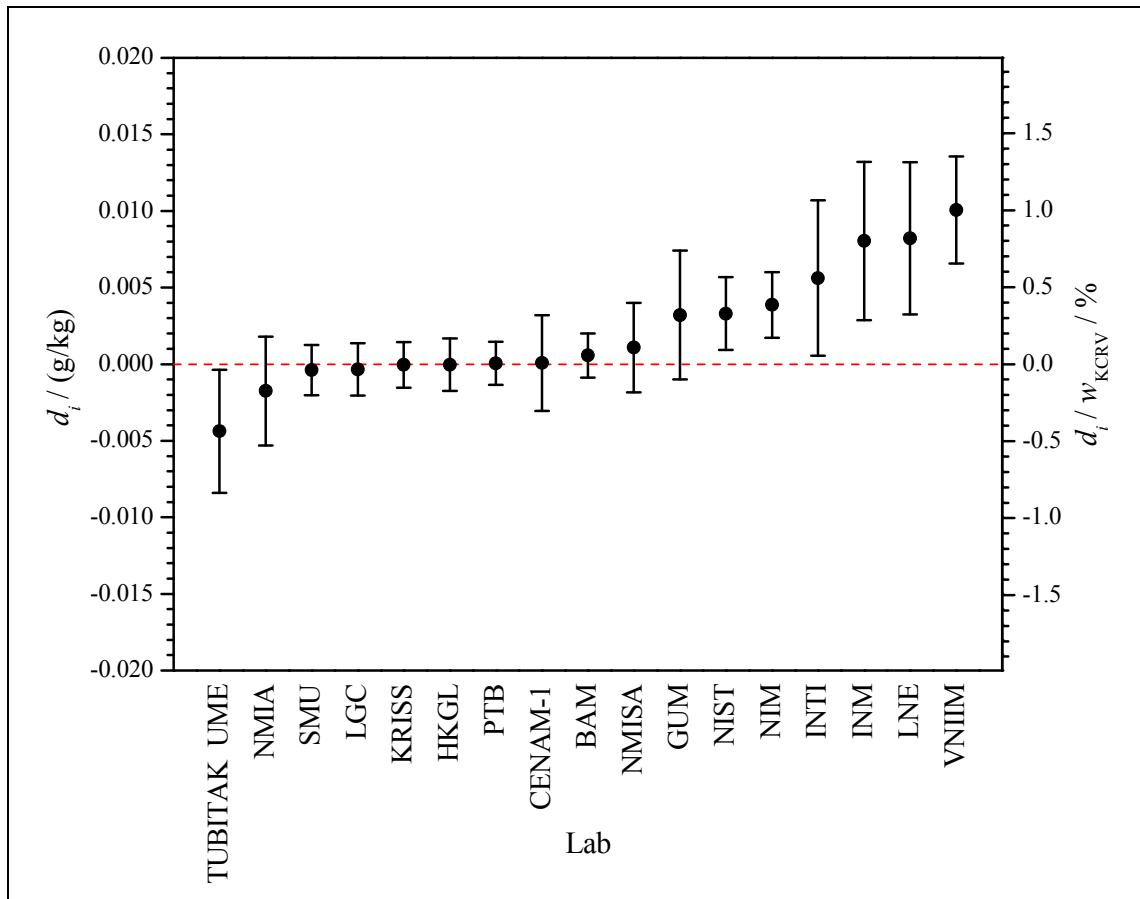


Figure 25: Chromium sample **Cr-B**. Graphical representation of the equivalence statements related to the gravimetric KCRV – DoE-plot of the data reported by the CCQM-K87 participants according to table 19. The black dots show the degree of equivalence d_i (DoE), while the error bars denote the expanded uncertainty associated with the degree of equivalence $U(d_i)$ according to eq. (22), calculated applying a coverage factor of $k = 2$, using $U(d_i) = k \cdot u(d_i)$. Results enclosing zero with their uncertainty interval are considered to be consistent with the KCRV.

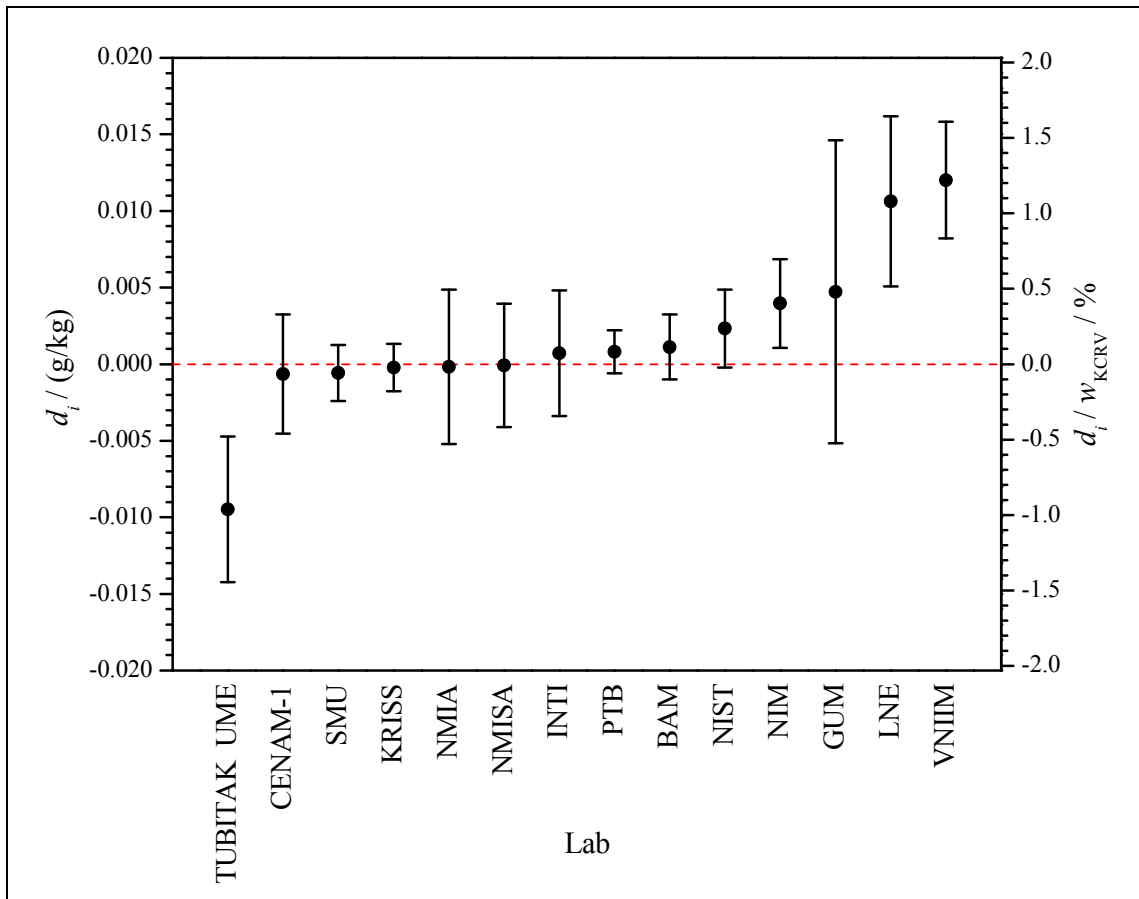


Figure 26: Chromium sample Cr-C. Graphical representation of the equivalence statements related to the gravimetric KCRV – DoE-plot of the data reported by the CCQM-K87 participants according to table 20. The black dots show the degree of equivalence d_i (DoE), while the error bars denote the expanded uncertainty associated with the degree of equivalence $U(d_i)$ according to eq. (22), calculated applying a coverage factor of $k = 2$, using $U(d_i) = k \cdot u(d_i)$. Results enclosing zero with their uncertainty interval are considered to be consistent with the KCRV.

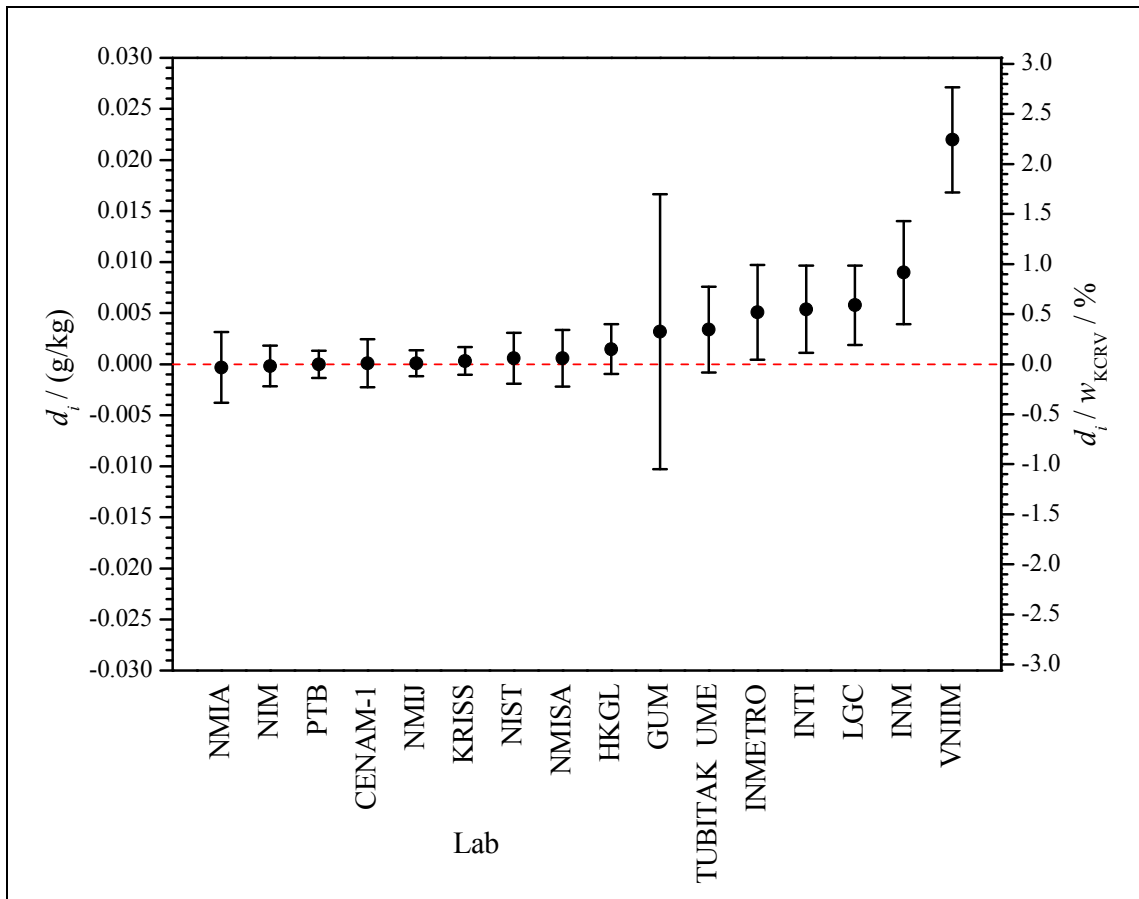


Figure 27: Cobalt sample Co-A. Graphical representation of the equivalence statements related to the gravimetric KCRV – DoE-plot of the data reported by the CCQM-K87 participants according to table 21. The black dots show the degree of equivalence d_i (DoE), while the error bars denote the expanded uncertainty associated with the degree of equivalence $U(d_i)$ according to eq. (22), calculated applying a coverage factor of $k = 2$, using $U(d_i) = k \cdot u(d_i)$. Results enclosing zero with their uncertainty interval are considered to be consistent with the KCRV.

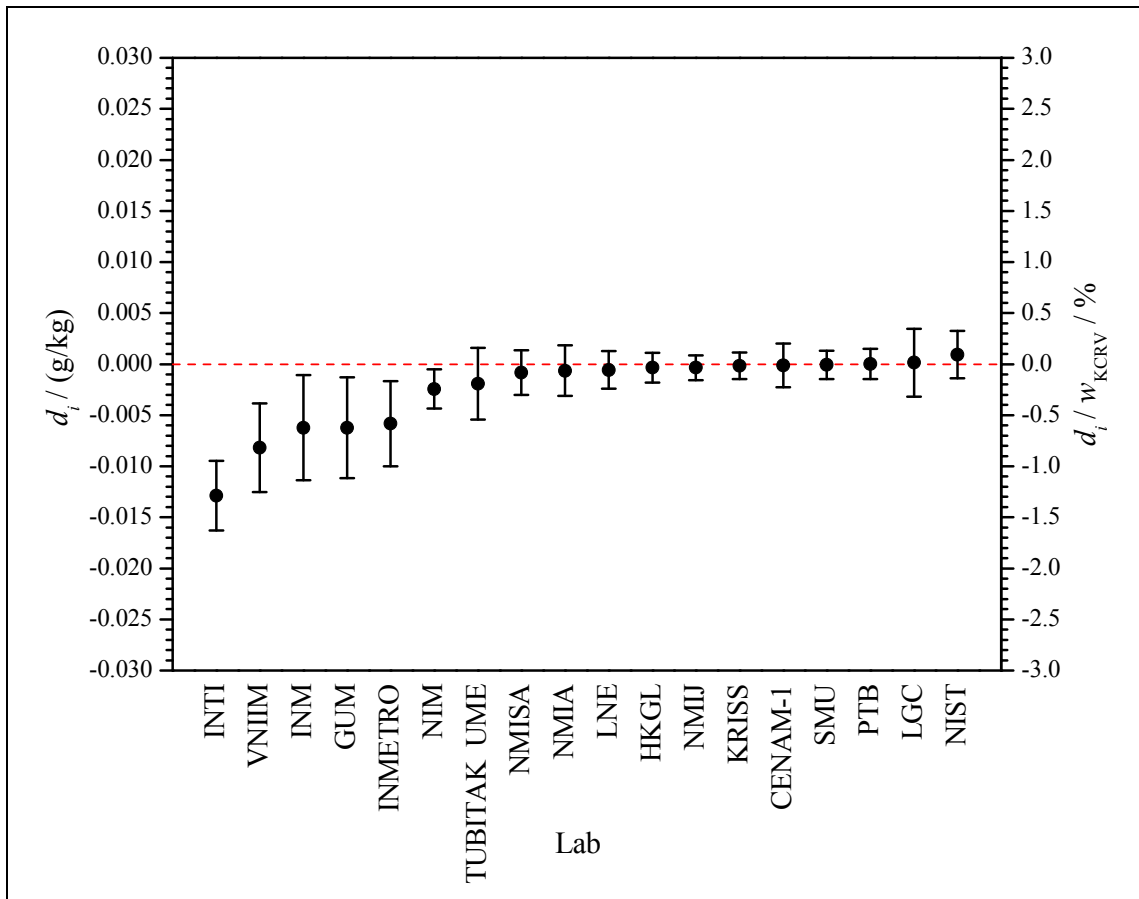


Figure 28: Cobalt sample **Co-B**. Graphical representation of the equivalence statements related to the gravimetric KCRV – DoE-plot of the data reported by the CCQM-K87 participants according to table 22. The black dots show the degree of equivalence d_i (DoE), while the error bars denote the expanded uncertainty associated with the degree of equivalence $U(d_i)$ according to eq. (22), calculated applying a coverage factor of $k = 2$, using $U(d_i) = k \cdot u(d_i)$. Results enclosing zero with their uncertainty interval are considered to be consistent with the KCRV.

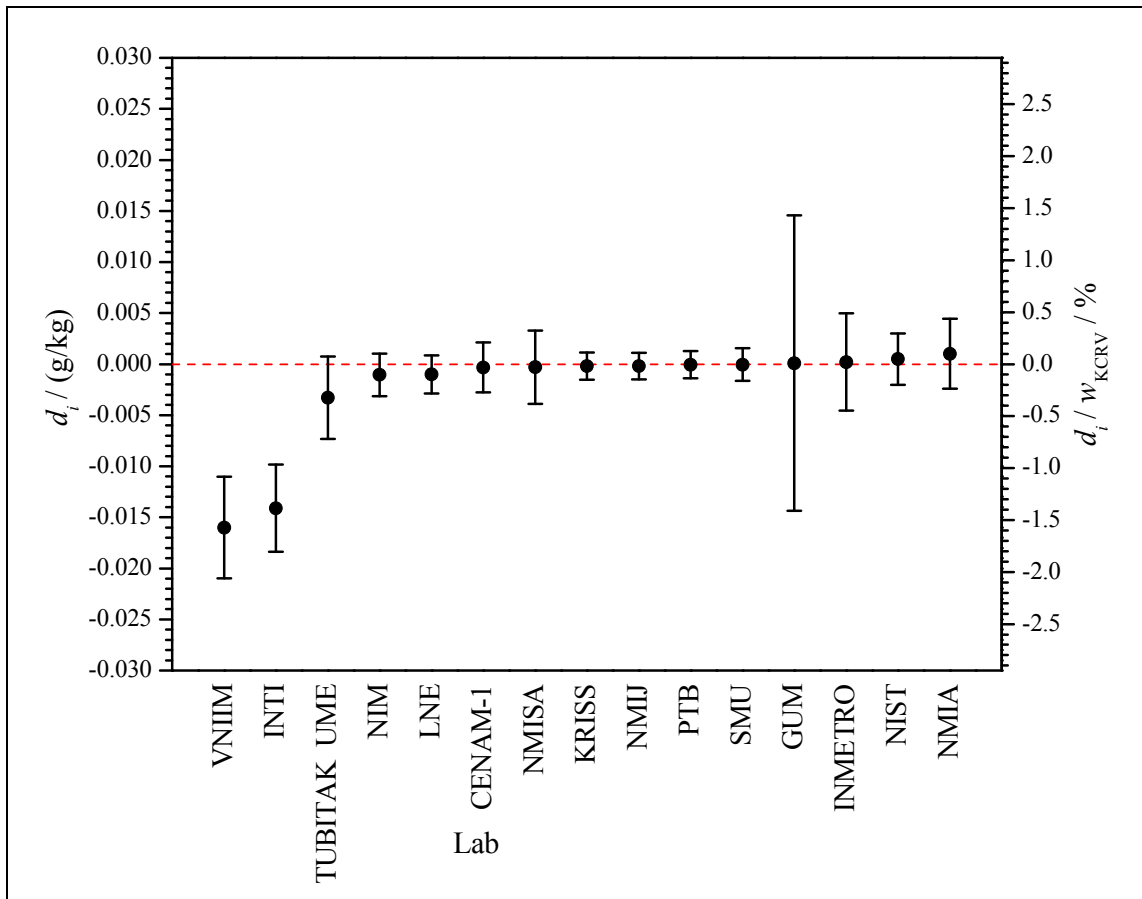


Figure 29: Cobalt sample Co-C. Graphical representation of the equivalence statements related to the gravimetric KCRV – DoE-plot of the data reported by the CCQM-K87 participants according to table 23. The black dots show the degree of equivalence d_i (DoE), while the error bars denote the expanded uncertainty associated with the degree of equivalence $U(d_i)$ according to eq. (22), calculated applying a coverage factor of $k = 2$, using $U(d_i) = k \cdot u(d_i)$. Results enclosing zero with their uncertainty interval are considered to be consistent with the KCRV.

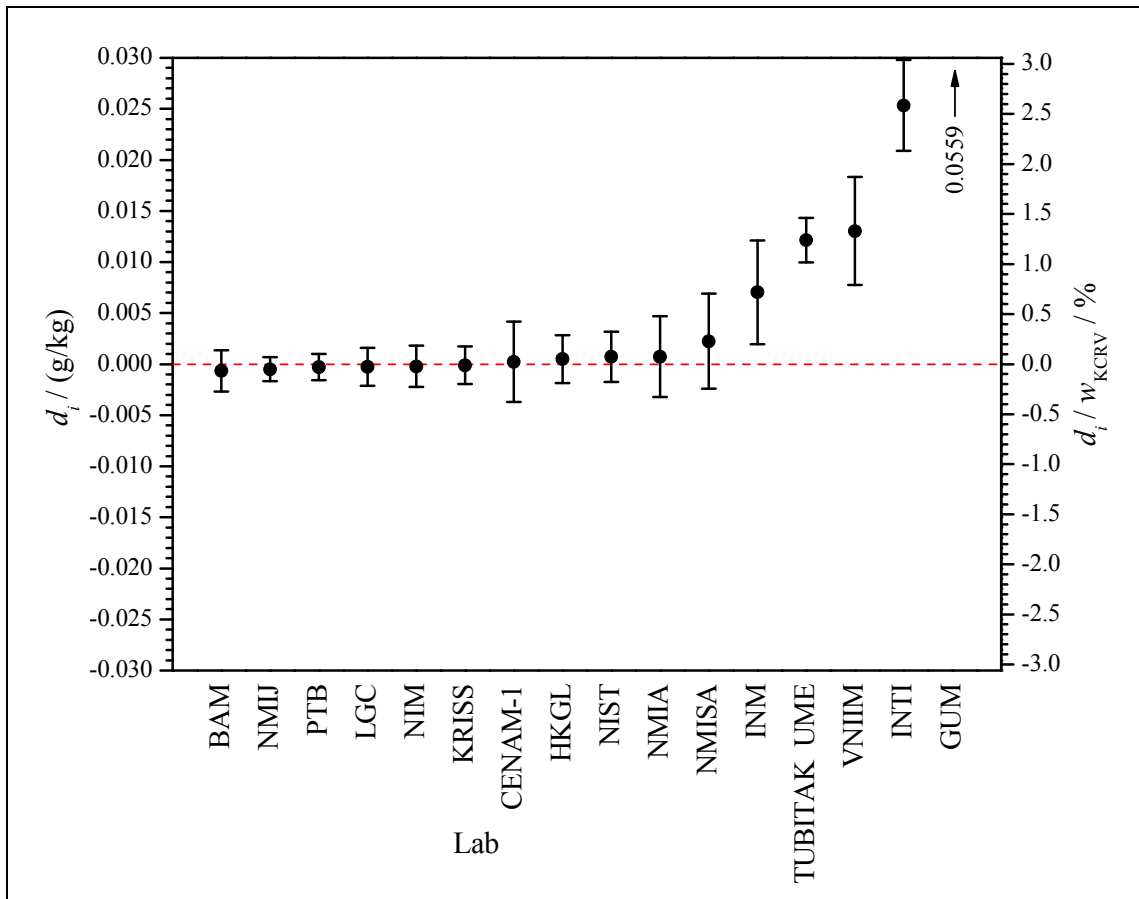


Figure 30: Lead sample **Pb-A**. Graphical representation of the equivalence statements related to the gravimetric KCRV – DoE-plot of the data reported by the CCQM-K87 participants according to table 24. The black dots show the degree of equivalence d_i (DoE), while the error bars denote the expanded uncertainty associated with the degree of equivalence $U(d_i)$ according to eq. (22), calculated applying a coverage factor of $k = 2$, using $U(d_i) = k \cdot u(d_i)$. Results enclosing zero with their uncertainty interval are considered to be consistent with the KCRV.

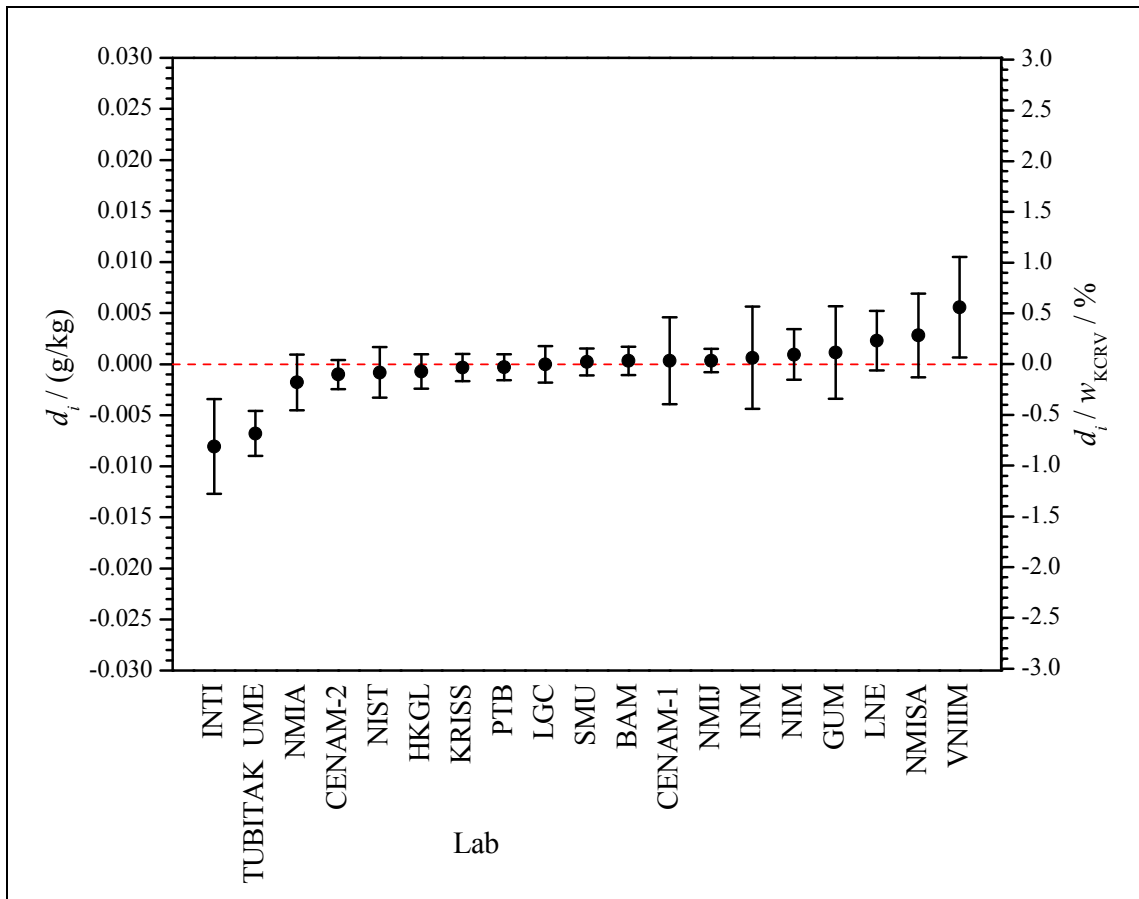


Figure 31: Lead sample **Pb-B**. Graphical representation of the equivalence statements related to the gravimetric KCRV – DoE-plot of the data reported by the CCQM-K87 participants according to table 25. The black dots show the degree of equivalence d_i (DoE), while the error bars denote the expanded uncertainty associated with the degree of equivalence $U(d_i)$ according to eq. (22), calculated applying a coverage factor of $k = 2$, using $U(d_i) = k \cdot u(d_i)$. Results enclosing zero with their uncertainty interval are considered to be consistent with the KCRV.

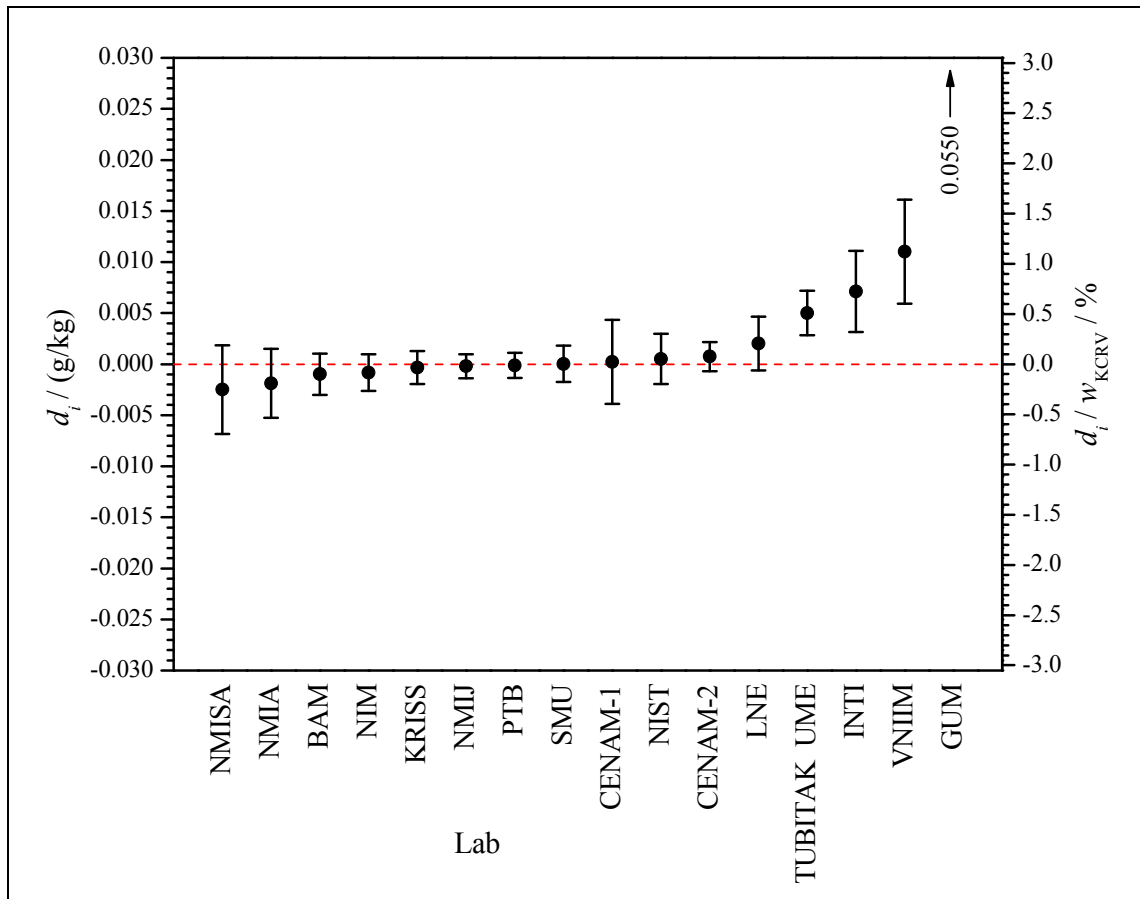


Figure 32: Lead sample **Pb-C**. Graphical representation of the equivalence statements related to the gravimetric KCRV – DoE-plot of the data reported by the CCQM-K87 participants according to table 26. The black dots show the degree of equivalence d_i (DoE), while the error bars denote the expanded uncertainty associated with the degree of equivalence $U(d_i)$ according to eq. (22), calculated applying a coverage factor of $k = 2$, using $U(d_i) = k \cdot u(d_i)$. Results enclosing zero with their uncertainty interval are considered to be consistent with the KCRV.

7.7 Precision and accuracy considerations

Based on [15] the elaborated comparison and measurement scheme was taken advantage of by calculating quantities related to the participants’ precision and accuracy. A possible bias due to the measurement and/or standard used should be reproduced by a particular participant with all three samples of one element. This bias can be expressed as the ratio of the measured mass fraction (e.g. w_A) and the respective KCRV ($w_{A,KCRV}$). Assuming a participant determined the mass fraction in samples A, B, and C (using A as the standard when determining B) the ratio of ratios below should be close to unity, meaning after subtracting one the difference should be close to zero in case the participant was able to reproduce its bias. Therefore, eq. (23) represents a possible expression to quantify the participants’ precision P . Equation (24) covers those cases where participants did not determine sample A but determined sample B using their standard.

$$P = \frac{\frac{w_C}{w_A}}{\frac{w_{C,KCRV}}{w_A}} - 1 \rightarrow 0 \quad (23)$$

$$P = \frac{\frac{w_C}{w_B}}{\frac{w_{C,KCRV}}{w_B}} - 1 \rightarrow 0 \quad (24)$$

Assuming all participants measured with perfect precision and the KCRV is completely accurate the accuracy of the participants own standards can be retrieved from the reported data applying eq. (25). The result A of eq. (25) expresses the relative deviation of a participant's standard from the respective KCRV that was used to determine sample A. For details refer to appendix D. The use of eq. (25) is limited to those participants who measured sample A as well as B, and at the same time used sample A as the standard when measuring sample B.

$$A = \left| \frac{\frac{w_A}{w_{A,KCRV}} \cdot \frac{w_{A,def}}{w_{A,KCRV}}}{\frac{w_B}{w_{B,KCRV}}} - 1 \right| \rightarrow 0 \quad (25)$$

Table 27–29 and figures 33–35 show the precision P and accuracy A according to the above equations. To draw conclusions from these data is complex and restricted to those cases where both P and A is available and additionally P is considerably smaller than A .

Table 27: Chromium. Precision P of the methods applied and accuracy A of the participants' own standards according to equations (23)–(25) in alphabetical order of the NMIs' acronyms. Please note that the validity of possible interpretations is restricted by several assumptions and preconditions. Refer to the text above and appendix D for details. Mass fraction data rounded to the number of digits of the KCRVs. Numbers in grey indicate the determination of sample B using an own standard instead of sample A. Numbers in brackets were calculated from results reported after the deadline. Mass fractions w_B differ from those in table 19 because A has to be calculated from the original data reported.

Chromium	A	B	C		
	$w_{A,KCRV}$ g/kg 1.0100	$w_{B,KCRV}$ g/kg 1.0050	$w_{C,KCRV}$ g/kg 0.9850	w_{def} g/kg 1.0000	
	w_A	w_B	w_C	P	A
NMI	g/kg	g/kg	g/kg	%	%
BAM	1.0109	0.9956	0.9861	0.024	0.033
CENAM-1	1.0063	0.9951	0.9843	0.306	0.378
GUM	1.0163	0.9982	0.9897	0.144	0.305
HKGL	1.0085	0.9950			0.145
INM	1.0110	1.0030			0.696
INTI	1.0047	1.0006	0.9857	0.601	1.078
KRISS	1.0099	0.9950	0.9848	0.014	0.005
LGC	1.0104	0.9947			0.073
LNE		1.0132	0.9956	0.258	
NIM	1.0150	1.0089 (0.9941)	0.9889	0.018	(0.589)
NIST	1.0121	0.9983	0.9873	0.027	0.120
NMIA	1.0101	0.9933	0.9848	0.028	0.184
NMISA	1.0096	0.9961	0.9849	0.031	0.147
PTB	1.0107	0.9951	0.9858	0.014	0.062
SMU		1.0046	0.9844	0.021	
TUBITAK UME	1.0028	0.9907	0.9755	0.251	0.279
VNIIM	0.9970	1.0050	0.9970	2.540	2.266

Table 28: Cobalt. Precision P of the methods applied and accuracy A of the participants' own standards according to equations (23)–(25) in alphabetical order of the NMIs' acronyms. Please note that the validity of possible interpretations is restricted by several assumptions and preconditions. Refer to the text above and appendix D for details. Mass fraction data rounded to the number of digits of the KCRVs. Numbers in grey indicate the determination of sample B using an own standard instead of sample A. Numbers in brackets were calculated from results reported after the deadline. Mass fractions w_B differ from those in table 22 because A has to be calculated from the original data reported.

Cobalt	A	B	C		
	$w_{A,KCRV}$ g/kg 0.9800	$w_{B,KCRV}$ g/kg 1.0000	$w_{C,KCRV}$ g/kg 1.0180	w_{def} g/kg 1.0000	
	w_A	w_B	w_C	P	A
NMI	g/kg	g/kg	g/kg	%	%
CENAM-1	0.9801	1.0202	1.0177	0.041	0.021
GUM	0.9832	1.0140	1.0181	0.313	0.952
HKGL	0.9815	1.0200			0.185
INM	0.9890	1.0140			1.548
INMETRO	0.9851	1.0144	1.0182	0.495	1.107
INTI	0.9854	1.0072	1.0039	1.923	1.861
KRISS	0.9803	1.0202	1.0178	0.051	0.048
LGC	0.9858	1.0205			0.575
LNE		0.9994	1.0170	0.041	
NIM	0.9798	0.9975	1.0170	0.141	
		(1.0180)			(0.208)
NIST	0.9806	1.0213	1.0185	0.009	0.034
NMIA	0.9797	1.0197	1.0190	0.132	0.031
NMIJ	0.9801	1.0200	1.0178	0.027	0.043
		0.9997		0.008	
NMISA	0.9806	1.0195	1.0177	0.088	0.142
PTB	0.9800	1.0000	1.0179	0.009	
SMU		0.9999	1.0180	0.002	
TUBITAK UME	0.9834	1.0184	1.0147	0.666	0.537
VNIIM	1.0020	1.0120	1.0020	3.730	3.086

Table 29: Lead. Precision P of the methods applied and accuracy A of the participants' own standards according to equations (23)–(25) in alphabetical order of the NMIs' acronyms. Please note that the validity of possible interpretations is restricted by several assumptions and preconditions. Refer to the text above and appendix D for details. Mass fraction data rounded to the number of digits of the KCRVs. Numbers in grey indicate the determination of sample B using an own standard instead of sample A. Numbers in brackets were calculated from results reported after the deadline. Mass fractions w_B differ from those in table 25 because A has to be calculated from the original data reported. Results reported in terms of amount contents n/m converted in mass fractions w applying a molar mass of $M(\text{Pb}) = (207.17782 \pm 0.00011)$ g/mol ($k = 2$), refer to section 2.3 for details.

Lead	A	B	C		
	$w_{A,KCRV}$ g/kg	$w_{B,KCRV}$ g/kg	$w_{C,KCRV}$ g/kg	w_{def} g/kg	
	0.9800	0.9940	0.9830	1.0000	
NMI	w_A g/kg	w_B g/kg	w_C g/kg	P %	A %
BAM	0.9793	1.0147	0.9820	0.032	0.100
CENAM-1	0.9802	1.0147	0.9832	0.0004	0.012
CENAM-2		0.9930	0.9837	0.178	
GUM	1.0359	1.0155	1.0380	0.108	5.585
HKGL	0.9805	1.0136			0.122
INM	0.9870	1.0150			0.654
INTI	1.0053	1.0061	0.9901	1.814	3.424
KRISS	0.9798	1.0140	0.9826	0.022	0.023
LGC	0.9797	1.0143			0.024
LNE		0.9963	0.9850	0.026	
NIM	0.9797	0.9950	0.9822	0.180	
		(1.0156)			(0.144)
NIST	0.9807	1.0135	0.9835	0.022	0.157
NMIA	0.9807	1.0125	0.9811	0.266	0.255
NMIJ	0.9795	1.0147	0.9828	0.031	0.086
		0.9938		0.004	
NMISA	0.9822	1.0172	0.9805	0.480	0.055
PTB	0.9797	0.9937	0.9829	0.018	
SMU		0.9942	0.9830	0.019	
TUBITAK UME	0.9921	1.0074	0.9880	0.719	1.934
VNIIM	0.9930	1.0200	0.9940	0.207	0.766

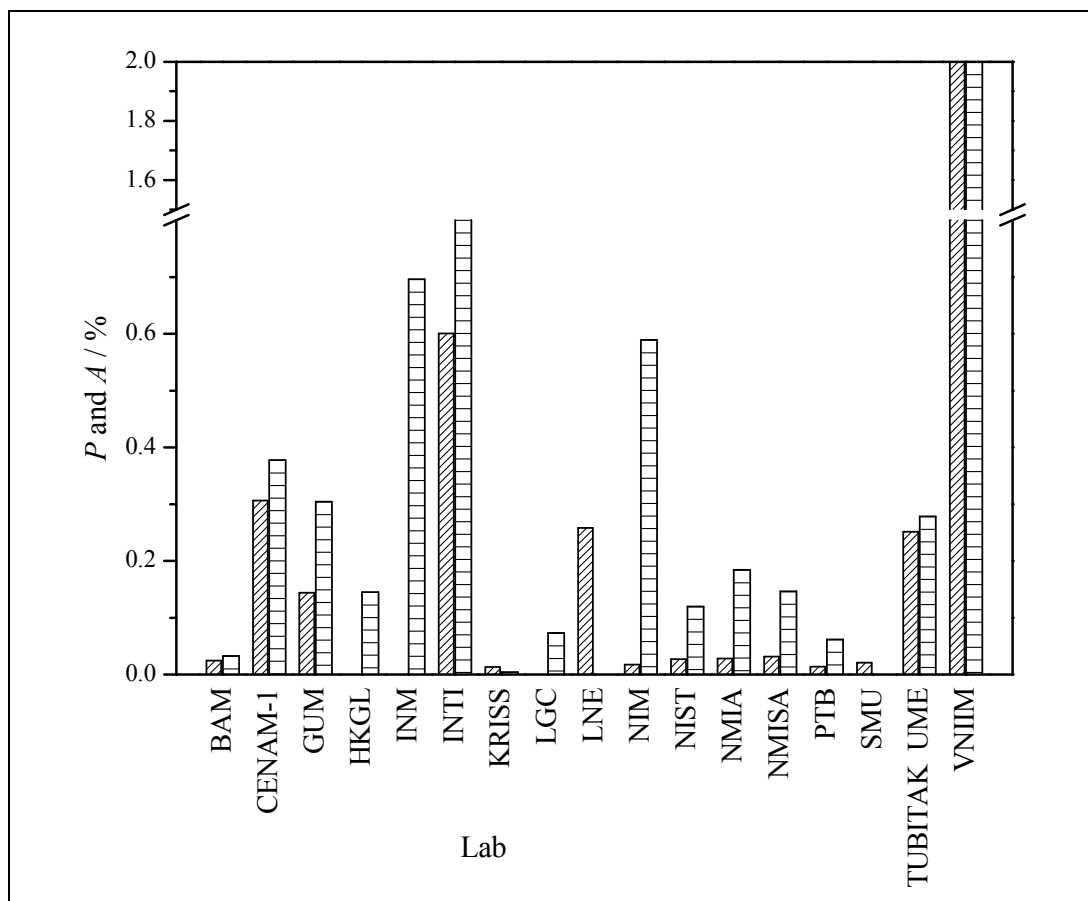


Figure 33: Chromium. Precision P (diagonal pattern) of the methods applied and accuracy A (horizontal pattern) of the participants' own standards according to equations (23)–(25) in alphabetical order of the NMIs' acronyms (see also table 27). Please note that the validity of possible interpretations is restricted by several assumptions and preconditions. Refer to the text above and appendix D for details.

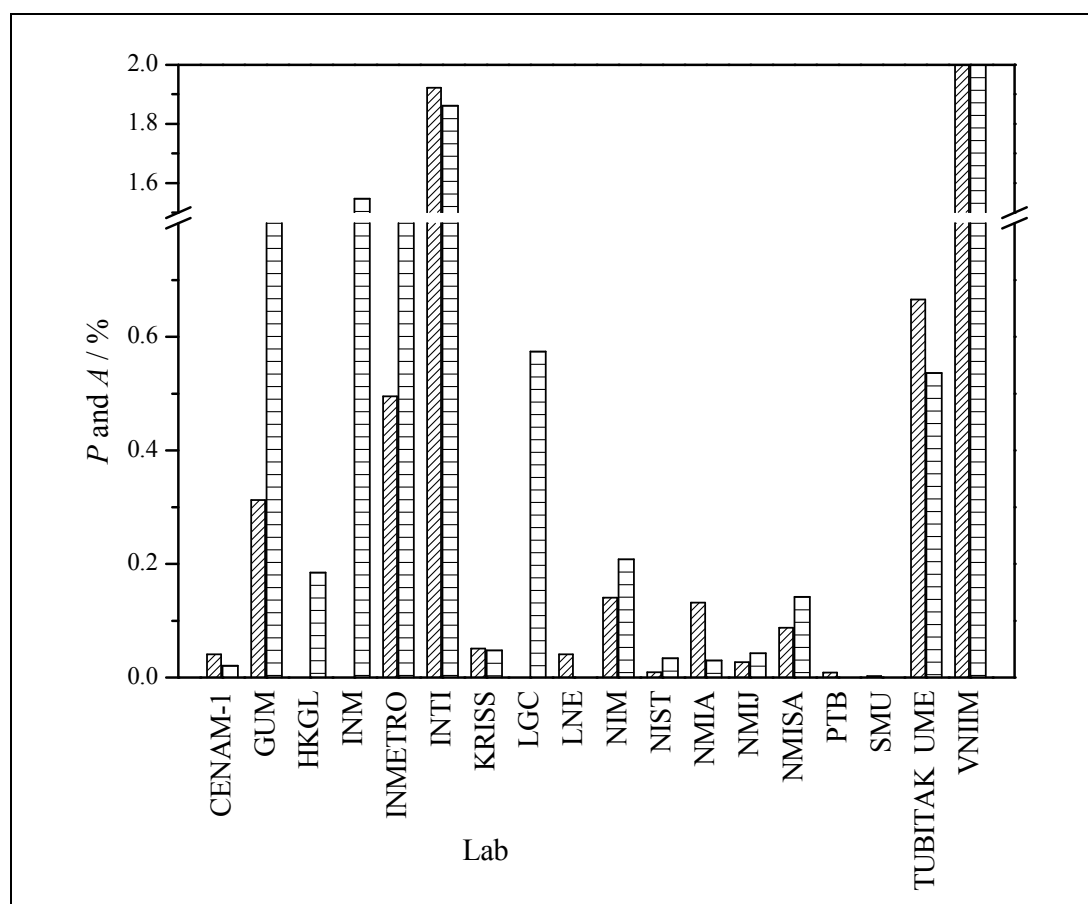


Figure 34: Cobalt. Precision P (diagonal pattern) of the methods applied and accuracy A (horizontal pattern) of the participants' own standards according to equations (23)–(25) in alphabetical order of the NMIs' acronyms (see also table 28). Please note that the validity of possible interpretations is restricted by several assumptions and preconditions. Refer to the text above and appendix D for details.

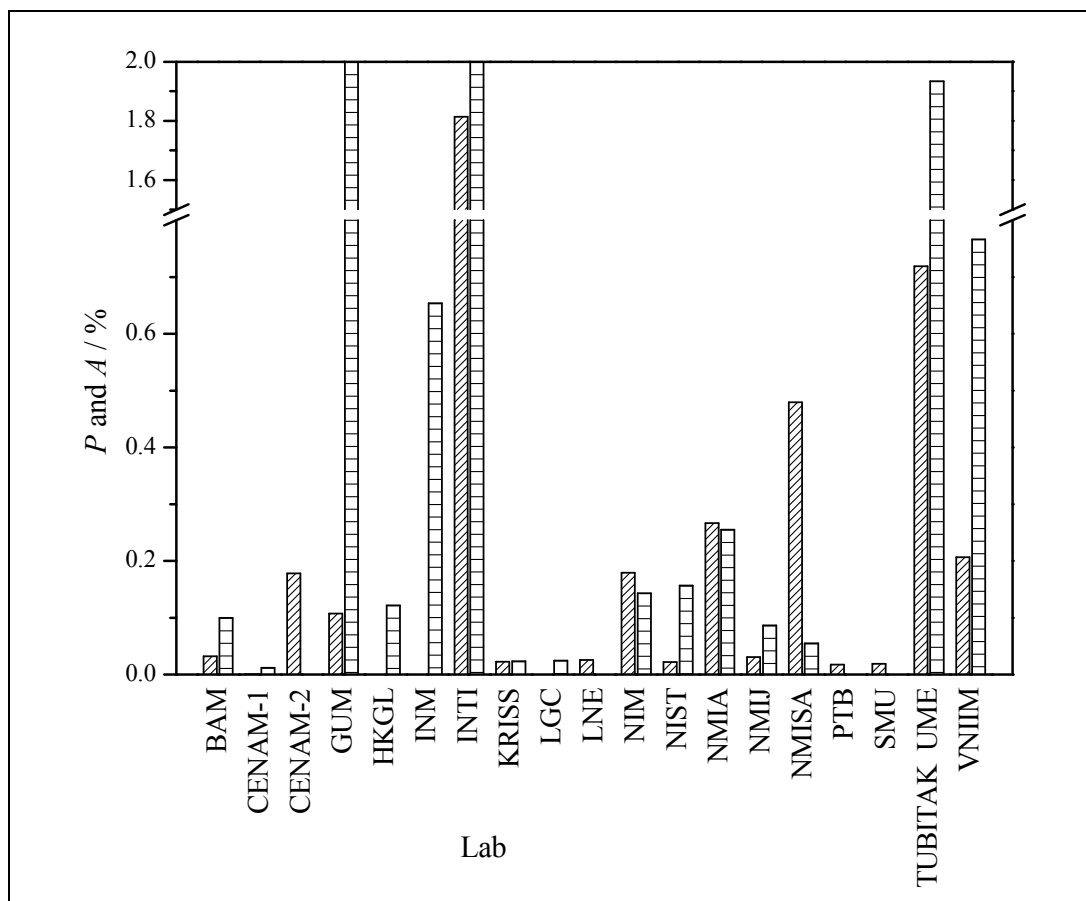


Figure 35: Lead. Precision P (diagonal pattern) of the methods applied and accuracy A (horizontal pattern) of the participants' own standards according to equations (23)–(25) in alphabetical order of the NMIs' acronyms (see also table 29). Please note that the validity of possible interpretations is restricted by several assumptions and preconditions. Refer to the text above and appendix D for details.

7.8 Dependency of methods and results

A considerably large variety of methods and instrumentation was applied by the participants (section 6, table 14). Nevertheless, no dependency between the results reported and the methods/instrumentation applied was obvious. Figures 36 and 37 show the results of samples Cr-B and Pb-B as examples to underpin this observation.

Table 30: Meaning of symbols in figures 36 and 37.

Symbol shape	Instrumentation	Symbol colour	Calibration strategy
circle	ICP OES	red	double IDMS
square	Q-ICP-MS	yellow	one-point-calibration
triangle, facing right	HR-ICP-MS	green	one-point-calibration + internal standard
triangle, facing down	MC-ICP-MS		
triangle, facing up	MC-TIMS	blue	bracketing
triangle, facing left	XRF		+ internal standard
diamond	FAAS	white	calibration curve
star	titrimetry	cyan	calibration curve + internal standard

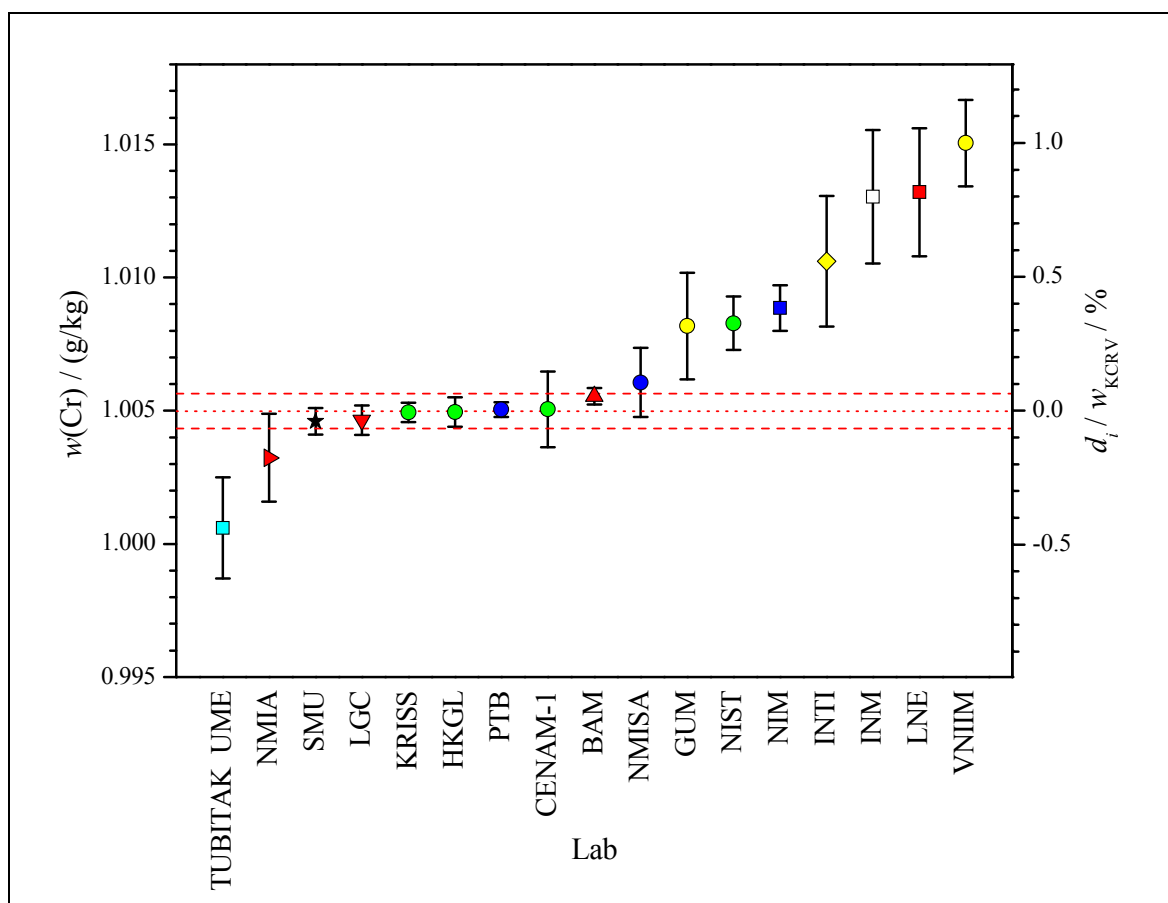


Figure 36: **Chromium Cr-B.** Chromium mass fraction $w(\text{Cr})$ as reported by the CCQM-K87 participants as a function of the methods used. All results reported as measured against Cr-A

under the assumption of $w(\text{Cr}) = 1 \text{ g/kg} \pm 0 \text{ g/kg}$ were converted using the actual value (KCRV) of Cr-A (appendix F). Error bars denote the combined uncertainty $u_c(w(\text{Cr}))$ for a coverage factor of $k = 1$ as reported. The dotted red line shows the **gravimetric KCRV**: $w_{\text{KCRV}}(\text{Cr}) = 1.0050 \text{ g/kg}$. The dashed red lines indicate the range of the combined uncertainty $u_c(w_{\text{KCRV}}(\text{Cr}))$ associated with the KCRV. The right y-axis shows the degree of equivalence d_i relative to the KCRV (for more details see section 7.6). Details about the meaning of shapes and colours see table 30.

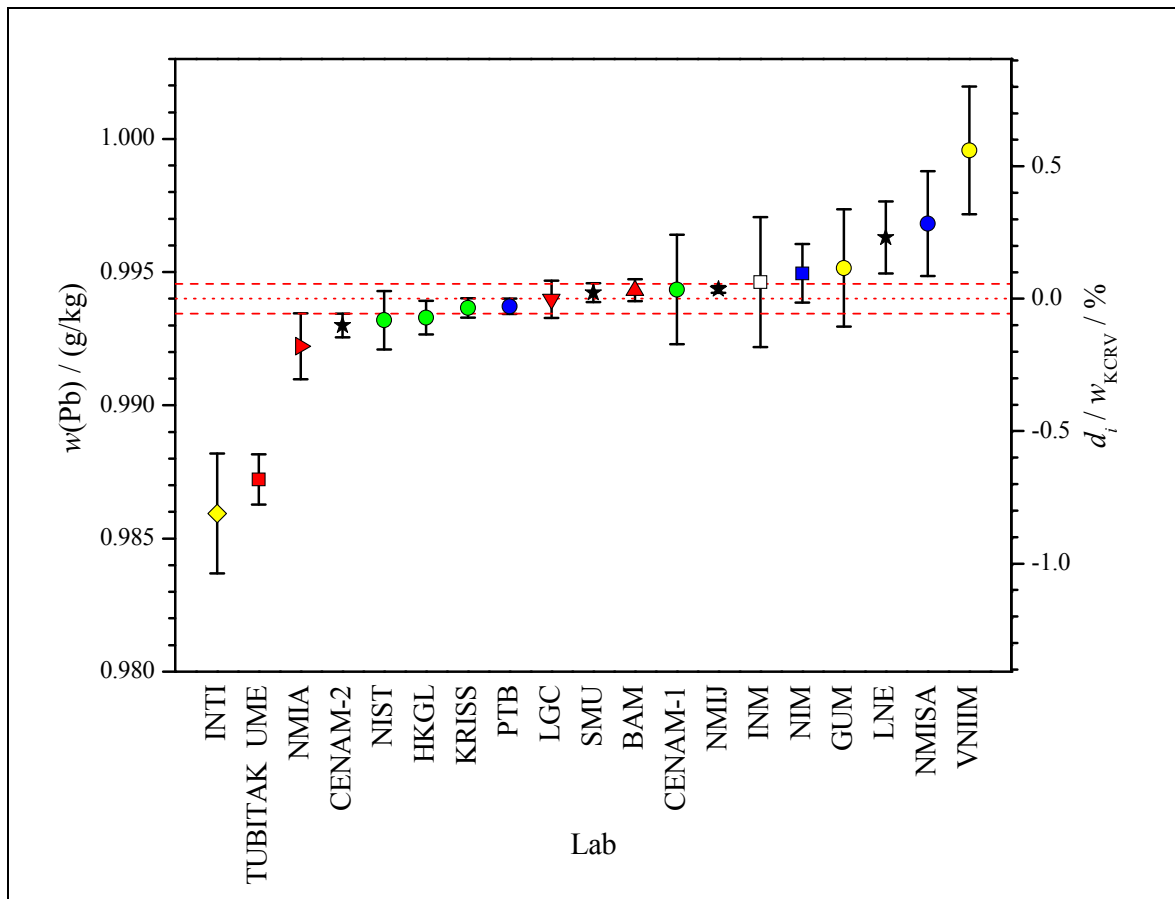


Figure 37: Lead Pb-B. Lead mass fraction $w(\text{Pb})$ as reported by the CCQM-K87 participants as a function of the methods used. All results reported as measured against Pb-A under the assumption of $w(\text{Pb}) = 1 \text{ g/kg} \pm 0 \text{ g/kg}$ were converted using the actual value (KCRV) of Pb-A (appendix F). Results reported in terms of amount contents n/m converted in mass fractions w applying a molar mass of $M(\text{Pb}) = (207.17782 \pm 0.00011) \text{ g/mol}$ ($k = 2$), refer to section 2.3 for details. Error bars denote the combined uncertainty $u_c(w(\text{Pb}))$ for a coverage factor of $k = 1$ as reported. The dotted red line shows the **gravimetric KCRV**: $w_{\text{KCRV}}(\text{Pb}) = 0.9940 \text{ g/kg}$. The dashed red lines indicate the range of the combined uncertainty $u_c(w_{\text{KCRV}}(\text{Pb}))$ associated with the KCRV. The right y-axis shows the degree of equivalence d_i relative to the KCRV (for more details see section 7.6). Details about the meaning of shapes and colours see table 30.

8. Discussion

A majority of the participants showed their ability to determine an element mass fraction in mono-elemental solutions as an important link in traceability chains for elemental analysis. Using the criterion of satisfactory equivalence ($|d_i| < U(d_i)$) an average of only 28 % of the participants did not meet this requirement. Compared to CCQM-K8 in which approximately 55 % of the participants did not achieve $|d_i| < U(d_i)$ [16] this means a considerable improvement. This demonstrates the important role of the CCQM working constantly on the international comparability of measurement results in analytical chemistry. Furthermore, around ten out of nineteen participants demonstrated an excellent performance: their results are located within a range of ± 0.1 % of the respective KCRV (figures 38–40 show examples).

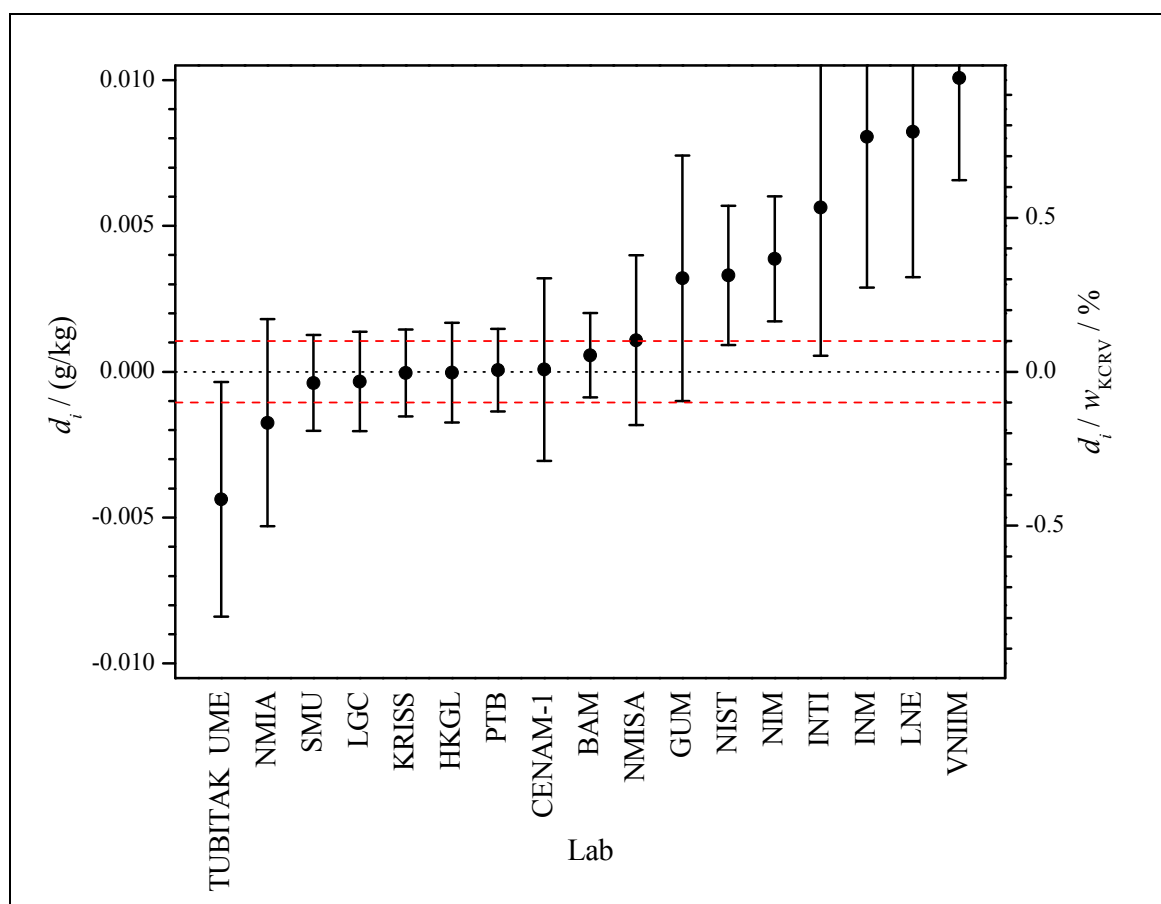


Figure 38: Zoomed-in version of figure 25 showing a core group in excellent agreement. Chromium sample **Cr-B**. Graphical representation of the equivalence statements related to the gravimetric KCRV – DoE-plot of the data reported by the CCQM-K87 participants according to table 19. The black dots show the degree of equivalence d_i (DoE), while the error bars denote the expanded uncertainty associated with the degree of equivalence $U(d_i)$ according to eq. (22), calculated applying a coverage factor of $k = 2$, using $U(d_i) = k \cdot u(d_i)$. Results enclosing zero with their uncertainty interval are considered to be consistent with the KCRV. The dashed red lines define a range ± 0.1 % deviation from the KCRV.

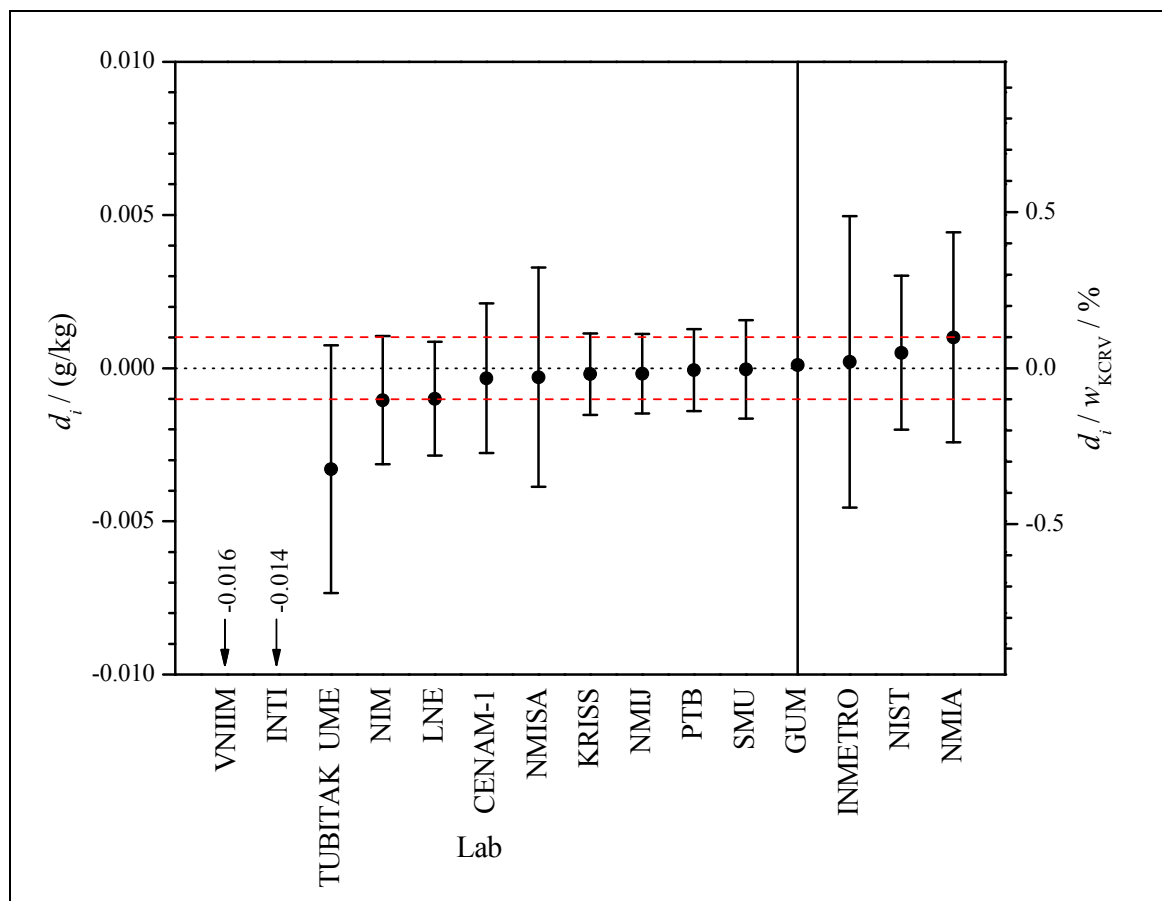


Figure 39: Zoomed-in version of figure 29 showing a core group in excellent agreement. Cobalt sample Co-C. Graphical representation of the equivalence statements related to the gravimetric KCRV – DoE-plot of the data reported by the CCQM-K87 participants according to table 23. The black dots show the degree of equivalence d_i (DoE), while the error bars denote the expanded uncertainty associated with the degree of equivalence $U(d_i)$ according to eq. (22), calculated applying a coverage factor of $k = 2$, using $U(d_i) = k \cdot u(d_i)$. Results enclosing zero with their uncertainty interval are considered to be consistent with the KCRV. The dashed red lines define a range ± 0.1 % deviation from the KCRV.

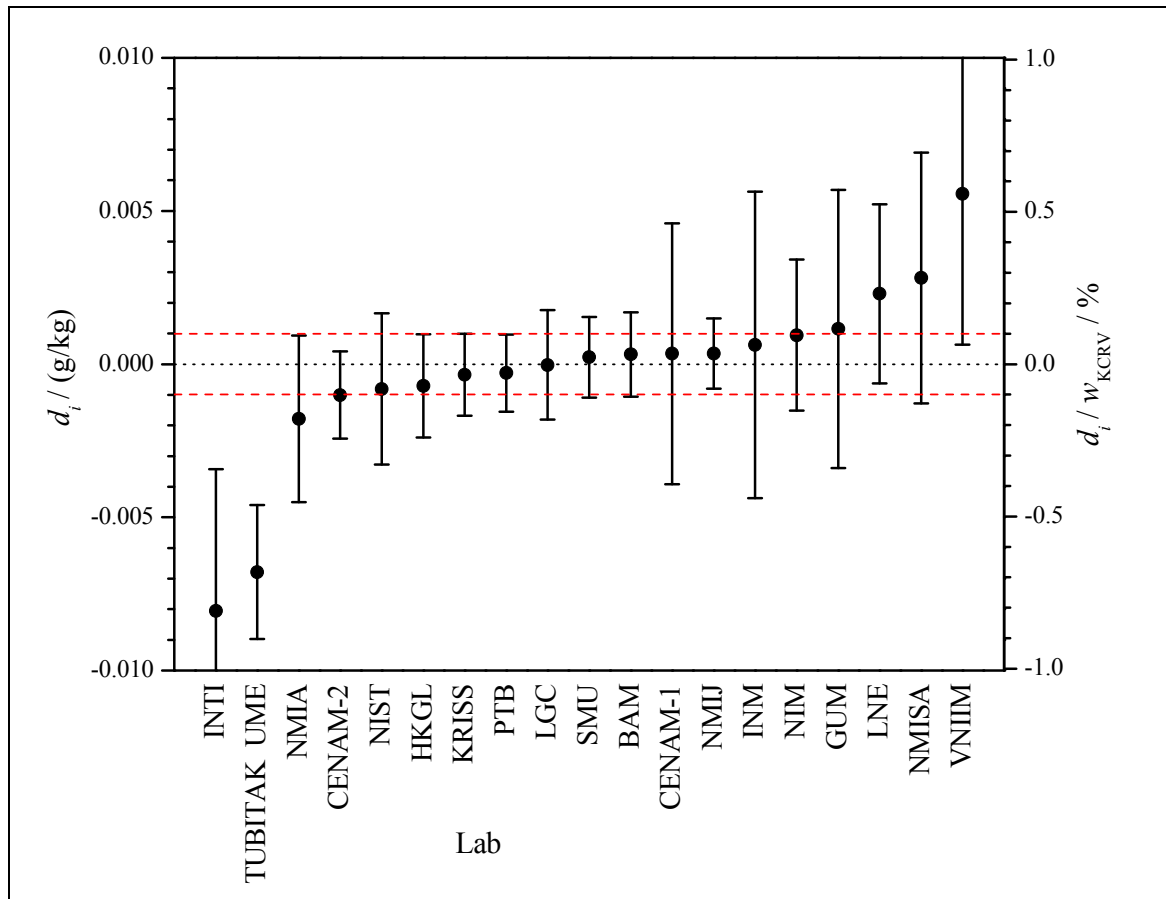


Figure 40: Zoomed-in version of figure 31 showing a core group in excellent agreement. Lead sample **Pb-B**. Graphical representation of the equivalence statements related to the gravimetric KCRV – DoE-plot of the data reported by the CCQM-K87 participants according to table 25. The black dots show the degree of equivalence d_i (DoE), while the error bars denote the expanded uncertainty associated with the degree of equivalence $U(d_i)$ according to eq. (22), calculated applying a coverage factor of $k = 2$, using $U(d_i) = k \cdot u(d_i)$. Results enclosing zero with their uncertainty interval are considered to be consistent with the KCRV. The dashed red lines define a range $\pm 0.1\%$ deviation from the KCRV.

Even though a majority of the participants applied ICP OES combined with a variety of calibration techniques (section 6, table 14 and section 7.8, figures 36 and 37), it is impossible to state a significant correlation between the method/measurement device and the particular result. This finding is underpinned by the observation that also the few double IDMS results showed no particular superiority.

The same holds true for any correlation between the results and the reference materials (sources of traceability): no such correlation was observed. The initial idea to exclude the influence due to the reference material used by applying solution A as the reference in order to see only the influence of the measurement/calibration technique itself was not entirely successful. The differences between the average performance when measuring solution B on the one hand and when measuring solutions A and C on the other hand showed a slight improvement, which should have been more pronounced when the reference materials would have been a major contribution to the participants' performance. Also the proposed approach to extract the accuracy of the references used from the participants' results (section 7.7) did not indicate decisive findings: in case a participant showed a "bad" accuracy (A large) almost always the

precision P was in the same order of magnitude which prevents any conclusion. On the other hand participants showing a sufficient precision P almost always shined with a small A . Even though this comparison is fortunately supported by a considerably large amount of data, this amount is insufficient to resolve such a delicate issue as possible differences of the references used.

The parallel pilot study CCQM-P124 (appendix C) demonstrated that at least the participating two industry laboratories (both supplier of secondary calibration solutions) are able to successfully measure mono-elemental calibration solutions on par with the majority of NMIs. This is an encouraging finding because the traceability in the field is usually achieved via secondary calibration solutions from manufacturers like the ones who participated.

This report includes no core competencies tables due to the clear and narrow range of competencies demonstrated and the absence of a complex and/or challenging matrix.

Median and uncertainty weighted mean KCRV estimators were in excellent agreement with the proposed gravimetric KCRVs (derived from the sample preparation). The average relative deviation of the median and uncertainty weighted mean KCRV estimators from the gravimetric KCRV was 0.05 % and 0.03 %, respectively.

The KCRVs were accepted by the IAWG during the Sydney meeting on 1 November 2011.

Therefore, this comparison was successfully completed.

9. References

- [1] CCQM Inorganic Analysis Working Group, Minutes of the meeting held on 1-4 November 2011, NMIA, Sydney, Australia.
<http://www.bipm.org/wg/CCQM/IAWG/Restricted/welcome.jsp>
- [2] Heinrich Kipphardt, Ralf Matschat, Olaf Rienitz, Detlef Schiel, Wolfgang Gernand, Dietmar Oeter, *Traceability system for elemental analysis*, *Accred Qual Assur* (2006) 10: 633-639
- [3] Heinrich Kipphardt, Ralf Matschat, *Purity assessment for providing primary standards for elemental determination – a snap shot of international comparability*, *Microchim Acta* (2008) 162: 269-275
- [4] Heinrich Kipphardt, Ralf Matschat, Jochen Vogl, Tamara Gusarova, Michael Czerwensky, Hans-Joachim Heinrich, Akiharu Hioki, Leonid A. Konopelko, Brad Methven, Tsutomu Miura, Ole Petersen, Gundel Riebe, Ralph Sturgeon, Gregory C. Turk, Lee L. Yu, *Purity determination as needed for the realisation of primary standards for elemental determination: status of international comparability*, *Accred Qual Assur* (2010) 15:29–37
- [5] Anna-Lisa Hauswaldt, Olaf Rienitz, Reinhard Jährling, Nicolas Fischer, Detlef Schiel, Guillaume Labarraque, Bertil Magnusson, *Uncertainty of standard addition experiments: a novel approach to include the uncertainty associated with the standard in the model equation*, *Accred Qual Assur* (2011) doi:10.1007/s00769-011-0827-5.
- [6] ISO Guide 35, Reference materials — General and statistical principles for certification, 3rd edition, International Organization for Standardization, Geneva, 2006.
- [7] *Evaluation of measurement data - Guide to the expression of uncertainty in measurement*, JCGM 100:2008.
http://www.bipm.org/utils/common/documents/jcgm/JCGM_100_2008_E.pdf
- [8] CCQM Guidance note: Estimation of a consensus KCRV and associated Degrees of Equivalence, Version 6, 2010-03-01, Draft.
- [9] Wolfgang Gottwald, *Statistik für Anwender*, WILEY-VCH, Weinheim, 2000.
- [10] W. J. Dixon, *Analysis of extreme values*, *The Annals of Mathematical Statistics* 21, 4 (1950), 488-506.
- [11] W. J. Dixon, *Processing data for outliers*, *J Biometrics* 9 (1953) 74-89.
- [12] R. B. Dean, W. J. Dixon, *Simplified statistics for small numbers of observations*, *Analytical Chemistry* 23 (1951) 636-638.
- [13] Lothar Sachs, *Angewandte Statistik*, Springer, Berlin, 1997.
- [14] Dieter Richter, Wolfgang Wöger, Werner Hässelbarth (eds.), *Data analysis of key comparisons*, Braunschweig and Berlin, 2003, ISBN 3-89701-933-3.
- [15] Michal Máriássy, personal communication, November 2011.
- [16] Helene Felber, Michael Weber, Cédric Rivier, *CCQM-K8 Key Comparison — Monoelemental Calibration Solutions*, *Metrologia*, 2002, 39, Tech. Suppl., 08002

CCQM-K87 and CCQM-P124

“Mono-elemental Calibration Solutions”

Technical Protocol

1. Introduction

Mono-elemental solutions are required for calibration purposes in elemental analysis and are therefore a prerequisite for reliable measurement results. This key comparison and the parallel pilot study address the particular importance of mono-elemental solutions. Cr, Co and Pb were carefully selected as the analytes. The comparisons are part of the broader context of “Traceability in elemental analysis” implemented with the aid of CCQM-P62, CCQM-P107, and CCQM-K72 (characterisation of impurities in pure substances serving as the traceability basis) as well as CCQM-P46 (preparation of primary elemental calibration solutions) and CCQM-K8 (determination of the element content in primary calibration solutions). The comparisons CCQM-K87 and CCQM-P124 are follow-ups of the key comparison CCQM-K8 (conducted in 2000) which was concerned with elemental solutions of Al, Cu, Fe and Mg. National metrology institutes and designated institutes were invited to participate in CCQM-K87 in order to confirm existing CMC claims or to facilitate the application of new CMC claims.

2. Samples

Nine mono-elemental solutions were prepared gravimetrically at PTB starting from the German national standards provided by BAM (cobalt and lead) and from a primary material provided by CENAM (chromium), respectively. The following table summarizes these solutions and shows the notation used:

type of solution	chromium	cobalt	lead
A – calibration solution	Cr-A	Co-A	Pb-A
B – sample solution	Cr-B	Co-B	Pb-B
C – “commercial” sample solution	Cr-C	Co-C	Pb-C

After cleaning the solid starting materials following the prescribed procedures taken from the certificates, aliquots of approximately 5 – 6 g were dissolved using stoichiometric amounts of HCl ($w = 0.2$ g/g) in case of Cr and excess amounts of HNO₃ ($w = 0.2$ g/g) in case of Co and Pb. These solutions were adjusted with HNO₃ ($w = 0.025$ g/g) and water, respectively, to form stock solutions (550 g each) with an element mass fraction of $w(E) \approx 10\,000$ µg/g. The final samples were gravimetrically prepared directly from the stock solutions by diluting each 550 g stock solution using HNO₃ ($w = 0.025$ g/g) yielding approximately 5.5 kg of each of the nine solutions. In case of the solution types A and B ultrapure HCl, subboiled HNO₃ and ultrapure water (type 1) was used for the preparation. In order to come as close as possible to a “commercial” solution, trace impurities were introduced into solution type C by using p.a. HNO₃ and p.a. HCl as well as only pure water (type 2) for the preparation instead of the chemicals mentioned above. Since even these p.a. chemicals are extremely pure, the differences between solution type B and C are fairly subtle, reflecting the fact that almost all commercial calibration solutions do not contain impurities above the trace level. All nine solutions were adjusted to feature an element mass fraction of 0.98 g/kg $\leq w(E) \leq 1.02$ g/kg. The solutions were filled in thoroughly cleaned, dried, labelled and weighed 100 mL-PFA bottles. Each bottle contains at least 100 g of the respective solution. Prior to sealing the bottles in film bags, each bottle was weighed again to keep track of losses during shipment and be able to distinguish between unavoidable losses due to evaporation (and correct for them, see section 6) and losses due to leaking bottles. The bottles were wrapped in tightly sealed film bags (12 µm polyester, 12 µm aluminium, 95 µm LDPE, type A 30 T, C. Waller, Eichstetten, Germany).

The following table compiles the densities determined at 21 °C immediately after bottling of the samples along with all the other important properties:

element, type of solution		matrix		element content	density $\rho / (\text{kg/m}^3)$
Cr	A	$w(\text{HCl}) < 0.002$ g/g	$w(\text{HNO}_3) \approx 0.025$ g/g	0.98 g/kg $\leq w(E) \leq 1.02$ g/kg	1014.1
	B				
	C				
Co	A				
	B				
	C				
Pb	A				1012.8
	B				
	C				

Please be aware that the molar mass of the lead in the samples Pb-A, Pb-B and Pb-C do not match the IUPAC representative molar mass of lead. Therefore, your reference material (source of traceability) may show a different molar mass than the sample. Please determine the molar mass in the sample to be able to correct for this issue or (if this is impossible) report your results in terms of an amount content n/m in mol/kg rather than in terms of a mass fraction w in g/kg.

3. Sample handling

Before opening the bags, please be prepared to weigh the bottles and to measure the ambient conditions (air pressure, air temperature, and relative humidity of the air). Please weigh the bottles immediately after opening the bags. Weigh them together with their screw-caps and labels. Please calculate possible losses according to section 6.

4. Analysis

Please apply your most accurate methods of measurement, preferably primary methods. Note that the relative expanded measurement uncertainty U_{rel} associated with your result must not exceed 0.5 % as already announced in the invitation. You are asked to determine the following quantities:

- Mass fraction $w_A(E)$ of the element E in solution A based on your own standard.
- Mass fraction $w_B(E)$ of the element E in solution B using the provided calibration solution A while assuming that its mass fraction is exactly $w_A(E) = 1 \text{ g/kg}$.
- Mass fraction $w_C(E)$ of the element E in solution C based on your own standard.
- In case you intend to use titrimetry, please determine $w_B(E)$ and $w_C(E)$ based on your own standard.
- In case you do not use titrimetry, the determination of $w_C(E)$ is voluntary, but every result would be appreciated very much.

5. Reporting

Note that the reporting deadline has been changed. The new **deadline** for the submission of results is **15 March 2011**. Please send your report via E-mail.

Please report all your results in terms of a mass fraction w in g/kg. Since it is necessary for the measurement of the lead samples, please determine and report also the molar mass of the lead $M(\text{Pb})$ in the lead samples along with the amount fraction $x(^i\text{Pb})$ in mol/mol of all the lead isotopes. Participants without the opportunity to determine the molar mass of the lead in the lead samples should report the lead results in terms of an amount content $n(\text{Pb})/m$ in mol/kg. Please report also all the masses of all solutions at the time of opening the bottles for the first time. Please refer to section 6 to do this.

Please calculate uncertainties for all the results reported according to the GUM [1]. Please, report also your sources of traceability along with a short description of the method(s) you used.

If you need further assistance or encounter any kind of problem, please contact Detlef Schiel and/or Olaf Rienitz.

Contact:

Dr. Detlef Schiel
Physikalisch-Technische Bundesanstalt
Bundesallee 100
38116 Braunschweig
Germany

Fax +49-531-592-3015

Phone +49-531-592-3110

E-Mail detlef.schiel@ptb.de

Dr. Olaf Rienitz

-3318

olaf.rienitz@ptb.de

6. Checking for losses / correcting evaporation effects

In addition to this “Technical Protocol” you should have received a table summarizing all bottles enclosed in your parcel together with the masses of the empty bottles m_{bottle} and the masses of the solutions in these bottles m_{solution} .

These masses were determined from the apparent masses (weighing values) of the empty bottle m_1 and the bottle containing the according solution m_2 determined at a time t_1 and t_2 , respectively. Since the ambient conditions (relative humidity of the air φ , air pressure p and air temperature ϑ) were different at these times (t_1 and t_2), according air buoyancy correction factors $K_{i,j}$ depending on the time j and the density of the weighed material i (PFA in case of the bottle, ρ_{bottle} , and the different solutions, ρ_{solution}) were calculated to convert the apparent masses m_1 and m_2 into the masses m_{bottle} and m_{solution} .

$$m_{\text{bottle}} = K_{\text{bottle},1} \cdot m_1$$

$$K_{\text{bottle},1} = \frac{1 - \frac{\rho_{\text{air},1}}{\rho_{\text{cal}}}}{1 - \frac{\rho_{\text{air},1}}{\rho_{\text{bottle}}}}$$

$$\rho_{\text{air},1} = \frac{0.34844 \frac{\text{kg/m}^3}{\text{hPa}} \cdot p_1 - \varphi_1 \cdot \left(0.252 \frac{\text{kg/m}^3}{^\circ\text{C}} \cdot \vartheta_1 - 2.0582 \frac{\text{kg}}{\text{m}^3} \right)}{273.15 + \frac{1}{^\circ\text{C}} \cdot \vartheta_1}$$

$$m_{\text{solution}} = K_{\text{solution},2} \cdot \left(m_2 - \frac{m_{\text{bottle}}}{K_{\text{bottle},2}} \right)$$

$$K_{\text{bottle},2} = \frac{1 - \frac{\rho_{\text{air},2}}{\rho_{\text{cal}}}}{1 - \frac{\rho_{\text{air},2}}{\rho_{\text{bottle}}}} \quad \text{and} \quad K_{\text{solution},2} = \frac{1 - \frac{\rho_{\text{air},2}}{\rho_{\text{cal}}}}{1 - \frac{\rho_{\text{air},2}}{\rho_{\text{solution}}}}$$

$$\rho_{\text{air},2} = \frac{0.34844 \frac{\text{kg/m}^3}{\text{hPa}} \cdot p_2 - \varphi_2 \cdot \left(0.252 \frac{\text{kg/m}^3}{^\circ\text{C}} \cdot \vartheta_2 - 2.0582 \frac{\text{kg}}{\text{m}^3} \right)}{273.15 + \frac{1}{^\circ\text{C}} \cdot \vartheta_2}$$

The following parameters were used to perform the calculations above: $\rho_{\text{bottle}} = 2150 \text{ kg/m}^3$, $\rho_{\text{solution,Cr}} = \rho_{\text{solution,Co}} = 1014.1 \text{ kg/m}^3$, and $\rho_{\text{solution,Pb}} = 1012,8 \text{ kg/m}^3$ in case of solution type A, B, and C, respectively, as well as $\rho_{\text{cal}} = 7950 \text{ kg/m}^3$ (please be aware that most modern balances feature internal calibration masses of $\rho_{\text{cal}} = 8000 \text{ kg/m}^3$, therefore refer to the manual of your balance).

Before sampling the first aliquot from a bottle, you are asked to weigh the bottle (including label and cap) at the time t_3 yielding its apparent mass m_3 , while also collecting the corresponding ambient conditions (relative humidity of the air φ_3 , air pressure p_3 and air temperature ϑ_3). This way you are able to observe even minor losses due to evaporation and are also able to correct for them. Please note: Directly before the weighing, you should unscrew the cap of the bottle and tighten it immediately afterwards to equilibrate the pressure

inside and outside the bottle. To calculate the correction, please follow the step-by-step recipe:

Step 1: Calculate the air density $\rho_{\text{air},3}$

$$\rho_{\text{air},3} = \frac{0.34844 \frac{\text{kg/m}^3}{\text{hPa}} \cdot p_3 - \varphi_3 \cdot \left(0.252 \frac{\text{kg/m}^3}{\text{°C}} \cdot \vartheta_3 - 2.0582 \frac{\text{kg}}{\text{m}^3} \right)}{273.15 + \frac{1}{\text{°C}} \cdot \vartheta_3}$$

Step 2: Calculate the air buoyancy correction factor of the bottle $K_{\text{bottle},3}$

$$K_{\text{bottle},3} = \frac{1 - \frac{\rho_{\text{air},3}}{\rho_{\text{cal},3}}}{1 - \frac{\rho_{\text{air},3}}{\rho_{\text{bottle}}}}$$

Step 3: Calculate the air buoyancy correction factor of the solution $K_{\text{solution},3}$

$$K_{\text{solution},3} = \frac{1 - \frac{\rho_{\text{air},3}}{\rho_{\text{cal},3}}}{1 - \frac{\rho_{\text{air},3}}{\rho_{\text{solution}}}}$$

Step 4: Calculate the mass $m_{\text{solution},3}$ of the solution at the time t_3 before sampling the first aliquot from the bottle

$$m_{\text{solution},3} = K_{\text{solution},3} \cdot \left(m_3 - \frac{m_{\text{bottle}}}{K_{\text{bottle},3}} \right)$$

Step 5: Calculate the loss Δm

$$\Delta m = m_{\text{solution},3} - m_{\text{solution}}$$

Step 6: In case it is reasonably small ($-10 \text{ mg} < \Delta m < 0 \text{ mg}$) this loss can be attributed to evaporation effects. In this case calculate an according evaporation losses correction factor f_{evap} (assuming the element content is still present completely in the bottle, causing a slightly elevated mass fraction of the element in question) and apply this to the mass fraction w_3 you have determined in the particular solution in order to retrieve the original mass fraction of the element at the time t_2 immediately after bottling the solution. Please report this corrected mass fraction w_2 .

$$w_2 = f_{\text{evap}} \cdot w_3 \quad \text{with} \quad f_{\text{evap}} = \left(1 + \frac{\Delta m}{m_{\text{solution}}} \right)$$

When setting up an uncertainty budget please use the following standard uncertainties (type B, normal distribution, coverage factor $k = 1$) associated with the mass of the empty bottle m_{bottle} and with the mass of the solution m_{solution} , respectively: $u(m_{\text{bottle}}) = 0.0005$ g and $u(m_{\text{solution}}) = 0.0007$ g.

The following table summarizes all the symbols used throughout the equations above.

Symbol	Unit	Quantity	Comment
m_{bottle}	g	Mass of the empty bottle (corrected for air buoyancy)	Individually listed for every bottle no. in the table sent to each participant
m_{solution}	g	Mass of the sample / calibration solution (corrected for air buoyancy)	Individually listed for every bottle no. in the table sent to each participant; determined immediately after bottling in the pilot laboratory (PTB)
$m_{\text{solution},3}$	g	Mass of the sample / calibration solution (corrected for air buoyancy)	To be determined prior to sampling the first aliquot in the participant's laboratory
Δm	g	Mass difference (loss) of the sample / calibration solution (corrected for air buoyancy)	Difference between m_{solution} and $m_{\text{solution},3}$; determined prior to sampling in the participant's laboratory
m_1	g	Apparent mass (reading of the balance) of the empty bottle	Determined in the pilot laboratory (PTB); used to calculate m_{bottle}
m_2	g	Apparent mass (reading of the balance) of the sum of the empty bottle and the sample/calibration solution	Determined in the pilot laboratory (PTB) immediately after bottling; used to calculate m_{solution}
m_3	g	Apparent mass (reading of the balance) of the sum of the empty bottle and the sample/calibration solution	Determined in the participant's laboratory prior to sampling; used to calculate $m_{\text{solution},3}$
w_2	g/kg	Mass fraction of the particular element	Value corrected for evaporation losses; calculated from w_3
w_3	g/kg	Mass fraction of the particular element	Value actually measured in the participant's laboratory
f_{evap}	1	Factor to correct the measured mass fraction for evaporation losses	To be calculated by the participant
$K_{\text{bottle},1}$	g/g	Air buoyancy correction factor	Valid for the bottle material (PFA) at the time of the determination of m_1
$K_{\text{bottle},2}$	g/g	Air buoyancy correction factor	Valid for the bottle material (PFA) at the time of the determination of m_2
$K_{\text{bottle},3}$	g/g	Air buoyancy correction factor	Valid for the bottle material (PFA) at the time of the determination of m_3

$K_{\text{solution},2}$	g/g	Air buoyancy correction factor	Valid for the solution A, B, and C, respectively, at the time of the determination of m_2
$K_{\text{solution},3}$	g/g	Air buoyancy correction factor	Valid for the solution A, B, and C, respectively, at the time of the determination of m_3
ρ_{cal}	kg/m ³	Density of the calibration masses of the balance	Value for Mettler H315 balance used in the pilot laboratory (PTB) to determine m_1 and m_2
$\rho_{\text{cal},3}$	kg/m ³	Density of the calibration masses of the balance	Value for the participant's balance used to determine m_3 ; usually 8000 kg/m ³
$\rho_{\text{air},1}$	kg/m ³	Air density	At the time of the determination of m_1 in the pilot laboratory (PTB)
$\rho_{\text{air},2}$	kg/m ³	Air density	At the time of the determination of m_2 in the pilot laboratory (PTB)
$\rho_{\text{air},3}$	kg/m ³	Air density	At the time of the determination of m_3 in the participant's laboratory
ρ_{bottle}	kg/m ³	Density of the bottle material (PFA)	Assumed to be sufficiently constant throughout the temperature range in question; $\rho_{\text{bottle}} = 2150 \text{ kg/m}^3$
ρ_{solution}	kg/m ³	Density of the particular sample/calibration solution	Determined in the pilot laboratory (PTB); listed in the text above; assumed to be sufficiently constant throughout the temperature range in question
p_1	hPa	Air pressure	At the time of the determination of m_1 in the pilot laboratory (PTB)
p_2	hPa	Air pressure	At the time of the determination of m_2 in the pilot laboratory (PTB)
p_3	hPa	Air pressure	At the time of the determination of m_3 in the participant's laboratory
φ_1	1	Relative air humidity	At the time of the determination of m_1 in the pilot laboratory (PTB)
φ_2	1	Relative air humidity	At the time of the determination of m_2 in the pilot laboratory (PTB)
φ_3	1	Relative air humidity	At the time of the determination of m_3 in the participant's laboratory; please use numerical values $0 \leq \varphi_3 \leq 1$
ϑ_1	°C	Air temperature	At the time of the determination of m_1 in the pilot laboratory (PTB)
ϑ_2	°C	Air temperature	At the time of the determination of m_2 in the pilot laboratory (PTB)
ϑ_3	°C	Air temperature	At the time of the determination of m_3 in the participant's laboratory

7. References

- [1] *Evaluation of measurement data – Guide to the expression of uncertainty in measurement*, JCGM 100:2008.
- [2] Frank Spieweck, Horst Bettin, *Methoden zur Bestimmung der Dichte von Festkörpern und Flüssigkeiten*, PTB Bericht W-46, ISBN 3-89429-132-X, Braunschweig, 1998.
- [3] Roland Nater, Arthur Reichmuth, Roman Schwartz, Michael Borys, Panagiotis Zervos, *Dictionary of Weighing Terms, A Guide to the Terminology of Weighing*, Springer, ISBN 978-3-642-02013-1, Berlin, 2009.

Physikalisch-Technische Bundesanstalt

Braunschweig und Berlin



Physikalisch-Technische Bundesanstalt, Bundesallee 100, 38116 Braunschweig, Germany

LGC Ltd.
Dr. Sarah Hill
Queens Road
TW11 0LY Teddington Middlesex

United Kingdom

Braunschweig, 2010-12-02

Dear CCQM-K87/CCQM-P124 participant,

The table below shows a compilation of the bottles your parcel should contain. Along with the unique bottle number, the corresponding mass of each empty bottle as well as the mass of the solution inside this bottle are listed. In case a cell reads "n.a.", you either have not registered for this particular element or stated that—due to your method of measurement—you would not need the calibration solution A. Please check the completeness as well as the consistency and condition of the contents of your parcel carefully. For more details concerning the correction of evaporation losses etc. refer to the technical protocol.

Laboratory code 017 / LGC					
Element	Type of solution		Bottle No.	m_{bottle} g	m_{solution} g
Cr	A	calibration	028	41.5060	107.5285
	B	sample	070	41.1197	112.8413
	C	"commercial" sample	111	40.6801	108.9716
Co	A	calibration	153	41.7032	106.8279
	B	sample	195	41.3354	105.2854
	C	"commercial" sample	236	41.1866	110.0777
Pb	A	calibration	281	41.3414	109.4610
	B	sample	325	41.1594	108.8299
	C	"commercial" sample	368	40.8049	109.8244

Appendix C – Results from CCQM-P124 compared to CCQM-K87

The comparisons CCQM-K87 and CCQM-P124 shared exactly the same samples and were running in parallel. Considering the smaller number of participants in the pilot study it is impossible to claim any differences concerning the performance of groups of participants. Two industry laboratories (both providers of mono-elemental calibration solutions) showed a performance very close to this of the most experienced NMIs. This observation is very encouraging since their commercially available calibration solutions are intended to provide traceability in the field. Figures 41–49 show the results of CCQM-P124 in comparison to CCQM-K87.

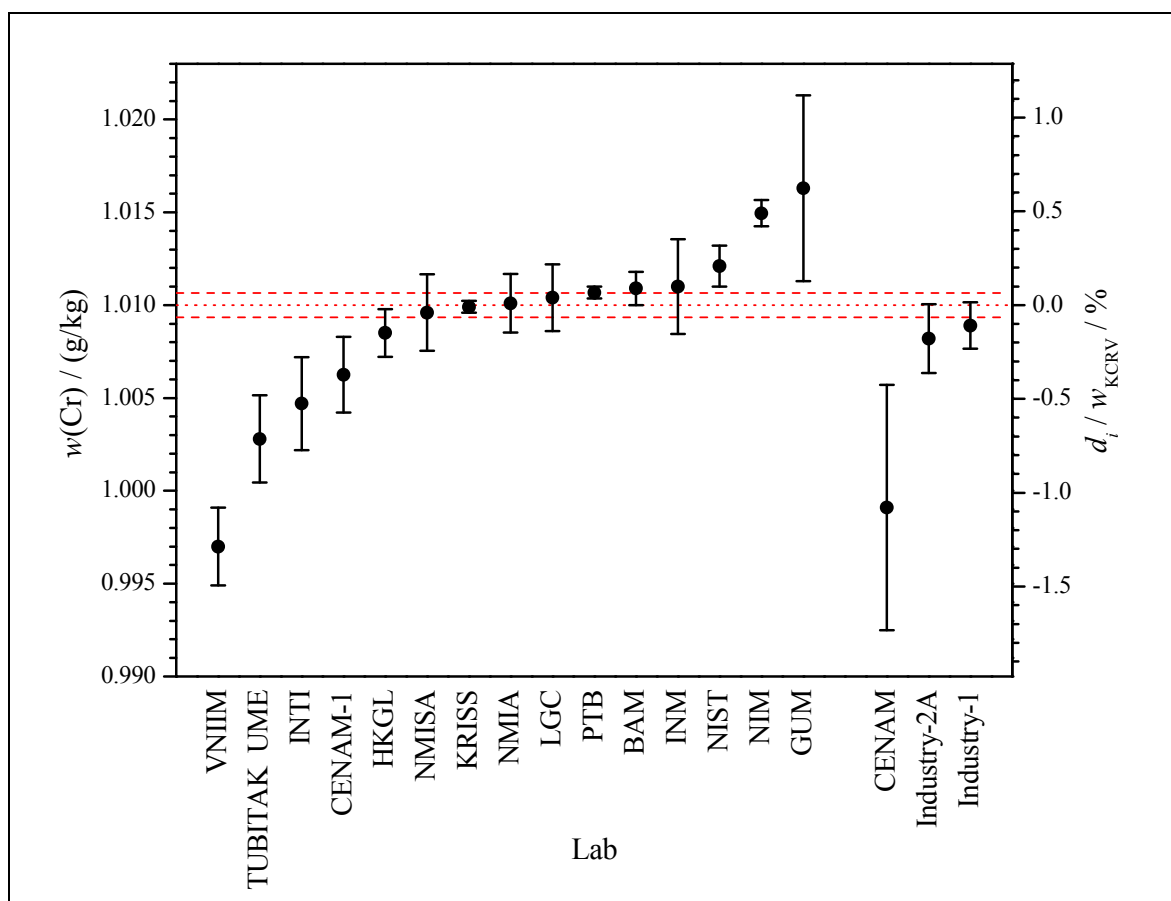


Figure 41: Chromium mass fraction $w(\text{Cr})$ in sample **Cr-A** as reported by the CCQM-K87 participants (left) and the CCQM-P124 participants (right), respectively. Error bars denote the combined uncertainty $u_c(w(\text{Cr}))$ for a coverage factor of $k = 1$ as reported. The dotted red line shows the **gravimetric KCRV**: $w_{\text{KCRV}}(\text{Cr}) = 1.0100$ g/kg. The dashed red lines indicate the range of the combined uncertainty $u_c(w_{\text{KCRV}}(\text{Cr}))$ associated with the KCRV. The right y-axis shows the degree of equivalence d_i relative to the KCRV (for more details see section 7.6).

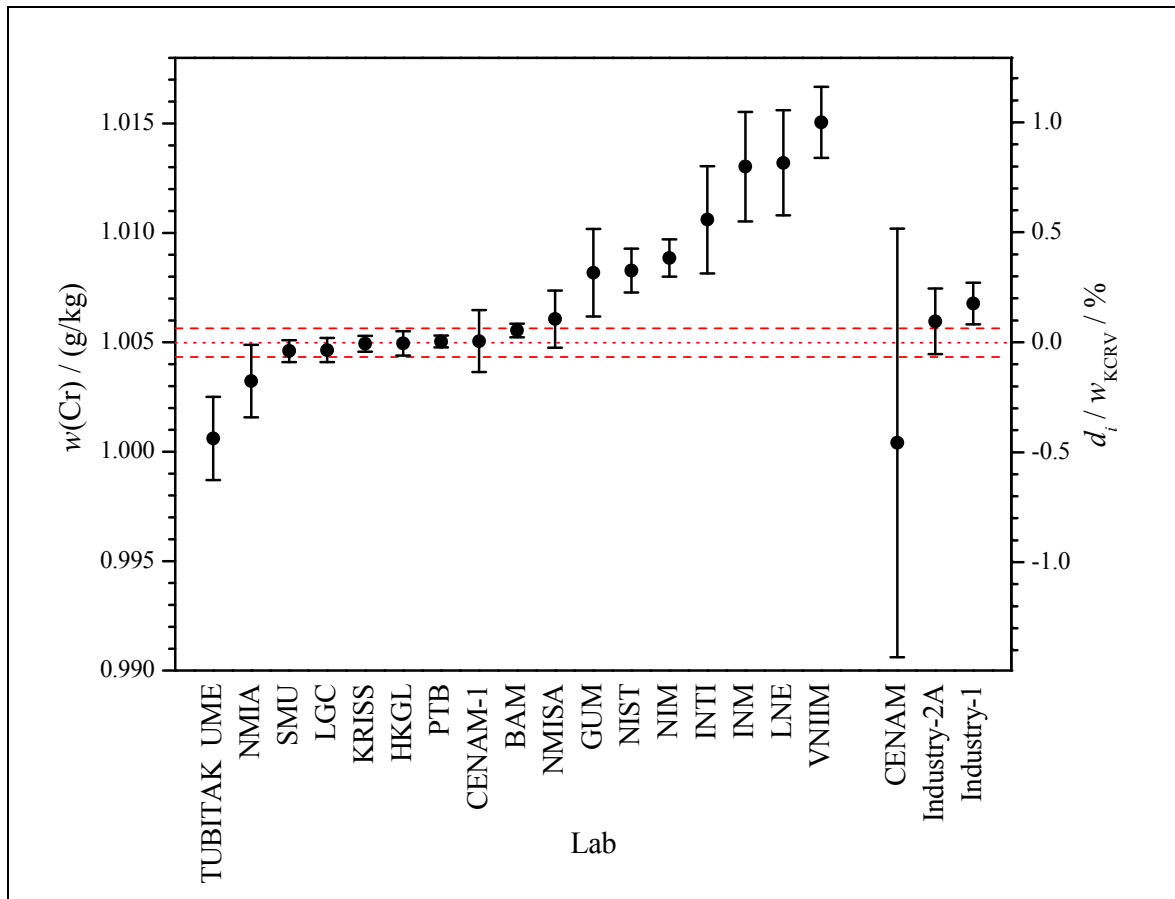


Figure 42: Chromium mass fraction $w(\text{Cr})$ in sample **Cr-B** as reported by the CCQM-K87 participants (left) and the CCQM-P124 participants (right), respectively. All results reported as measured against Cr-A under the assumption of $w(\text{Cr}) = 1 \text{ g/kg} \pm 0 \text{ g/kg}$ were converted using the actual value (KCRV) of Cr-A (appendix F). Error bars denote the combined uncertainty $u_c(w(\text{Cr}))$ for a coverage factor of $k = 1$ as reported. The dotted red line shows the **gravimetric KCRV**: $w_{\text{KCRV}}(\text{Cr}) = 1.0050 \text{ g/kg}$. The dashed red lines indicate the range of the combined uncertainty $u_c(w_{\text{KCRV}}(\text{Cr}))$ associated with the KCRV. The right y-axis shows the degree of equivalence d_i relative to the KCRV (for more details see section 7.6).

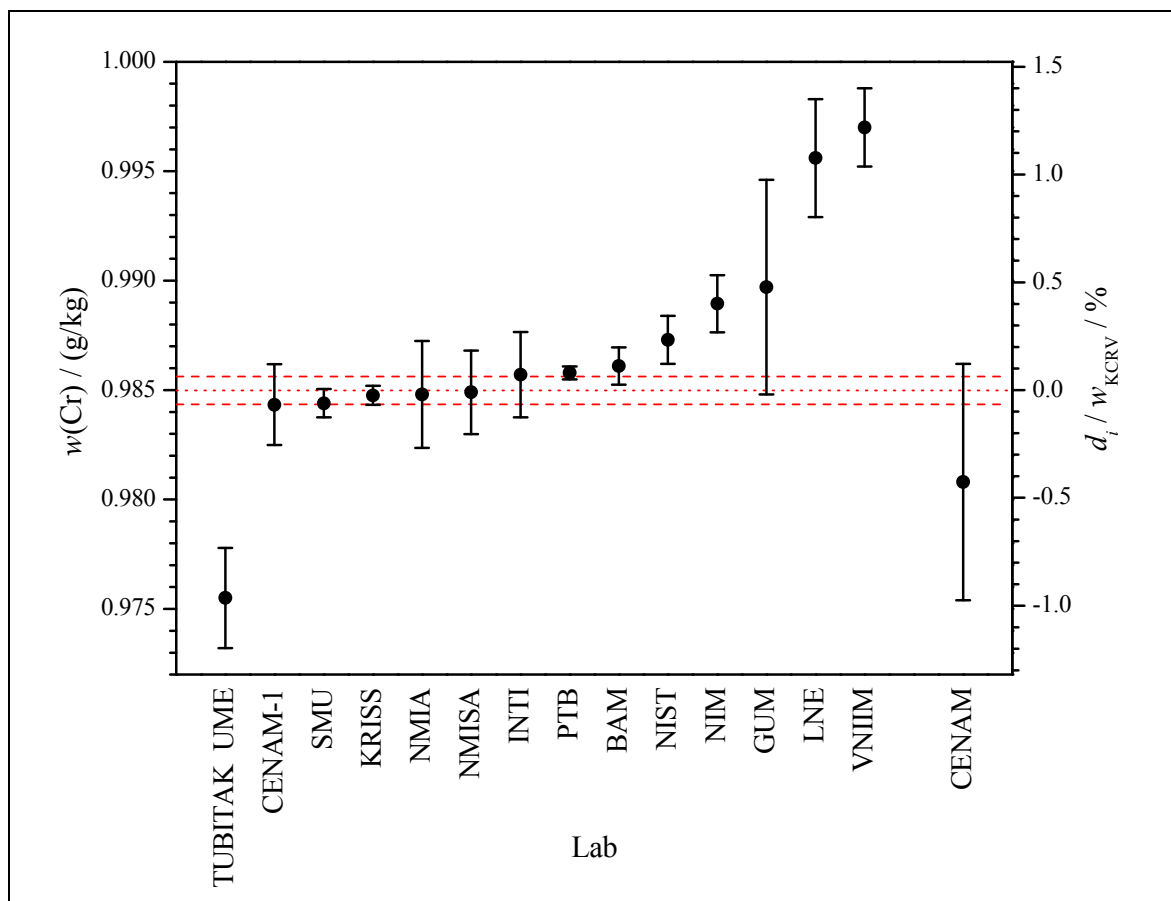


Figure 43: Chromium mass fraction $w(\text{Cr})$ in sample **Cr-C** as reported by the CCQM-K87 participants (left) and the CCQM-P124 participants (right), respectively. Error bars denote the combined uncertainty $u_c(w(\text{Cr}))$ for a coverage factor of $k = 1$ as reported. The dotted red line shows the **gravimetric KCRV**: $w_{\text{KCRV}}(\text{Cr}) = 0.9850 \text{ g/kg}$. The dashed red lines indicate the range of the combined uncertainty $u_c(w_{\text{KCRV}}(\text{Cr}))$ associated with the KCRV. The right y-axis shows the degree of equivalence d_i relative to the KCRV (for more details see section 7.6).

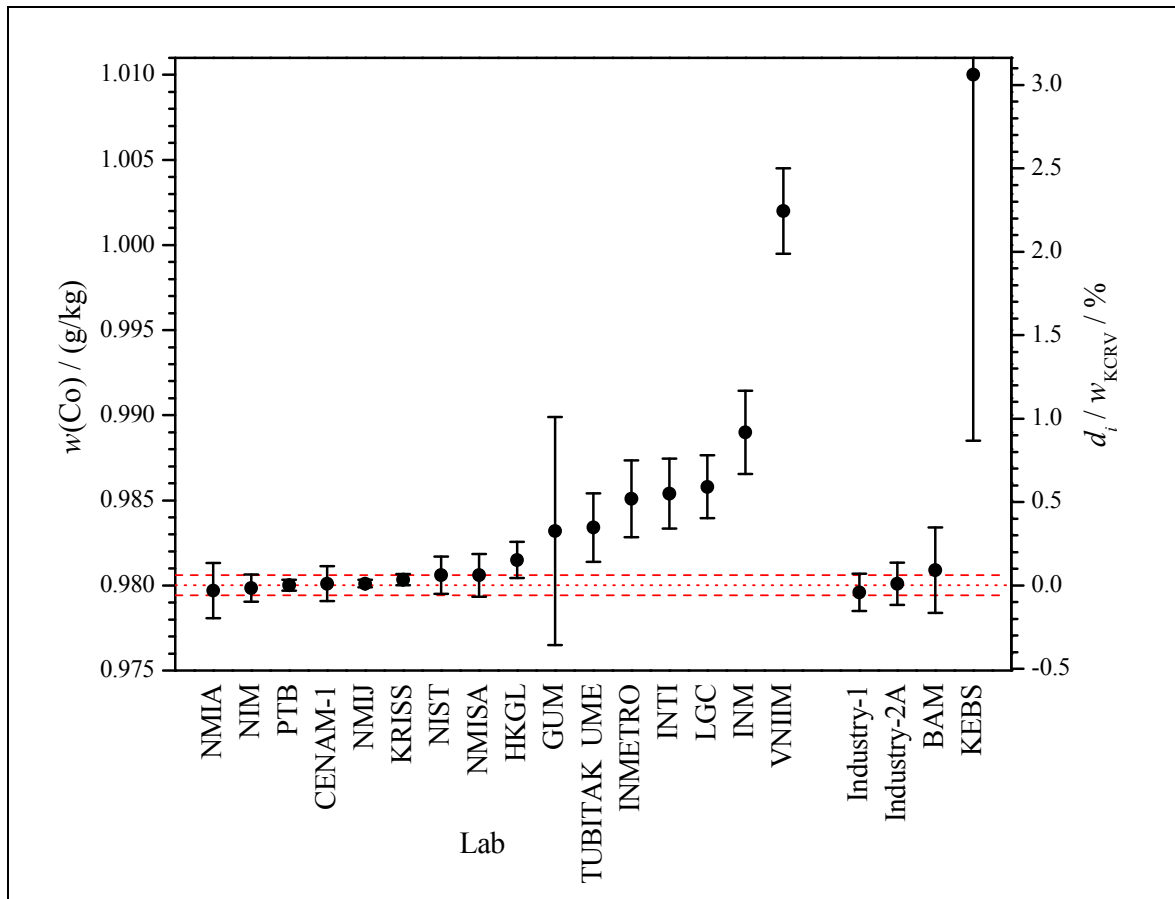


Figure 44: Cobalt mass fraction $w(\text{Co})$ in sample **Co-A** as reported by the CCQM-K87 participants (left) and the CCQM-P124 participants (right), respectively. Error bars denote the combined uncertainty $u_c(w(\text{Co}))$ for a coverage factor of $k = 1$ as reported. The dotted red line shows the **gravimetric KCRV**: $w_{\text{KCRV}}(\text{Co}) = 0.9800 \text{ g/kg}$. The dashed red lines indicate the range of the combined uncertainty $u_c(w_{\text{KCRV}}(\text{Co}))$ associated with the KCRV. The right y-axis shows the degree of equivalence d_i relative to the KCRV (for more details see section 7.6).

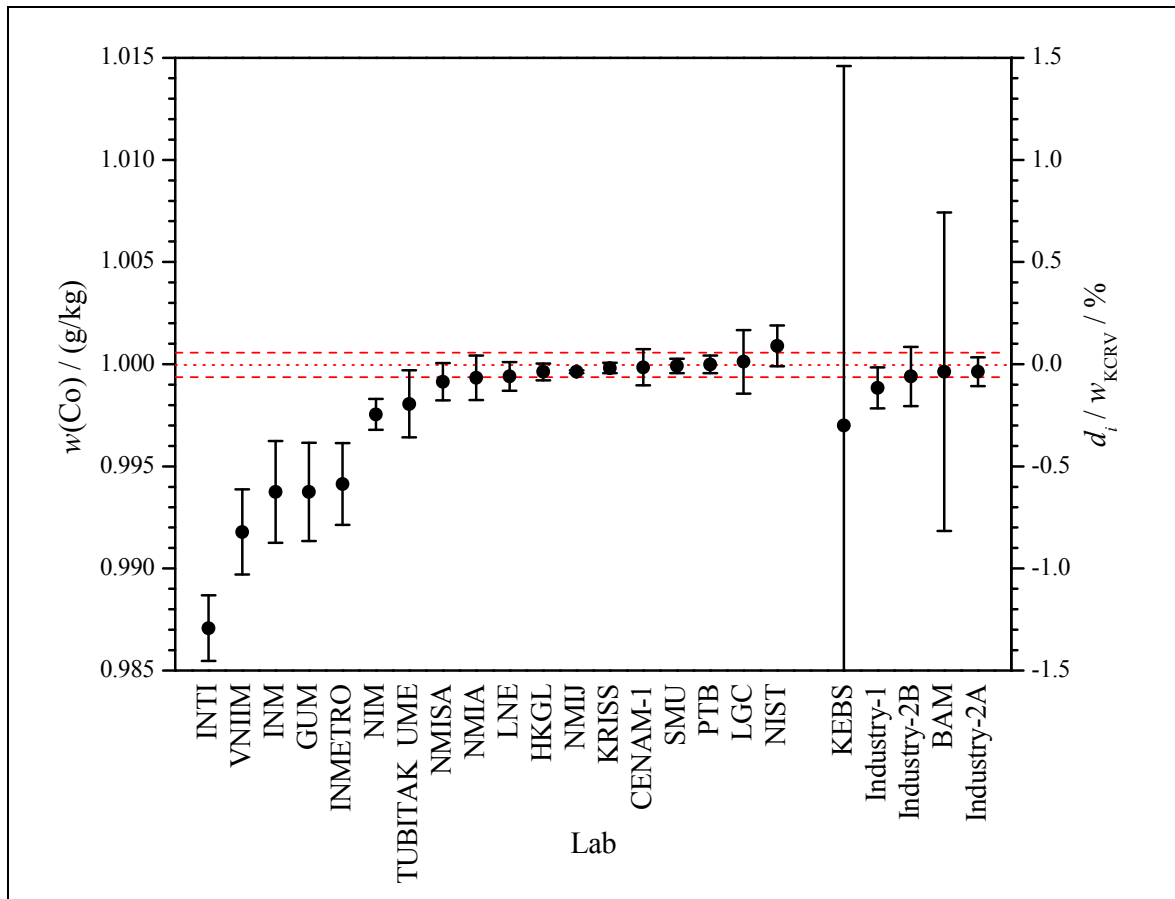


Figure 45: Cobalt mass fraction $w(\text{Co})$ in sample **Co-B** as reported by the CCQM-K87 participants (left) and the CCQM-P124 participants (right), respectively. All results reported as measured against Co-A under the assumption of $w(\text{Co}) = 1 \text{ g/kg} \pm 0 \text{ g/kg}$ were converted using the actual value (KCRV) of Co-A (appendix F). Error bars denote the combined uncertainty $u_c(w(\text{Co}))$ for a coverage factor of $k = 1$ as reported. The dotted red line shows the **gravimetric KCRV**: $w_{\text{KCRV}}(\text{Co}) = 1.0000 \text{ g/kg}$. The dashed red lines indicate the range of the combined uncertainty $u_c(w_{\text{KCRV}}(\text{Co}))$ associated with the KCRV. The right y-axis shows the degree of equivalence d_i relative to the KCRV (for more details see section 7.6).

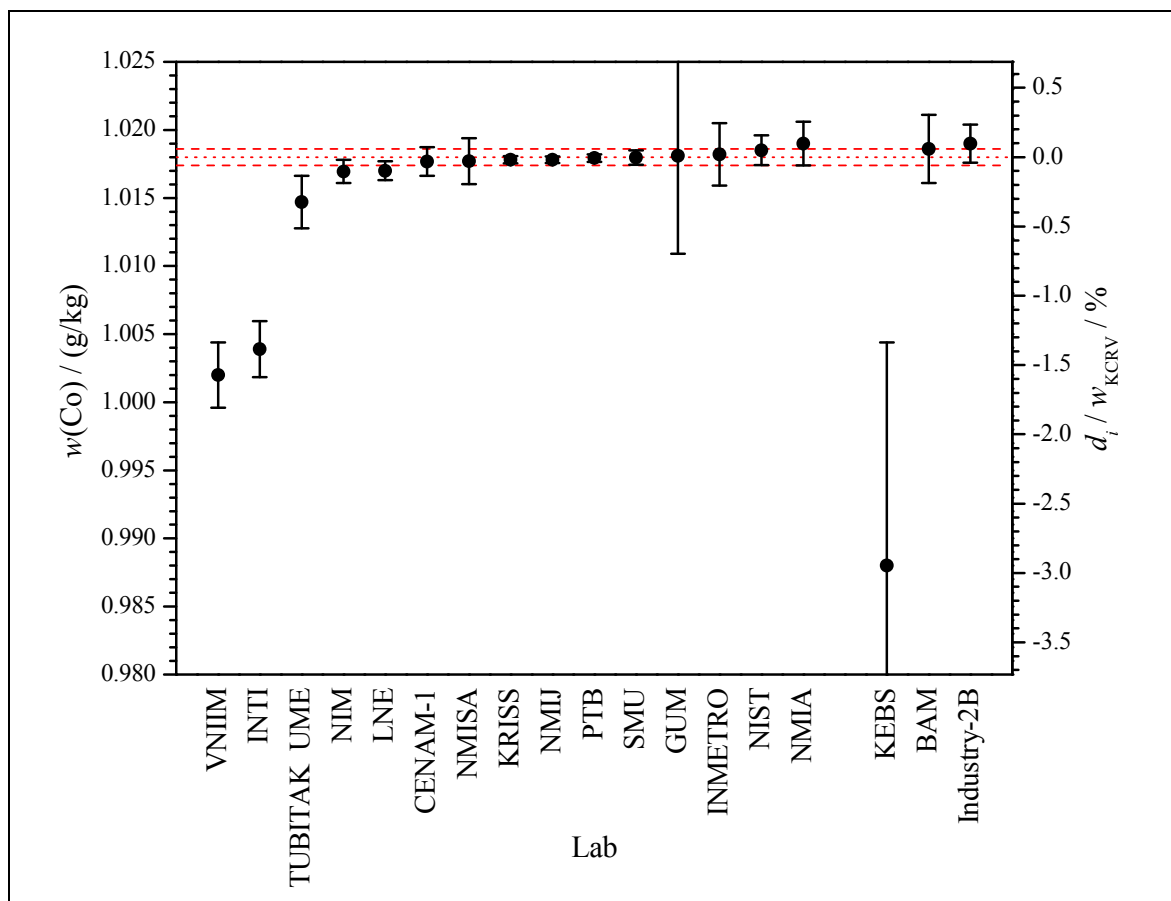


Figure 46: Cobalt mass fraction $w(\text{Co})$ in sample Co-C as reported by the CCQM-K87 participants (left) and the CCQM-P124 participants (right), respectively. Error bars denote the combined uncertainty $u_c(w(\text{Co}))$ for a coverage factor of $k = 1$ as reported. The dotted red line shows the **gravimetric KCRV**: $w_{\text{KCRV}}(\text{Co}) = 1.0180 \text{ g/kg}$. The dashed red lines indicate the range of the combined uncertainty $u_c(w_{\text{KCRV}}(\text{Co}))$ associated with the KCRV. The right y-axis shows the degree of equivalence d_i relative to the KCRV (for more details see section 7.6).

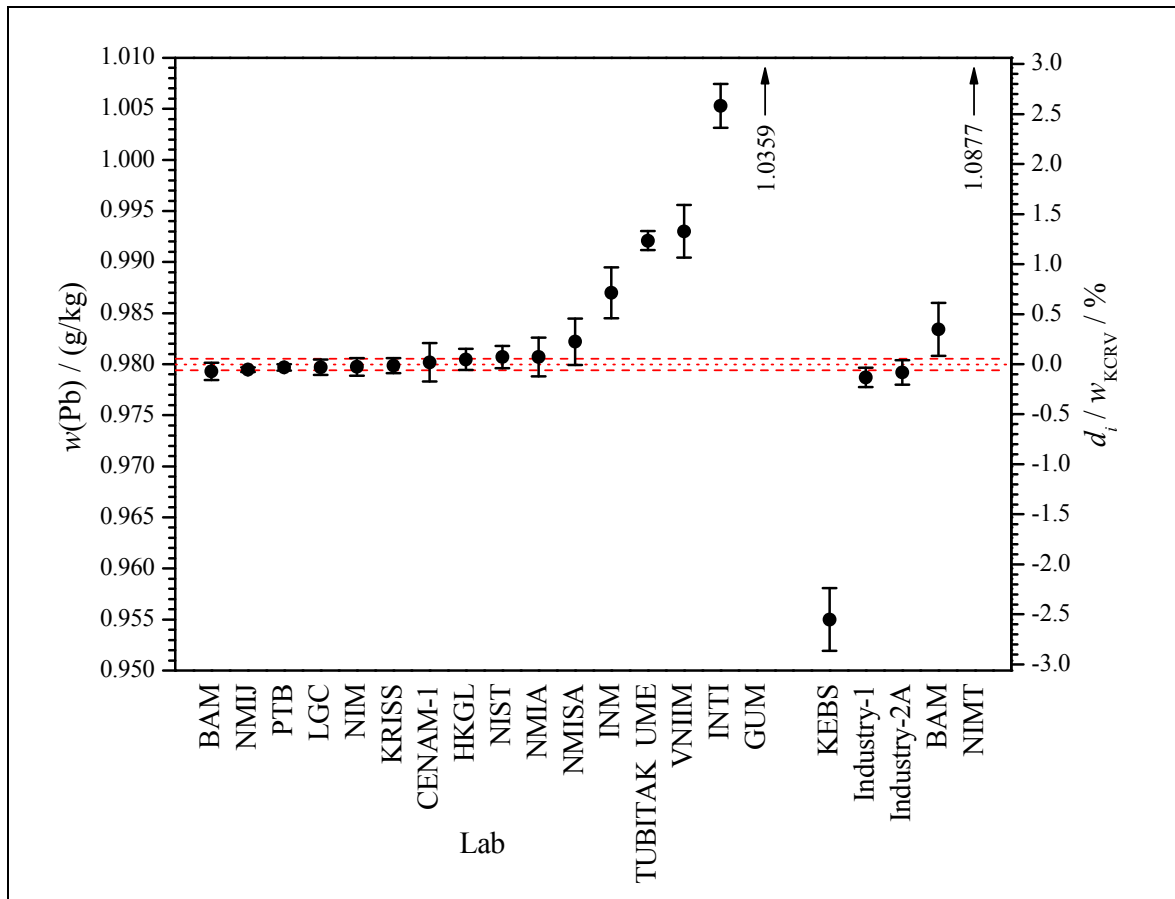


Figure 47: Lead mass fraction $w(\text{Pb})$ in sample **Pb-A** as reported by the CCQM-K87 participants (left) and the CCQM-P124 participants (right), respectively. Results reported in terms of amount contents n/m converted in mass fractions w applying a molar mass of $M(\text{Pb}) = (207.17782 \pm 0.00011) \text{ g/mol}$ ($k = 2$), refer to section 2.3 for details. Error bars denote the combined uncertainty $u_c(w(\text{Pb}))$ for a coverage factor of $k = 1$ as reported. The dotted red line shows the **gravimetric KCRV**: $w_{\text{KCRV}}(\text{Pb}) = 0.9800 \text{ g/kg}$. The dashed red lines indicate the range of the combined uncertainty $u_c(w_{\text{KCRV}}(\text{Pb}))$ associated with the KCRV. The right y-axis shows the degree of equivalence d_i relative to the KCRV (for more details see section 7.6).

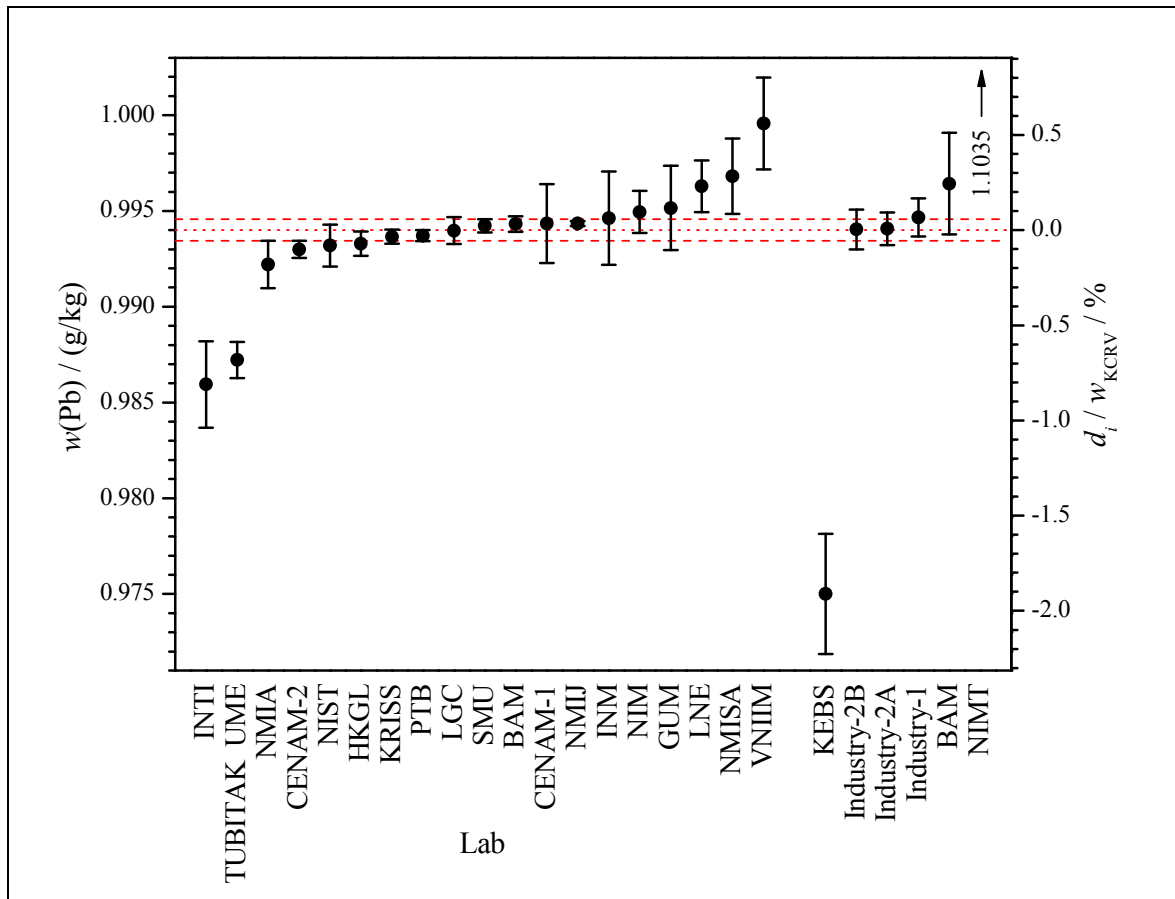


Figure 48: Lead mass fraction $w(\text{Pb})$ in sample **Pb-B** as reported by the CCQM-K87 participants (left) and the CCQM-P124 participants (right), respectively. All results reported as measured against Pb-A under the assumption of $w(\text{Pb}) = 1 \text{ g/kg} \pm 0 \text{ g/kg}$ were converted using the actual value (KCRV) of Pb-A (appendix F). Results reported in terms of amount contents n/m converted in mass fractions w applying a molar mass of $M(\text{Pb}) = (207.17782 \pm 0.00011) \text{ g/mol}$ ($k = 2$), refer to section 2.3 for details. Error bars denote the combined uncertainty $u_c(w(\text{Pb}))$ for a coverage factor of $k = 1$ as reported. The dotted red line shows the **gravimetric KCRV**: $w_{\text{KCRV}}(\text{Pb}) = 0.9940 \text{ g/kg}$. The dashed red lines indicate the range of the combined uncertainty $u_c(w_{\text{KCRV}}(\text{Pb}))$ associated with the KCRV. The right y-axis shows the degree of equivalence d_i relative to the KCRV (for more details see section 7.6).

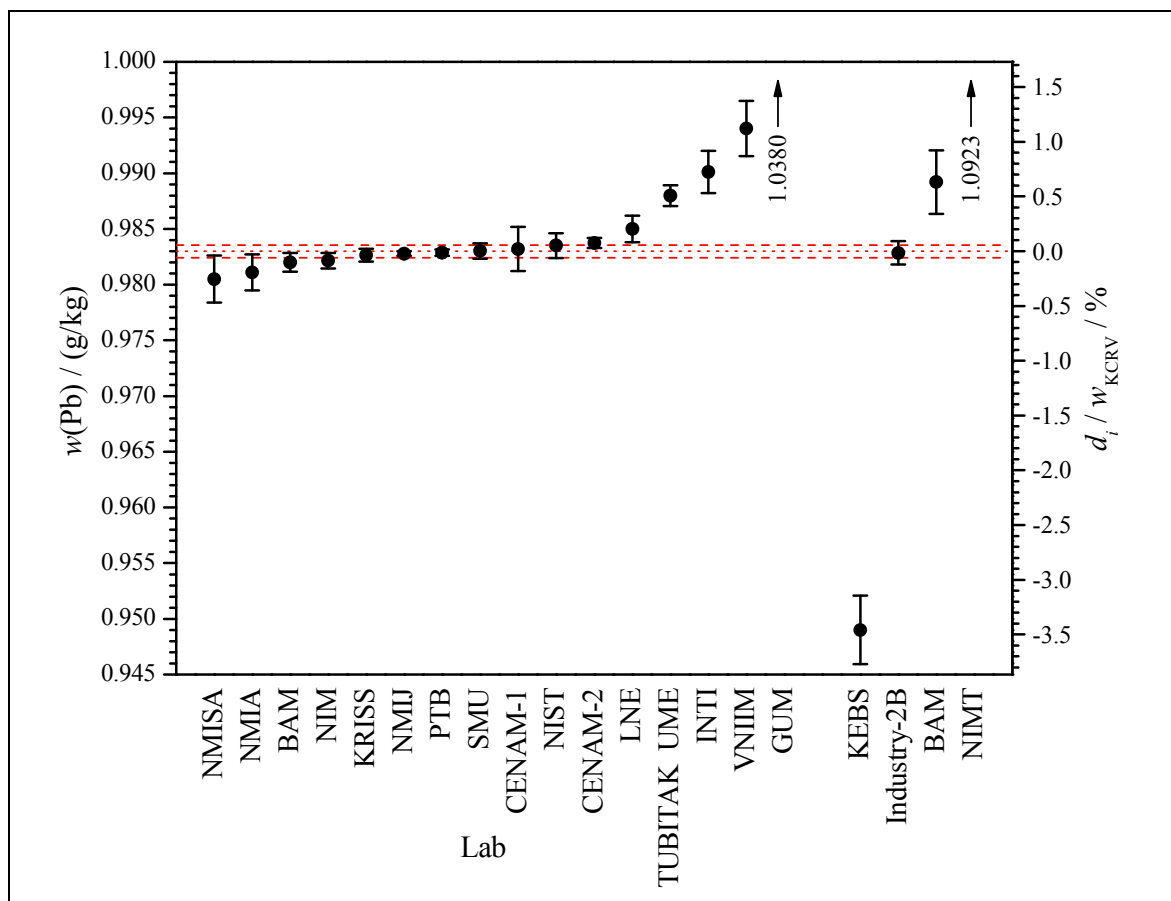


Figure 49: Lead mass fraction $w(\text{Pb})$ in sample **Pb-C** as reported by the CCQM-K87 participants (left) and the CCQM-P124 participants (right), respectively. Results reported in terms of amount contents n/m converted in mass fractions w applying a molar mass of $M(\text{Pb}) = (207.17782 \pm 0.00011) \text{ g/mol}$ ($k = 2$), refer to section 2.3 for details. Error bars denote the combined uncertainty $u_c(w(\text{Pb}))$ for a coverage factor of $k = 1$ as reported. The dotted red line shows the **gravimetric KCRV**: $w_{\text{KCRV}}(\text{Pb}) = 0.9830 \text{ g/kg}$. The dashed red lines indicate the range of the combined uncertainty $u_c(w_{\text{KCRV}}(\text{Pb}))$ associated with the KCRV. The right y-axis shows the degree of equivalence d_i relative to the KCRV (for more details see section 7.6).

Appendix D – Accuracy of the participants' standards

Based on considerations proposed in [15] an equation (section 7.7, eq. (25)) was derived to calculate a quantity reflecting the accuracy A of the standards applied by the participants.

The measured mass fraction w_A determined in solution A using the own standard z (having an element mass fraction of w_z) is biased. The actual (“true”) mass fraction $w_{A,KCRV}$ and the measured one are coupled by a factor $k_{\text{bias,A}}$. This factor can be understood as the product of two factors, namely the factor k_z representing the bias caused by an inaccurate own standard (being off by a relative deviation $\Delta_{\text{rel}w_z}$) and the factor k_{meth} representing the bias caused by the measurement itself (eq. (26)).

$$w_A = k_{\text{bias,A}} \cdot w_{A,KCRV} = k_{\text{meth}} \cdot k_z \cdot w_{A,KCRV} \quad (26)$$

The relative deviation $\Delta_{\text{rel}w_z}$ is defined as the difference between the assigned mass fraction w_z and its true value $w_{z,\text{true}}$ related to the true value $w_{z,\text{true}}$ (eq. (27)).

$$k_z = 1 + \Delta_{\text{rel}w_z} \quad \text{where} \quad \Delta_{\text{rel}w_z} = \frac{w_z - w_{z,\text{true}}}{w_{z,\text{true}}} \quad (27)$$

When measuring solution B applying solution A as the standard under the assumption of an arbitrary mass fraction $w_{A,\text{def}}$, the result w_B will again be biased compared to the “true” mass fraction $w_{B,KCRV}$. The factor $k_{\text{bias,B}}$ describing this observation consists of two contributions: the bias k_{meth} caused by the measurement itself and the bias k_{def} caused by the difference between the arbitrarily defined and the “true” mass fraction ($w_{A,\text{def}}$ and $w_{A,KCRV}$, respectively) of solution A.

$$w_B = k_{\text{bias,B}} \cdot w_{B,KCRV} = k_{\text{meth}} \cdot k_{\text{def}} \cdot w_{B,KCRV} \quad (28)$$

$$k_{\text{def}} = \frac{w_{A,\text{def}}}{w_{A,KCRV}} \quad (29)$$

Under the assumption of a total absence of any precision problem the factors k_{meth} in case of these two measurements are exactly the same. This way the equations above can be taken advantage of in order to extract the relative deviation $\Delta_{\text{rel}w_z}$ of the participant's own standard (accuracy A). Solving eq. (26) for k_z yields eq. (30).

$$k_z = \frac{w_A}{w_{A,KCRV}} \cdot \frac{1}{k_{\text{meth}}} \quad (30)$$

Solving eq. (28) for k_{meth} yields eq. (31).

$$k_{\text{meth}} = \frac{w_B}{w_{B,KCRV}} \cdot \frac{1}{k_{\text{def}}} \quad (31)$$

Eq. (32) follows from replacing k_{def} using eq. (29) in eq. (31).

$$k_{\text{meth}} = \frac{\frac{w_B}{w_{B,KCRV}}}{\frac{w_{A,def}}{w_{A,KCRV}}} \quad (32)$$

Using Eq. (32) k_{meth} is replaced in eq. (30) yielding eq. (33).

$$k_z = \frac{\frac{w_A}{w_{A,KCRV}}}{\frac{w_B}{w_{B,KCRV}}} = \frac{\frac{w_A}{w_{A,KCRV}} \cdot \frac{w_{A,def}}{w_{A,KCRV}}}{\frac{w_B}{w_{B,KCRV}}} \quad (33)$$

Eq. (27) rearranged for $\Delta_{\text{rel}}w_z$ yields using eq. (33):

$$\Delta_{\text{rel}}w_z = k_z - 1 \quad (34)$$

$$\Delta_{\text{rel}}w_z = \frac{\frac{w_A}{w_{A,KCRV}} \cdot \frac{w_{A,def}}{w_{A,KCRV}}}{\frac{w_B}{w_{B,KCRV}}} - 1 \quad (35)$$

Eq. (35) represents the desired equation to express the accuracy A of the participants' own standards ($A \equiv |\Delta_{\text{rel}}w_z|$).

$$A = \left| \frac{\frac{w_A}{w_{A,KCRV}} \cdot \frac{w_{A,def}}{w_{A,KCRV}}}{\frac{w_B}{w_{B,KCRV}}} - 1 \right| \quad (25)$$

The assumptions made to derive eq. (25) limit its validity and applicability and therefore render possible interpretations of calculated accuracy values very difficult (section 7.7).

Appendix E – Unprocessed results as reported

Since several participants used their own standard to determine the element mass fractions in type B solutions the results determined using sample A as the standard under the assumption of a mass fraction of 1 g/kg were converted applying the particular KCRV of sample A to ensure comparability among all results (appendix F). In case two results for sample type B, the result quoted first is the one originally reported while the second was reported after the deadline to enable precision/accuracy calculations (section 7.7). Furthermore, several participants reported their lead results in terms of an amount content n/m to avoid the necessity to determine the molar mass of lead in the sample. All these amount content results were converted to yield mass fractions, again to ensure comparability among all results. The uncertainties were reported relative or absolute, as combined or expanded uncertainties. To enable a consistent data evaluation and presentation all missing data were retrieved from the reported. For the sake of completeness tables 31–39 summarize all reported data unprocessed, “as reported”.

Table 31: Cr-A, unprocessed data, in alphabetical order of the participants’ acronyms.

Cr-A	w	$u_c(w)$	$u_{c,rel}(w)$	k	$U(w)$	$U_{rel}(w)$
	g/kg	g/kg	%	1	g/kg	%
BAM	1.0109			2	0.0018	
CENAM-1	1.0063			2	0.0041	
GUM	1.0163			2	0.0100	
HKGL	1.0085			2.11		0.27
INM	1.0110			2	0.0051	
INTI	1.0047			2	0.0050	0.48
KRISS	1.00991			2.57	0.00080	
LGC	1.0104			2	0.0036	
NIM	1.0150			2	0.0014	
NIST	1.0121	0.0011		2.045	0.0022	
NMIA	1.0101			2.10	0.0033	
NMISA	1.0096			1.99	0.0041	
PTB	1.01068			2	0.00065	
TUBITAK UME	1.0028			2		0.47
VNIIM	0.997			2		0.42

Table 32: Cr-B, unprocessed data, in alphabetical order of the participants’ acronyms. Numbers in grey indicate the determination using an own standard instead of sample A.

Cr-B	w	$u_c(w)$	$u_{c,rel}(w)$	k	$U(w)$	$U_{rel}(w)$
	g/kg	g/kg	%	1	g/kg	%
BAM	0.99559			2	0.00062	
CENAM-1	0.9951			2	0.0028	

Cr-B	w	$u_c(w)$	$u_{c,rel}(w)$	k	$U(w)$	$U_{rel}(w)$
	g/kg	g/kg	%	1	g/kg	%
GUM	0.9982			2	0.0040	
HKGL	0.9950			2.36		0.13
INM	1.0030			2	0.0050	
INTI	1.0006			2	0.0049	0.49
KRISS	0.99499			2.45	0.00088	
LGC	0.9947			2	0.0011	
LNE	1.0132			2	0.0048	
NIM	1.0089			2	0.0017	
	0.9941			2	0.0017	
NIST	0.9983	0.0010		2.052	0.0021	
NMIA	0.9933			2.36	0.0039	
NMISA	0.9961			2.00	0.0026	
PTB	0.99509			2	0.00055	
SMU	1.0046			2	0.0010	
TUBITAK UME	0.9907			2		0.38
VNIM	1.005			2		0.32

Table 33: Cr-C, unprocessed data, in alphabetical order of the participants' acronyms.

Cr-C	w	$u_c(w)$	$u_{c,rel}(w)$	k	$U(w)$	$U_{rel}(w)$
	g/kg	g/kg	%	1	g/kg	%
BAM	0.9861			2	0.0017	
CENAM-1	0.9843			2	0.0037	
GUM	0.9897			2	0.0098	
INTI	0.9857			2	0.0039	0.40
KRISS	0.98476			2.78	0.00122	
LNE	0.9956			2	0.0054	
NIM	0.9889			2	0.0026	
NIST	0.9873	0.0011		2.042	0.0022	
NMIA	0.9848			2.01	0.0049	
NMISA	0.9849			1.99	0.0038	
PTB	0.98578			2	0.00059	
SMU	0.9844			2	0.0013	
TUBITAK UME	0.9755			2		0.47
VNIM	0.997			2		0.36

Table 34: Co-A, unprocessed data, in alphabetical order of the participants' acronyms.

Co-A	w	$u_c(w)$	$u_{c,rel}(w)$	k	$U(w)$	$U_{rel}(w)$
	g/kg	g/kg	%	1	g/kg	%
CENAM-1	0.9801			2	0.0021	
GUM	0.9832			2	0.0134	
HKGL	0.9815			2.2		0.24
INM	0.9890			2	0.0049	
INMETRO	0.9851			2	0.0045	
INTI	0.9854			2	0.0041	0.42
KRISS	0.98034			2.78	0.00090	
LGC	0.9858			2	0.0037	
NIM	0.9798			2	0.0016	
NIST	0.9806	0.0011		2.042	0.0022	
NMIA	0.9797			2.03	0.0033	
NMIJ	0.98011		0.023			
NMISA	0.9806			1.99	0.0025	
PTB	0.98002			2	0.00063	
TUBITAK UME	0.9834			2		0.41
VNIM	1.002			2		0.50

Table 35: Co-B, unprocessed data, in alphabetical order of the participants' acronyms. Numbers in grey indicate the determination using an own standard instead of sample A.

Co-B	w	$u_c(w)$	$u_{c,rel}(w)$	k	$U(w)$	$U_{rel}(w)$
	g/kg	g/kg	%	1	g/kg	%
CENAM-1	1.0202			2	0.0018	
GUM	1.0140			2	0.0048	
HKGL	1.0200			2.45		0.10
INM	1.0140			2	0.0050	
INMETRO	1.0144			2	0.0040	
INTI	1.0072			2	0.0032	0.32
KRISS	1.02019			2.45	0.00062	
LGC	1.0205			2	0.0031	
LNE	0.9994			2	0.0014	
NIM	0.9975			2	0.0015	
	1.0180			2	0.0015	
NIST	1.0213	0.0010		2.052	0.0022	
NMIA	1.0197			2.03	0.0022	
NMIJ	1.02000		0.007			

Co-B	w	$u_c(w)$	$u_{c,rel}(w)$	k	$U(w)$	$U_{rel}(w)$
	g/kg	g/kg	%	1	g/kg	%
NMIJ	0.99971		0.022			
NMISA	1.0195			1.97	0.0018	
PTB	0.99999			2	0.00086	
SMU	0.99991			2	0.00070	
TUBITAK UME	1.0184			2		0.33
VNIIM	1.012			2		0.42

Table 36: Co-C, unprocessed data, in alphabetical order of the participants' acronyms.

Co-C	w	$u_c(w)$	$u_{c,rel}(w)$	k	$U(w)$	$U_{rel}(w)$
	g/kg	g/kg	%	1	g/kg	%
CENAM-1	1.0177			2	0.0021	
GUM	1.0181			2	0.0144	
INMETRO	1.0182			2	0.0046	
INTI	1.0039			2	0.0041	0.41
KRISS	1.01780			2.57	0.00069	
LNE	1.0170			2	0.0014	
NIM	1.0170			2	0.0017	
NIST	1.0185	0.0011		2.052	0.0022	
NMIA	1.0190			2.06	0.0033	
NMIJ	1.01781		0.023			
NMISA	1.0177			2.02	0.0034	
PTB	1.01793			2	0.00055	
SMU	1.01796			2	0.00105	
TUBITAK UME	1.0147			2		0.38
VNIIM	1.002			2		0.48

Table 37: **Pb-A**, unprocessed data, in alphabetical order of the participants' acronyms.

Pb-A	w	$u_c(w)$	$u_{c,rel}(w)$	k	$U(w)$	$U_{rel}(w)$	n/m	k	$U(n/m)$
	g/kg	g/kg	%	1	g/kg	%	mmol/kg	1	mmol/kg
BAM	0.9793			2	0.0017				
CENAM-1	0.9802			2	0.0038				
GUM							5.00	2	0.07
HKGL	0.98046			2.08		0.22			
INM							4.764	2	0.024
INTI	1.0053			2	0.0043	0.43			
KRISS							4.7295	2.18	0.0078
LGC	0.9797			2	0.0015				
NIM	0.9797			2	0.0017				
NIST	0.9807	0.0011		2.040	0.0022				
NMIA	0.9807			2.00	0.0038				
NMIJ	0.97946		0.022						
NMISA	0.9822			1.99	0.0045				
PTB	0.97968			2	0.00065				
TUBITAK UME	0.9921			2		0.19			
VNIIM	0.993			2		0.52			

Table 38: **Pb-B**, unprocessed data, in alphabetical order of the participants' acronyms. Numbers in grey indicate the determination using an own standard instead of sample A.

Pb-B	w	$u_c(w)$	$u_{c,rel}(w)$	k	$U(w)$	$U_{rel}(w)$	n/m	k	$U(n/m)$
	g/kg	g/kg	%	1	g/kg	%	mmol/kg	1	mmol/kg
BAM	1.01465			2	0.00081				
CENAM-1	1.0147			2	0.0041				
CENAM-2	0.99299			2	0.00089				
GUM	1.0155			2	0.0044				
HKGL	1.0136			2.36		0.15			
INM							4.899	2	0.024
INTI	1.0061			2	0.0045	0.45			
KRISS							4.8942	2.06	0.0037
LGC	1.0143			2	0.0014				
LNE	0.9963			2	0.0027				
NIM	0.9950			2	0.0022				
	1.0156			2	0.0023				
NIST	1.0135	0.0011		2.040	0.0023				

Pb-B	w	$u_c(w)$	$u_{c,rel}(w)$	k	$U(w)$	$U_{rel}(w)$	n/m	k	$U(n/m)$
	g/kg	g/kg	%	1	g/kg	%	mmol/kg	1	mmol/kg
NMIA	1.0125			2.02	0.0025				
NMIJ	1.01468		0.013						
	0.99384		0.023						
NMISA	1.0172			1.98	0.0039				
PTB	0.99371			2	0.00058				
SMU							4.7989	2	0.0034
TUBITAK UME	1.0074			2		0.19			
VNIIM	1.020			2		0.48			

Table 39: **Pb-C**, unprocessed data, in alphabetical order of the participants' acronyms.

Pb-C	w	$u_c(w)$	$u_{c,rel}(w)$	k	$U(w)$	$U_{rel}(w)$	n/m	k	$U(n/m)$
	g/kg	g/kg	%	1	g/kg	%	mmol/kg	1	mmol/kg
BAM	0.9820			2	0.0017				
CENAM-1	0.9832			2	0.0040				
CENAM-2	0.98373			2	0.00089				
GUM							5.01	2	0.08
INTI	0.9901			2	0.0038	0.38			
KRISS							4.7430	2.23	0.0063
LNE	0.9850			2	0.0024				
NIM	0.9822			2	0.0014				
NIST	0.9835	0.0011		2.042	0.0022				
NMIA	0.9811			2.00	0.0032				
NMIJ	0.98278		0.022						
NMISA	0.9805			2.00	0.0042				
PTB	0.98287			2	0.00056				
SMU							4.7448	2	0.0068
TUBITAK UME	0.9880			2		0.19			
VNIIM	0.994			2		0.50			

Appendix F – Conversion applied to results reported for type B solutions

The participants were asked to determine the mass fractions of the elements (E) in type B solutions using the according type A solution as the standard assuming a mass fraction of $w_{A,def}(E) = 1 \text{ g/kg} \pm 0 \text{ g/kg}$. Those participants applying methods which need no calibrator of the same type as the sample (e.g. coulometric titrimetry) were asked to skip solution type A and report the mass fraction in solution type B against their own standards. Please refer to section 2.1 and appendix A for more details. A few participants determined solutions B against their own standards even though they applied methods requiring calibration solutions of the same type as the sample. To be able to compare all results, those reported as determined against solution A under the above assumption were converted using the KCRV of solution A as the best representation of the “true” value:

$$w_{B,conv}(E) = \frac{w_{A,KCRV}(E)}{w_{A,def}(E)} \cdot w_{B,reported}(E) \quad (36)$$

Appendix G – Molar mass of lead, additional data

Figure 2 in section 2.3 shows the molar masses of lead as “reported” by the participants. Several participants reported individual molar masses for each type of solution. One participant reported the isotope ratios $^{204}\text{Pb}/^{206}\text{Pb}$. To achieve comparability among all results the reported molar masses and their associated uncertainties were averaged:

$$M(\text{Pb}) = \frac{M_A(\text{Pb}) + M_B(\text{Pb}) + M_C(\text{Pb})}{3} \quad (37)$$

$$u(M(\text{Pb})) = \sqrt{\frac{u^2(M_A(\text{Pb})) + u^2(M_B(\text{Pb})) + u^2(M_C(\text{Pb}))}{3}} \quad (38)$$

From the isotope ratios $R_{i/206}$ the molar mass of lead and its associated uncertainty was calculated (after averaging the isotope ratios) using the GUM Workbench 2.4.

$$R_i = \frac{R_{A,i/206} + R_{B,i/206} + R_{C,i/206}}{3} \quad (39)$$

$$M(\text{Pb}) = \frac{1}{R_{204} + R_{206} + R_{207} + R_{208}} \times [R_{204}M(^{204}\text{Pb}) + R_{206}M(^{206}\text{Pb}) + R_{207}M(^{207}\text{Pb}) + R_{208}M(^{208}\text{Pb})] \quad (40)$$

Table 40 summarizes all reported data related to the molar mass of lead as well as the molar masses calculated from the data (figure 2).

Table 40: Molar masses of lead $M(\text{Pb})$ as reported or calculated using eq. (37)-(40).

Institute	M g/mol	$u(M)$ g/mol
BAM	207.177980	0.000085
CENAM	207.169	0.067
HKGL	207.178	
KRISS	207.178	0.040
LGC	207.177834	0.000049
LNE	207.200	0.014
NIM	207.178	
NIST	207.18	0.105
NMIA	207.178	0.022
NMIJ	207.1776	0.0009
PTB	207.177797	0.000093
TUBITAK UME	207.177	0.001

Appendix H – Remarks on rounding

All results reported, all input quantities of the gravimetric KCRVs, the KCRVs themselves as well as all intermediate results or final results (like DoEs etc.) were handled throughout the complete data processing without any rounding. The data processing was carried out using Microsoft Excel 2007 (15 digits internal precision). Figures showing data were plotted using Origin Lab Corporation Origin 8.5 G SR1. Data transfer from Excel to Origin without rounding. All numbers printed in this report were rounded usually considering their associated uncertainties in accordance with [7] or in some cases to yield the same number of digits to simplify comparability. This means that in rare cases intermediate results cannot be retrieved to their last digits due to the rounding, but this does not influence the accuracy of the printed numbers.